INFORMATION TO USERS

The most advanced technology has been used to photograph and reproduce this manuscript from the microfilm master. UMI films the text directly from the original or copy submitted. Thus, some thesis and dissertation copies are in typewriter face, while others may be from any type of computer printer.

The quality of this reproduction is dependent upon the quality of the copy submitted. Broken or indistinct print, colored or poor quality illustrations and photographs, print bleedthrough, substandard margins, and improper alignment can adversely affect reproduction.

In the unlikely event that the author did not send UMI a complete manuscript and there are missing pages, these will be noted. Also, if unauthorized copyright material had to be removed, a note will indicate the deletion.

Oversize materials (e.g., maps, drawings, charts) are reproduced by sectioning the original, beginning at the upper left-hand corner and continuing from left to right in equal sections with small overlaps. Each original is also photographed in one exposure and is included in reduced form at the back of the book.

Photographs included in the original manuscript have been reproduced xerographically in this copy. Higher quality 6" x 9" black and white photographic prints are available for any photographs or illustrations appearing in this copy for an additional charge. Contact UMI directly to order.

U·M·I

University Microfilms International
A Bell & Howell Information Company
300 North Zeeb Road, Ann Arbor, MI 48106-1346 USA
313 761 4700 800 521 0600

Order Number 9020764

Soil-structure interaction influence of lift off

Gu, Yongtai, Ph.D.

City University of New York, 1990

U·M·I
300 N. Zeeb Rd.
Ann Arbor, MI 48106

SOIL STRUCTURE INTERACTION

INFLUENCE OF LIFT OFF

by

Yongtai Gu

A dissertation submitted to the Graduate Faculty in Engineering in partial fulfillment of the requirement for the degree of Doctor of Philosophy, the City University of New York.

1990

This manuscript has been read and accepted for the Graduate Faculty in Engineering in satisfaction of the dissertation requirement for the degree of Doctor of Philosophy.

January 25, 1990
date

Charles A. Miller
Chair of Examining Committee

1/25/90
date

Jacques E. Bevenniste
Executive Officer

Professor, Aspasia Zerva

Professor, Jacques E. Bevenniste

Professor, Carl J. Costantino

Profeffor, Charles A. Miller
Supervisory Committee

The City University Of New York

ABSTRACT

Soil-Structure Interaction
Influence of Lift-Off
b y
Yong tai Gu
Adviser: Professor Charles A. Miller

In this research the effects of lift off on soil-structure interaction are discussed. Two types of lift off model are introduced in two different parts. In part one, the Wolf's discrete model is modified as a discrete lift off model. The vertical and rocking concentrated spring and dampers from wolf's model are converted to distributed springs and dampers so that lift off effects may be included. The horizontal spring and damper are used in lift off model directly. The equations of motion during lift off are taken to be nonlinear. Two different models for spring/damper distributing are established and studied.

In part two, a continuum mechanic model derived by use of Pekeris solution and Chao's solution. It is assumed that the base of foundation is divided into segments(strips). The relationship of unit uniform pulse on a strip and displacement due to the pulse is established first. A solution is obtain sequentially in time for the unknown magnitudes of the uniform pulses applied to each strip of foundation. When the pressures in a strip are in tensile, the lift off occurs. For developing lift off model, the pressure in tensile must be set as zero since soil can not carry tensile force.

The validity of these two lift off models is evaluated by two set of experiment data. The acceleration spectra predicted by the lift off models are compared with the measured data in these two experiments respectively. The dynamic stiffness coefficients calculated by these two models are compared with Wolf's formula when lift off neglecting.

The lift off effects on soil structure interaction are studied by evaluating the peak acceleration required to lift off. The peak acceleration required to lift off are effect by interaction damping ratio, depth of burial,and height of the structure's center of gravity above base. Also, the results predicted by lift off models when lift off neglected and considered are compared and studied.

ACKNOWLEDGEMENT

Foremost, I wish to thank my adviser, Professor Charles A. Miller, for his continuous guidance, insight and encouragement that make this thesis possible. Also I am thankful to him for giving me financial support during my study.

I am grateful to professor Carl J. Costantino, Jacques E. Bevenniste, and Aspasia Zerva for kindly providing useful information, reference in SSI and all valuable discussion with them.

Specially, I want to thank Professor G. Donald Brandt, the Chairman of Civil Engineering Department,for giving me the opportunity to be a teaching assistant during my research.

Finally, I thank my mother,my wife and my son for their patient support and genuine interest in my completion of this dissertation.

TABLE OF CONTENTS

page

PART II CONTINUUM MECHANICS MODEL

LIST OF FIGURES

Chapter
Introduction

The effects of the soil-structure interaction process on the response of a structure to an earthquake has long been a topic of interest in engineering and geophysics. The response of a structure during an earthquake depends on the characteristics of the ground motion, the dynamic properties of the surrounding soil, and the stiffness and inertial properties of the structure and foundations. An appropriate model must properly account for the different structural elements (shell, slabs, walls and frames), and must accurately represent the material behavior of concrete, steel and soil. The condition at the foundation-soil interface must be properly modeled including the possibility of lateral separation and foundation uplift. Finally, the model must be capable of properly modeling the seismic free field environment which consists of body waves (shear and dilatation) arriving at some angle of incidence and surface waves (Raleigh and Love).

The requirements just described imply that a complete soil structure interaction model must be fully three dimensional and non-linear. For a structure which is founded on rock or a very stiff soil, the foundation motion is essentially that which would exist in the soil at the level of the foundation in the absence of the structure and any excavation; this motion is denoted as the free field ground motion. For soft soil, the foundation motion differs from that in the free field due to the coupling of the soil and structure during the earthquake. This interaction results from the scattering of waves from the foundation and the radiation of energy from the structure due to the structural vibrations. Because of these effects, the state of deformation in the supporting soil is different from that in the free field. Therefore, the dynamic response of a structure supported on soft soil may differ substantially in amplitude and frequency content from the response of an identical structure supported on very stiff soil or rock.

Several non-linear effects become significant at high acceleration levels. The soil may behave in a non-linear fashion at strain levels associated with the large earthquakes. These nonlinearities are approximately accounted for in a linear analysis through an adjustment in the values of modulus and damping for the soil. Iterative solutions are obtained until the assumed soil properties match the calculated soil strain levels. A second source of nonlinearity occurs at the soil/structure interface when the foundation lifts off from the soil. This thesis focus on the SSI problem and particular the non linear effects associated with lift off. A brief description of the state of the art for treating SSI without lift off is first given followed with a discussion of the lift off problem.

Most of the solutions to the SSI problem treat the foundation as a rigid plate, either circular or rectangular, resting on an isotropic, homogeneous, linear elastic half space. The earlier solutions to the problem have been obtained assuming that the distribution of contact stresses is the same under both static and dynamic loading and is independent of the frequency of vibration. Actually the distribution of contact stresses depends on the frequency. Lysmer [3] has succeeded in solving the problem of a rigid plate under steady state vertical oscillation taking into account the proper distribution of contact stresses. Using a somewhat similar approach, Elorduy [5] has developed a method applicable to the vibrations of a rigid plate of arbitrary shape resting on an elastic half space. He makes use of the known solution for the free-field response due to a vertical (Pekeris [6]) or a horizontal (Chao [7]) concentrated step pulse applied at a point of the elastic half space. He then solves two sets of simultaneous equations to satisfy the boundary conditions at the base of the plate. Elorduy's application to rectangular plate is based on the simplifying assumption that the phase lag between force and displacement is the same at all points of contact between the plate and half space.

Elorduy's approach, after removing the simplifying assumption and incorporating an explicit consideration of coupling between vertical and horizontal displacements, can give results as accurate as desired for plates of arbitrary shape. However, as in

Lysmer's treatment, the method gives rise to very ill-conditioned equations in some range of the variables. This difficulty was obviated by Robertson [9] through a transformation of the integral equation from which these sets of equations are derived. He was thus able to arrive at an exact solution for the vertical oscillations of a rigid circular plate on an elastic half space. His method can be adopted to analyses of the rocking, torsional and translational oscillations of rigid circular plates and to the vibrations of infinitely long rigid plates. However, it is not applicable in any form to finite square or rectangular plates.

Talimi [10] has been able to solve the problems of rocking and translational oscillations of a rigid circular cylindrical pier embedded in an elastic half space. Parmelee [11], and Wilson [12] have obtained solutions using a high-speed computer for specific two dimensional cases using lumped-parameter models and finite elements.

The response of an infinitely long foundation having a circular cross section and subjected to shear waves with partial motion in the direction of the long axis of the foundation has been obtained by Luco [17] and Trifunic [18]. Results for the case of a semi-elliptical cross section have been presented by Wong [19]. An integral equation approach for foundations of arbitrary cross section and numerical results for the partial case of a rectangular cross section have been presented by Wong [19]. Oien [20] obtained the response of a plate strip foundation subjected to Raleigh waves.

The translational and torsional response of a circular foundation, supported on an elastic half space and subjected to plane non-vertically incident shear waves has been studied by Kobori [21]. The torsional response of a circular foundation to non-vertical incident shear waves has also been studied by Luco [22]. Tani and Lguchi [23] and Scanlan [24] have obtained approximate values for the response of rectangular foundations subjected to non-vertically incident waves. Finally

Dominguez [26] has obtained the response of a rigid foundation of rectangular shape embedded in an uniform half space.

All of the above solutions are based on the assumption that the foundation is "welded" to the soil. It implies that tensile stresses in the soil/foundation interface can be developed under large seismic loadings. In reality, such tensile pressures cannot develop at the interface. When the stresses at the interface tend to be tensile, a portion of the foundation will separate from ground (foundation uplift). At that moment, the contact stresses at the soil foundation interface will be "redistributed." The magnitude of the SSI system forces must be changed when lift off occurs. By investigating seismic induced rocking motion, Meet [13] was first to recognize the effect of foundation lift off and the performance of seemingly unstable structures during an earthquake. Experiments [16] on steel building frames with column uplift during vibration demonstrated that column uplift, occurring under an extreme earthquake, would have a considerable effect on the response of the structure. A simple model was recently studied in [4], in which the lumped parameter analysis method was modified by representing the typical lumped soil-structure interaction springs and dampers with equivalent models distributed over the area of the structure foundation. The distributed springs and dampers were then modified so that they can only transmit compressive stresses. Important differences were found for the rocking and vertical motion between the results obtained considering and neglecting lift off.

In this dissertation, it is intend to investigate the influence of lift off on soil-structure interaction during an earthquake by using two different models. One is the discrete model method and another is the continuum mechanics method. With both methods, it is assumed that 1.) the free field motion is directly used as input; 2). the foundation is rigid and rests on or is embedded in an elastic half space.

In the first case, Wolf's discrete model [1] is modified in a manner similar to [4]. This is an improvement over the work in [4] since Wolf's model has more

parameters than that was used in [4] and has the ability to dissipate energy during impact of the foundation with the soil. Chapter 2 briefly introduces Wolf's discrete model. Wolf presented a discrete model, as shown in Fig.(2.1), to perform a time domain analysis of the response of an embedded structure. The structure is assumed to be a rigid cylinder with mass that is supported from a rigid base. A vertical spring/damper, a rocking spring/damper and a horizontal spring and damper placed at different heights models the SSI effects. A virtual additional mass, representing the soil's behavior, is connected to the foundation node through a damper acting in the vertical direction. An additional rocking mass is connected with a rocking damper to the base. All these parameters are frequency independent. This model is semi-empirical. It is based on a semi-infinite truncated cone model of the soil whereby, after enforcing a match with the static stiffness, the remaining parameters are modified to achieve an optimal fit of the dynamic-stiffness coefficients in the frequency domain.

Chapter 3 is devoted to developing a discrete lift off model. Wolf's model is converted into a lift off model in a manner similar to Miller [4]. Since lift off has little effect on the horizontal direction response of the foundation, Wolf's coefficients for the horizontal spring/damper are directly used in the lift off model. However, the coefficients in the vertical and rocking directions are modified, since the contact area between foundation and soil will change at each time step as varying degrees of liftoff occurs. The main idea is to distribute the lumped parameters from Wolf's discrete model over the foundation area, and then, assuming that the distributed spring/damper model can only transmit compression pressure. During the earthquake, the mass, spring and dampers in the tensile area are omitted. In order to make the distributed parameter model match the no lift off model, It is necessary to add a lumped spring, damper, and mass at the center of the base.

A computer program code is developed for this discrete lift off model and it is

described in Chapter 3. The equations of motion are integrated in the time domain using the Wlson-θ method. Chapter 4. gives several examples of results obtained with the discrete lift off model developed in Chapter 3. Two sets of experimental data are used to compare with the results predicted by the lift off model. The first one, Simquake II [29], was performed on June 2 ,1977 at the University of New Mexico. The test was conducted by the Civil Engineering Research Facility of the University for the Electric Power Research Institute. The structure was a scale model of a reactor containment building. The second set of experimental data comes from a large scale model containment (Taiwan Seismic Experiment [30]) placed in a region of high seismicity in Taiwan. This work was sponsored by the Electric Power Research Institute and Taiwan Power Company.

In Chapter 5, a variation of parameters study is performed to evaluate the significance of lift off. First, the peak acceleration required to cause lift off are determined. Many parameters ,such as the position of the structure's center of gravity, depth of embedment, and frequency of the system, effect this peak acceleration. Second, the significance of including lift off effects considering lift off in the soil structure interaction are investigated Comparisons are made for response spectra generated for cases including lift off and neglecting lift off.

In the second part of the thesis, a continuum mechanics method is developed to investigate the effects of lift off. This model is also used to evaluate the validity of the discrete lift off model that is developed in part 1. The foundation is treated as rigid and divided into strips. Influence functions are developed by integrating known solution of the response of an elastic half space to unit pulses in the horizontal and vertical directions. The interaction force at each strip is treated as the unknown at each time step and a set of simultaneous equations developed based on the equations of motion of the structure and the compatibility condition at the soil/structure interface. The soil motion is the sum of the seismic input plus the effects of the interaction forces which locally perturb the free field motion. These simultaneous equations are solved for the interaction forces.

In Chapter 6 several assumptions are made to simplify the soil structure interaction system. The compatibility and equilibrium equations of motion are then established. Chapter 7 deals with the computation of the horizontal and vertical displacements in an elastic half space due to unit pulses. In this Chapter, Perkeris [6] and Chao [7] 's solution are used to compute the displacements when a pulse is applied on the surface of an elastic half space. The Perkeris solution gives the horizontal and vertical displacement in an elastic half space at time(t) caused at a distance (r) by a step vertical force applied at time (t_o); Similar to this, Chao's solution gives the horizontal and vertical displacement caused by a horizontal step load. The sensitivity of results to the time step, special discretion of foundation and the explicit form of unit pulse solution are considered.

Chapter 8 introduces the numerical technique, A fourth order Runge-Kutta numerical integration scheme is introduced in Chapter 8 to solve the equations derived in Chapter 6. A computer program for this model is developed. Sensitivity studies are performed considering the size of the elements used to model the foundation and the effects of different time steps used in the numerical solution. It will be seen that the pressure values converge to a fixed value as the time increment Δt and the width Δx become smaller.

In Chapter 9 the validity of this model is evaluated. Similar to Chapter 4, the dynamic stiffness coefficients are computed and studied. Several examples of analysis by this mode are given in this Chapter. The comparisons are made with the results predicted by both the discrete model and the continuum mechanics method when lift off is neglected or considered. The lift off effect on the soil structure interaction process is evaluated by this model. The pressures and accelerations in the foundation are computed and studied when lift off occurs. Chapter 10 gives some conclusions and suggestions .

Chapter 2
Discrete Model Neglecting Lift Off

2.1 Wolf's Discrete Model

The soil/structure interaction (SSI) solutions, discussed in Chapter 1, generally require the solution of coupled integral equations to obtain numerical results. These results are therefore often simplified by obtaining "equivalent' models which yield comparable results over the frequency ranges of interest. These equivalent models usually are constructed with spring/dashpot elements. One of these equivalent models has been developed by Wolf [1]. This model is modified in Chapter 3 of this thesis to accommodate liftoff effects. Wolf's original model is described in this Chapter.

Consider a cylindrical structure of radius (R), height (H), and embedded in an elastic half space by an amount (e) as shown in Fig. (2.1). The elastic half space has a shear modulus (G), Poisson's ratio (m), and mass density (r). The structure has a mass (M_S), and rotary inertia (J_S) about the structure's center of gravity, located a distance (Z_O) above the base. Wolf developed the model shown on Fig. 2.2 connecting the structure to the free field to model SSI effects. The structure is coupled to the soil: vertically through the spring and dashpot (K_V, C_V); horizontally through the spring and dashpot (K_h, C_h); and rotationally through the spring and dashpot (K_r, C_r). Additional masses (M_{OV}, M_{Oh}, J_O) are attached to the foundation to represent the soil
mass vibrating with the foundation in the vertical, horizontal, and rotational directions respectively. The masses (M_1, and J_1) are attached to the foundation through the dampers (C_{1V}, and C_{1r}) to model the energy that is radiated from the structure to the soil as the structure vibrates.

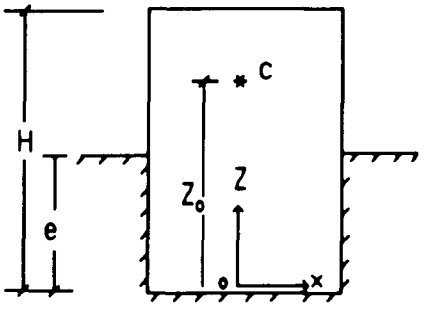

FIG (2.1) EMBEDDED STRUCTURE

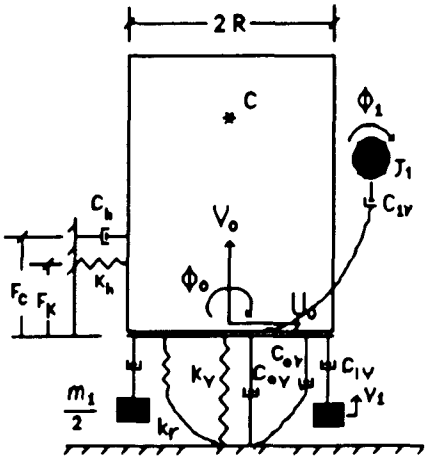

FIG (2.2) DIICRETE MODEL

Wolf developed the following expressions for these SSI parameters by fitting the static stiffness and obtaining best fits to the frequency dependent solutions obtained by rigorous treatment of the SSI problem.

$$K_h = \frac{8GR}{(2-\mu)}\left(1 + \frac{e}{R}\right) \qquad (2.1)$$

$$K_v = \frac{4GR}{(1-\mu)}\left(1 + 0.54\frac{e}{R}\right) \qquad (2.2)$$

$$K_r = \frac{8GR^3}{3(1-\mu)}\left[1 + 1.3\frac{e}{R} + \left(\frac{e}{R}\right)^3\right] \qquad (2.3)$$

$$C_{oh} = \frac{R\,K_h}{c_s}\left[0.68 + 0.57\sqrt{\frac{e}{R}}\right] \qquad (2.4)$$

$$C_{or} = \frac{R\,K_r}{c_s}\left[0.16\,\frac{e}{R}\right] \qquad (2.5)$$

$$C_{1r} = \frac{R^3 K_r}{c_s}\left[0.40 + 0.03\left(\frac{e}{R}\right)^2\right] \tag{2.6}$$

$$C_{ov} = \frac{R\,K_v}{c_s}\left[0.85 + 0.35\left(\frac{e}{R}\right)\right] \tag{2.7}$$

$$C_{1v} = \frac{R\,K_v}{c_s}\left[0.32 - 0.001\left(\frac{e}{R}\right)\right] \tag{2.8}$$

$$M_{oh} = \frac{R^2 K_h}{c_s^2}\mu_{oh} \tag{2.9}$$

$$J_o = \frac{R^2 K_r}{c_s^2}\mu_{or} \tag{2.10}$$

$$M_{ov} = \frac{R^2 K_v}{c_s^2}\mu_{ov} \tag{2.11}$$

$$J_1 = \frac{R^2 K_r}{c_s^2}\mu_{1r} \tag{2.12}$$

$$M_1 = \frac{R^2 K_r}{c_s^2}\mu_{1v} \tag{2.13}$$

in which,

$$\mu_{oh} = 0 \tag{2.14}$$

$$\mu_{or} = 0 \tag{2.15}$$

$$\mu_{ov} = 0 \tag{2.16}$$

$$\mu_{1r} = 0.33 + 0.1\left(\frac{e}{R}\right)^2 \tag{2.17}$$

$$\mu_{1v} = 0.38 \tag{2.18}$$

in whoch

$c_s = \sqrt{\frac{G}{\rho}}$, wave velocity

2.2 Assumptions

In order to analyze the response of the system during an earthquake by using this discrete model, the following assumptions are made:

1. A rigid structure is embedded into an elastic homogeneous half space.
2. The structure is "welded" to the soil, that is, tensile stresses can develop between the foundation and soil.
3. All of the parameters of the system are independent of frequency.
4. Free field surface motions are used directly as input to the dynamic system.

2.3 The Equilibrium Equations of Motion

From Fig (2.2), the system has five degree of freedom so that five equilibrium equations of motion must be established to analyze the responses of this system during an earthquake. As shown in Fig (2.1) and Fig (2.2), V_o, U_o are the displacements at the center of the foundation in the vertical and horizontal directions respectively; and ϕ_o is the rotation of the structure (measured about the base); V_1 and ϕ_1 correspond to the vertical displacement of mass M_1 and the rotation of mass J_1 respectively. If the accelerations of the ground motion are X_h and X_v in the horizontal and vertical directions respectively, the total kinetic energy of the system is

$$T = \frac{1}{2}M_h(\dot{U} + Z_o\dot{\phi}_o)^2 + \frac{1}{2}J\dot{\phi}_o^2 + \frac{1}{2}J_1\dot{\phi}_1^2 + \frac{1}{2}M_v\dot{V}_o^2 + \frac{1}{2}M_1\dot{V}_1^2 \qquad (2.19)$$

and the potential energy of the system is

$$P = \frac{K_h}{2}(U + F_k\phi_o)^2 + \frac{K_r}{2}\phi_o^2 + \frac{K_v}{2}V_o^2 \qquad (2.20)$$

If a set of virtual displacements δU, $\delta \phi_0$, $\delta \phi_1$, δV_0 and δV_1 are imposed on each of the generalized coordinates U, ϕ_0, ϕ_1, V_0, and V_1 the virtual work done is

$$W_{nc} = -M_h \ddot{X}_h \delta u - M_v \ddot{X}_v \delta v_o - C_h (\dot{U} + F_c \dot{\phi}_o) \delta u$$
$$- [C_{ov} \dot{V}_o + C_{1v} (\dot{V}_o - \dot{V}_1)] \delta v_o - C_{1v} (\dot{V}_1 - \dot{V}_o) \delta v_1$$
$$- (C_{or} \dot{\phi}_o + F_c C_h \dot{U}) \delta \phi_o - C_{1r} (\dot{\phi}_o - \dot{\phi}_1) \delta \phi_o - C_{1r} (\dot{\phi}_1 - \dot{\phi}_o) \delta \phi_1 \qquad (2.21)$$

Using Lagrange's equation

$$\frac{\partial}{\partial t} \left(\frac{\partial T}{\partial \dot{q}_i} \right) - \frac{\partial T}{\partial q_i} + \frac{\partial P}{\partial q_i} = Q_i \qquad (2.22)$$

where, q_i (i= 1, 2, $\cdots$ 5) are generalized coordinate, specialy for this system they are: U, ϕ_o , ϕ_1 , V_o , V_1 .

$$Q_1 = -M_h \ddot{X}_h - C_h (\dot{U} + F_c \dot{\phi}_o) \qquad (2.23)$$

$$Q_2 = -C_{or} \dot{\phi}_o - F_c C_h \dot{U} - C_{1r} (\dot{\phi}_o - \dot{\phi}_1) \qquad (2.24)$$

$$Q_3 = -C_{1r} (\dot{\phi}_1 - \dot{\phi}_o) \qquad (2.25)$$

$$Q_4 = -M_v \ddot{X}_v - [C_{ov} \dot{V}_o + C_{1v} (\dot{V}_o - \dot{V}_1)] \qquad (2.26)$$

$$Q_5 = - C_{1v} (\dot{V}_1 - \dot{V}_o) \qquad (2.27)$$

Finally, the equilibrium equations of motion for the discrete model system are

$$M_h(\ddot{U} + Z_o\ddot{\phi}_o) + C_h(\dot{U} + F_c\dot{\phi}_o) + K_h(U + F_h\phi_o) = -M_h\ddot{X}_h \qquad (2.28)$$

$$J\ddot{\phi}_o + M_h(\ddot{U} + Z_o\ddot{\phi}_o)Z_o + C_h F_c\dot{U} + C_{or}\dot{\phi}_o + C_{1r}(\dot{\phi}_o - \dot{\phi}_1) + K_r\phi_o + K_h(U + F_k\phi_o)F_k = 0 \qquad (2.29)$$

$$J_1\ddot{\phi}_1 + C_{1r}(\dot{\phi}_1 - \dot{\phi}_o) = 0 \qquad (2.30)$$

$$M_v\ddot{V}_o + C_{ov}\dot{V}_o + (\dot{V}_o - \dot{V}_1)C_{1v} + K_v V_o = -M_v\ddot{X}_v \qquad (2.31)$$

$$M_1\ddot{V}_1 + (\dot{V}_1 - \dot{V}_o)C_{1v} = 0 \qquad (2.32)$$

in which,

$M_h = M_S + M_{oh}$

$M_v = M_S + M_{ov}$

$J = J_S + J_O$

M_S and J_S are the mass and mass moment of inertia for the structure. The other coefficients of these equations given in Section 2.1.

The equations from (2.10) to (2.14) can be expressed in matrix notation as,

$$[M]\{\ddot{U}\} + [C]\{\dot{U}\} + [K]\{U\} = \{P\} \qquad (2.33)$$

in which,

$$[M] = \begin{bmatrix} M_h & Z_o M_h & & & \\ Z_o M_h & J + Z_o^2 M_h & & & \\ & & J_1 & & \\ & & & M_v & \\ & & & & M_1 \end{bmatrix} \tag{2.34}$$

$$[C] = \begin{bmatrix} C_h & F_c C_h & & & \\ F_c C_h & C_{or} + C_{1r} & -C_{1r} & & \\ & -C_{1r} & C_{1r} & & \\ & & & C_{ov} + C_{1v} & -C_{1v} \\ & & & -C_{1v} & C_{1v} \end{bmatrix} \tag{2.35}$$

$$[K] = \begin{bmatrix} K_h & F_k K_h & & & \\ F_k K_h & K_r + F_k^2 K_h & & & \\ & & 0 & & \\ & & & K_v & \\ & & & & 0 \end{bmatrix} \tag{2.36}$$

where,

$$\{\ddot{U}\} = [\ \ddot{U}\ ,\ \ddot{\phi}_o\ ,\ \ddot{\phi}_1\ ,\ \ddot{V}_o\ ,\ \ddot{V}_1\ ]^T \tag{2.37}$$

$$\{\dot{U}\} = [\ \dot{U}\ ,\ \dot{\phi}_o\ ,\ \dot{\phi}_1\ ,\ \dot{V}_o\ ,\ \dot{V}_1\ ]^T \tag{2.38}$$

$$\{U\} = [\ U\ ,\ \phi_o\ ,\ \phi_1\ ,\ V_o\ ,\ V_1\ ]^T \tag{2.39}$$

$$\{P\} = -[M_h \ddot{X}_h, 0\ ,\ 0\ ,M_v \ddot{X}_v\ ,\ 0\ ]^T \tag{2.40}$$

Chapter 3
Discrete Lift Off Model

3.1 Introduction

The large lateral loads acting on a structure during an earthquake may lead to a substantial overturning moment. It is possible for these moments to result in tensile forces occurring at the soil/structure interface based on a linear,"welded" model as discussed in previous Chapter. Since tension is incompatible with the constitutive law of soil, the base mat will become partially separated and corresponding shear stresses (friction) can occur in the area of contact. A model for analyzing soil structure interaction including the effects of partial lift off is derived. The model is developed by distributing the lumped parameters (springs/dampers and masses) of wolf's discrete model over the foundation area.

For example, as shown in Fig(3.1) a, K_v and K_r are the vertical and rocking spring interaction coefficients from Wolf's discrete model, and are modeled with a foundation modulus k. The concentrated parameters(K_v^* and K_r^*) are added so that the vertical and rocking stiffness of the two models may be equaled. These three values k, K_v^* and K_r^* are illustrated in Fig (3.2) (1), (2), and (3). Similarly, the other parameters C_0, C_1, M_0, M_1 ,J_0

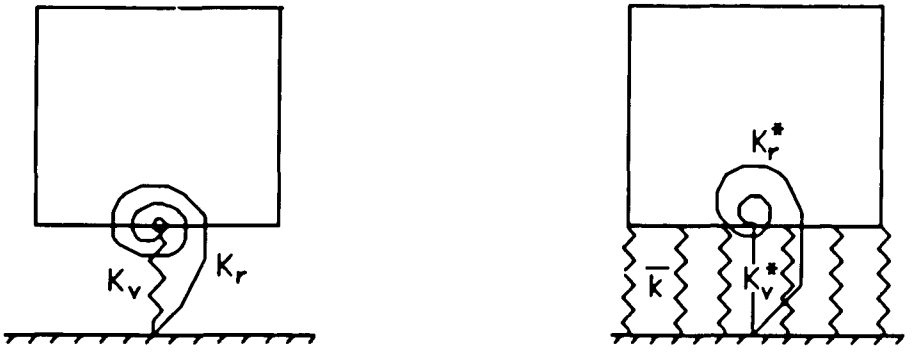

a) WELDED MODEL b) LIFT OFF MODEL

FIG. (3.1) DISTRIBUTED PARAMETERS

and J_1 can also be distributed over the foundation base as shown in Fig (3.2). Fig (3.2) (1) illustrates a set of distributed parameters at each point of the foundation base. Two sets of lumped parameters in the center of base are shown in Fig (3.2) (2) and (3).

Two distributed models are developed in this Chapter. In the first, the parameter is uniformly distributed over the foundation and in the second, the parameters have a parabolic distribution.In section 3.2, the uniformly distributed parameters will derived from Wolf's model. The equations of equilibrium of motion developed in Chapter 2 are modified. Since the coefficients of the stiffness,damper and mass vary with time step due to lift off, these equations of motion are no longer

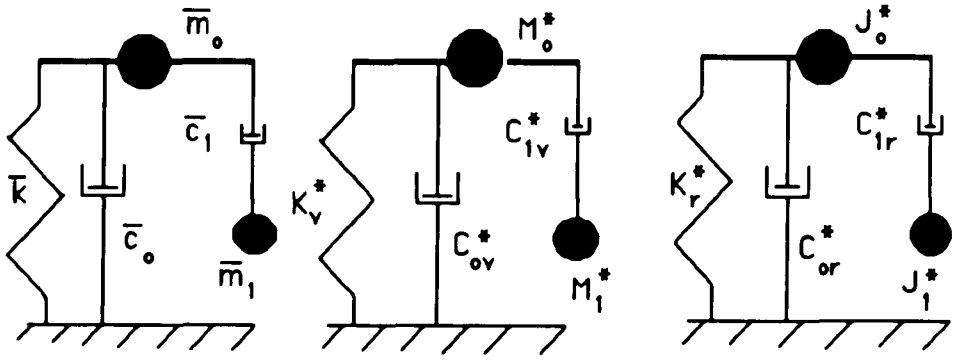

(1) typical distributed parameters

(2)vertical concentrate model at center

(3) rocking concentrate model at center

FIG (3.2) THE DETAIL OF LIFT OFF MODEL

linear. The parabolic parameter distribution model is introduced in section 3.3. Section 3.4 briefly introduces a computer code for analyzing this lift off influence on soil structure interaction. The Wilson-θ integration method is used to solve the nonlinear equations.

3.2 Uniformly Distributed model

According to the analysis in reference [4], lift off has only a small effect on the base horizontal motion. Therefore, the parameters of the spring/damper and mass in the horizontal direction can be used for the lift off model without any modification.

The distributed vertical spring value k is found from the distributed the lumped spring values (K_v and K_r) given in Chapter 2. Since either the vertical or rocking set of springs cannot completely determines the springs, the additional single vertical spring K_v^* and rocking spring K_r^* are required to be placed at the center of the base to complete the model. The total forces in the spring of the discrete model must be equivalent to that of lift off model. Foundation module (K_v and K_r) are derived to match the lumped parameter model and combined with a parameter (α) to the model foundation modulus (k) as follows:

For the equivalency between lift off and "welded" model a concentrated vertical and a rocking spring must be placed in the center of base as shown in Fig (3.1) . The values of these parameters are as following:

$$\bar{k}_v = \frac{K_v}{\pi R^2} = \frac{4G}{\pi R(1-\mu)}\left[1+0.54\left(\frac{e}{R}\right)\right] \qquad (3.1)$$

$$\bar{k}_r = \frac{4K_r}{\pi R^4} = \frac{32G}{3\pi R(1-\mu)}\left[1+1.3\left(\frac{e}{R}\right)+0.58\left(\frac{e}{R}\right)^3\right] \qquad (3.2)$$

$$\bar{k} = \bar{k}_v + \alpha(\bar{k}_r - \bar{k}_v) \qquad (0 \leq \alpha \leq 1) \qquad (3.3)$$

$$K_v^* = K_v - \pi R^2 \bar{k} \qquad (3.4)$$

$$K_r^* = K_r - \frac{\pi R^4}{4}\bar{k} \qquad (3.5)$$

Plots of the distributed and lumped parameters are shown in Fig (3.3) and (3.4), and (3.5). From Fig (3.3), the uniform vertical spring value k is always positive and increases with α value ; the value K_v^* and K_r^* as shown in Fig (3.4) and Fig (3.5) respectively decrease with value α, but K_v^* is negative for all positive values of(α). To avoid negative spring rates, α is taken to be 0.

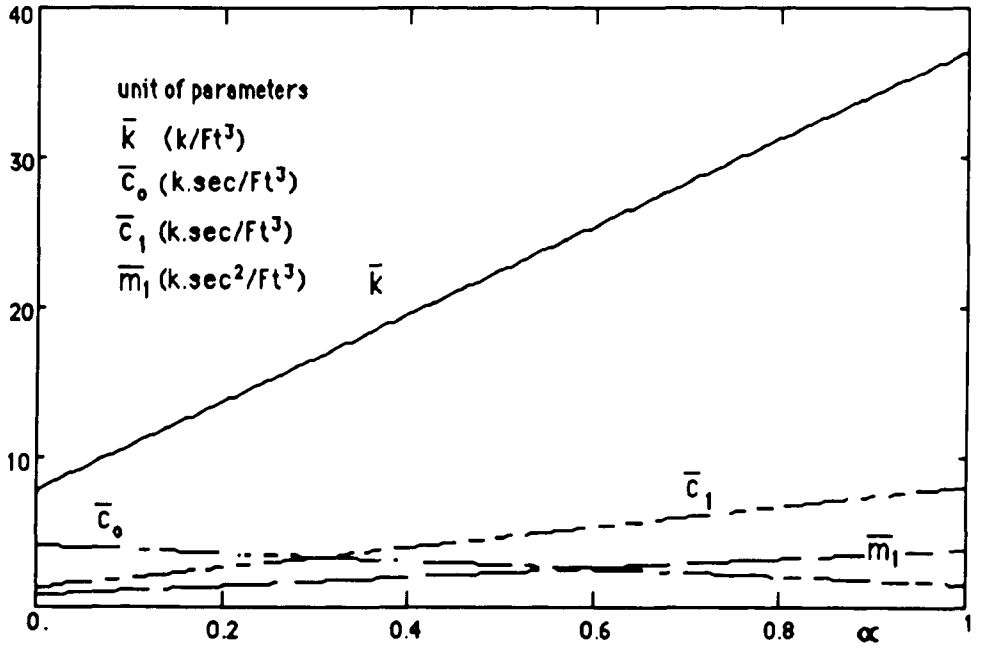

FIG (3.3) DISTRIBUTED PARAMETERS VARY WITH α

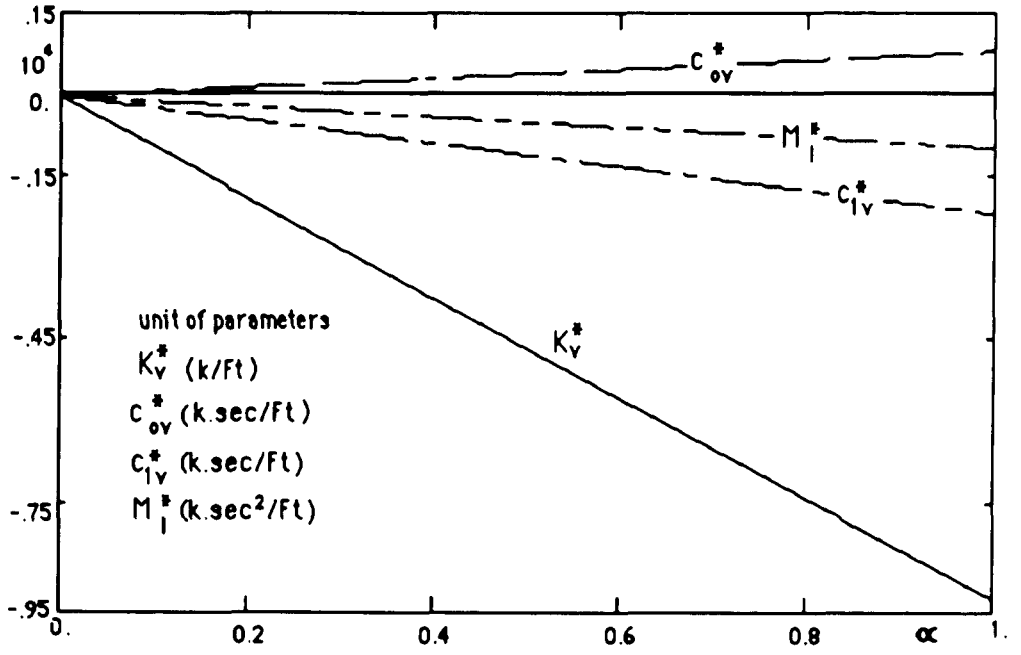

FIG (3.4) CONCENTRATE VERTICAL PARAMETERS VARY WITH α

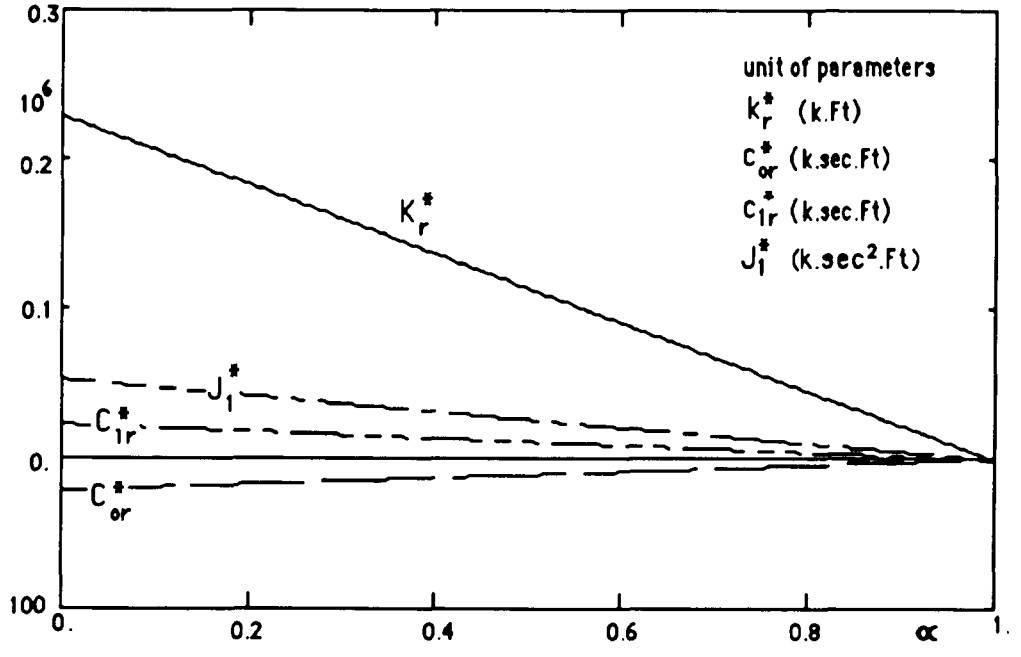

FIG(3.5) CONVENTRATE ROCKING PARAMETERS VARY WITH α

Therefore, the final modified parameters of the spring are:

$$\bar{k} = \bar{k}_v = \frac{4G}{\pi R(1-\mu)}\left[1+0.54\left(\frac{e}{R}\right)\right] \tag{3.6}$$

$$K_v^* = 0 \tag{3.7}$$

$$K_r^* = \frac{GR^3}{1-\mu}\left[1.67+5.59\left(\frac{e}{R}\right)+0.58\left(\frac{e}{R}\right)^3\right] \tag{3.8}$$

Similarly, the magnitudes of dampers and masses for the lift off model are

$$\bar{c}_1 = \frac{G}{\pi R(1-\mu)}\left[1.28+0.69\left(\frac{e}{R}\right)-0.01\left(\frac{e}{R}\right)^4-0.022\left(\frac{e}{R}\right)^5\right] \tag{3.9}$$

$$C_{1v}^* = 0 \tag{3.10}$$

$$C_{1r}^* = \frac{GR^3}{\pi c_s(1-\mu)}\left[1.39+2.63\left(\frac{e}{R}\right)+0.08\left(\frac{e}{R}\right)^2+0.8\left(\frac{e}{R}\right)^3-0.0025\left(\frac{e}{R}\right)^4 +0.0124\left(\frac{e}{R}\right)^5\right] \tag{3.11}$$

$$\bar{m}_1 = \frac{G}{\pi c_s^2(1-\mu)}\left[1.52+2.16\left(\frac{e}{R}\right)\right] \tag{3.12}$$

$$M_1^* = 0 \tag{3.13}$$

$$J_1^* = \frac{GR^5}{c_s^2(1-\mu)}\left[1.26+1.5\left(\frac{e}{R}\right)+0.267\left(\frac{e}{R}\right)^2 1.12\left(\frac{e}{R}\right)^3+0.155\left(\frac{e}{R}\right)^4\right] \tag{3.14}$$

Since C_{or} is negative for value ($\alpha<1$) as shown in Fig (3.5), ($\alpha=1$) must be used for the distribution of the dampers, and;

$$\bar{c}_o=\frac{G}{\pi R(1-\mu)}\left[1.7\left(\frac{e}{R}\right)+3.93\left(\frac{e}{R}\right)^2+0.99\left(\frac{e}{R}\right)^4\right] \tag{3.15}$$

$$C^*_{ov}=\frac{GR}{\pi c_s(1-\mu)}\left[3.2+3.129\left(\frac{e}{R}\right)-0.056\left(\frac{e}{R}\right)^2-0.062\left(\frac{e}{R}\right)^4\right] \tag{3.16}$$

$$C^*_{or}=0 \tag{3.17}$$

in which,

k, c_o, c_1, m are distributed parameters corresponding spring, damper,additional damper and additional mass.

K_v^*,K_r^* are the concentrated spring at the center of foundation base.

C_{ov}^*,C_{or}^* are the concentrated damper at the center of foundation base.

M_1^*,J_1^* are the additional mass and mass moment of inertia after lift off.

C_{1v}^*,C_{1r}^* are the additional damper in vertical and rocking direction respectively after lift off.

3.3 Alternative Model For Parameter Distribution

Another model for distributing the parameters of the lumped model is introduced in this section. The distributed parameters are assumed to vary in a parabolic manner along x direction as shown in Fig (3.6).

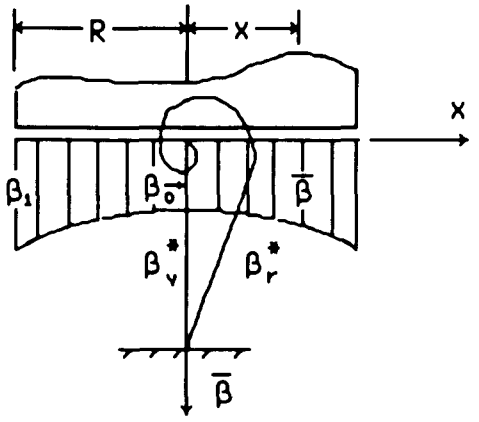

Fig(3.6) Parabolic Distribute model

If β_1 and $\beta_o = \theta\ \beta_1$ (θ from o to 1) are the values of the vertical distributed parameters at the edge and the center of the foundation respectively, the value inside the base should be

$$\overline{\beta} = \beta_1 [\theta - (\theta - 1)\frac{x^2}{R^2}] \tag{3.18}$$

In order to match the no lift off condition, a concentrate vertical and rocking parameter must be placed in the center of the foundation base as shown in Fig (3.6),and the expressions for these conditions are

$$\beta_v^* = \beta_v - \int_A \overline{\beta}\ dA = \frac{3}{4}\beta_v(1-\theta) \tag{3.19}$$

$$\beta_r^* = \beta_r - \int_A \overline{\beta}\ x^2\ dA = \beta_r - \frac{\beta_v}{32}(7\theta+1) \tag{3.20}$$

in which,

$\beta_1 = \beta_V/(\pi R^2)$, A= area of foundation base.

β_V is the distributed parameters based on the lumped vertical parameter

β_r is the distributed parameters based on the lumped rocking parameter For the

spring, $\beta_1 = K_v/(\pi R^2)$, the modified springs should be

$$\bar{K} = \frac{K_v}{\pi R^2}\left[\theta-(\theta-1)\frac{x^2}{R^2}\right] \tag{3.21}$$

$$K_v^* = \frac{3}{4} K_v (1-\theta) \tag{3.22}$$

$$K_r^* = K_r - \frac{R^2 K_v}{32}(7\theta+1) \tag{3.23}$$

Similarly, we can get the expression for the dampers and mass as follows:

$$\bar{C}_o = \frac{C_{ov}}{\pi R^2}\left[\theta-(\theta-1)\frac{x^2}{R^2}\right] \tag{3.24}$$

$$C_{ov}^* = \frac{3}{4} C_{ov}(1-\theta) \tag{3.25}$$

$$C_{or}^* = C_{or} - \frac{R^2 C_{ov}}{32}(7\theta+1) \tag{3.26}$$

$$\bar{C}_1 = \frac{C_{1v}}{\pi R^2}\left[\theta-(\theta-1)\frac{x^2}{R^2}\right] \tag{3.27}$$

$$C_{1v}^* = \frac{3}{4} C_{1v}(1-\theta) \tag{3.28}$$

$$C_{1r}^* = C_{1r} - \frac{R^2 C_{1v}}{32}(7\theta+1) \tag{3.29}$$

$$\bar{M} = \frac{M_1}{\pi R^2}\left[\theta-(\theta-1)\frac{x^2}{R^2}\right] \tag{3.30}$$

$$M_1^* = \frac{3}{4} M_1 (1-\theta) \tag{3.31}$$

$$J_1^* = J_1 - \frac{R^2 M_1}{32}(7\theta+1) \tag{3.32}$$

Plots of these parameters as function of θ are shown in Fig (3.7) (3.8) and (3.9). As shown in these figures, all of parameters except C_{01}^* are positive when θ varies from 0 to 1. When $\theta < 0.25$ the values of C_{01}^* are also positive.

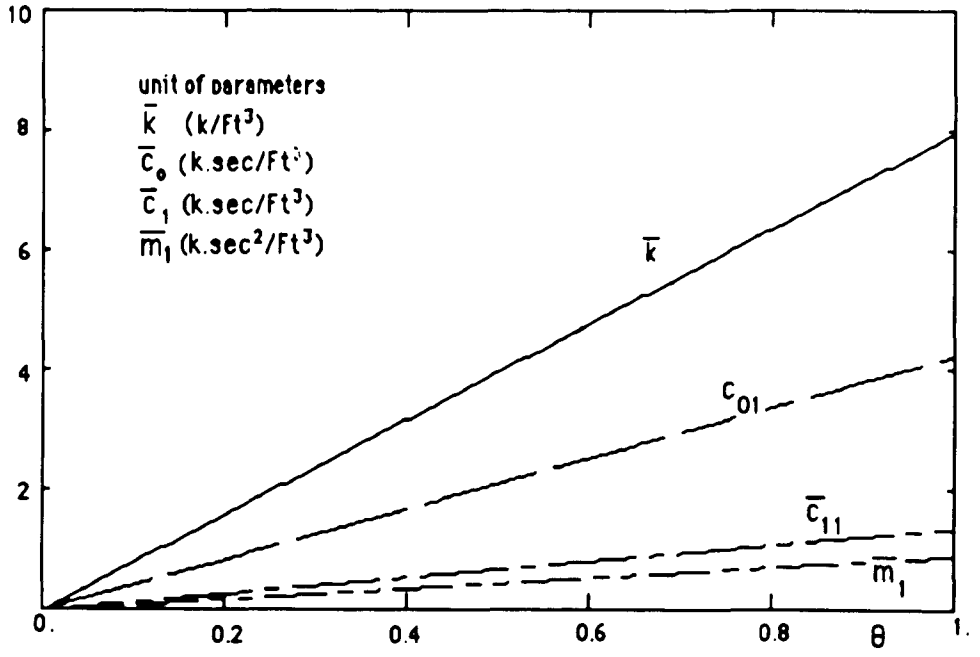

FIG (3.7) DISTRIBUTED PARAMETERS VARY WITH θ (X=0, R=10)

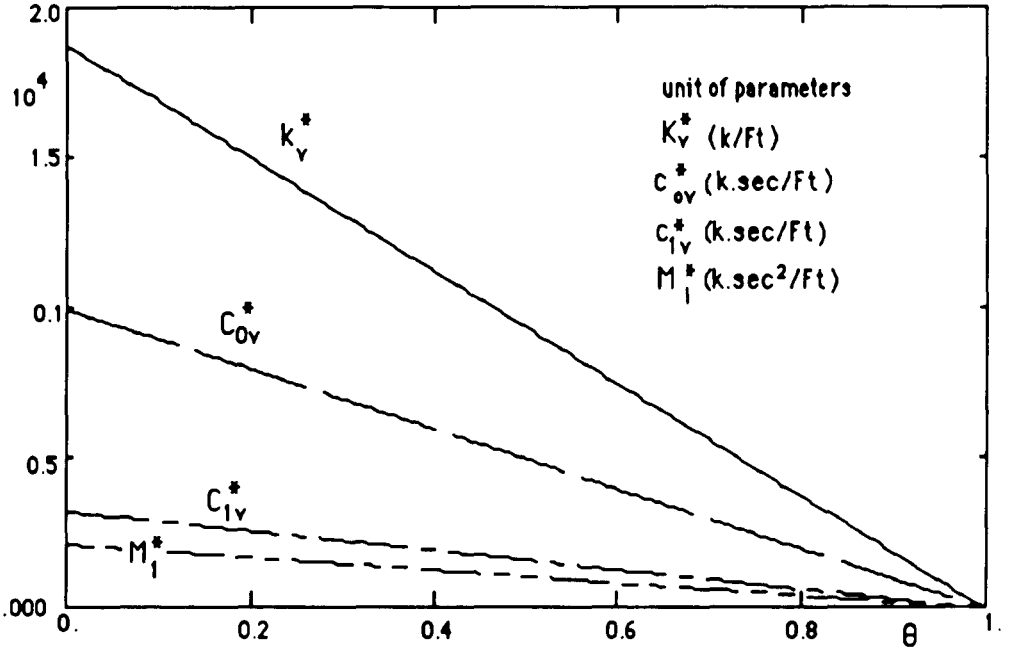

FIG (3.8) VERTICAL CONCENTRATE PARAMETERS VARY WITH θ (X=0, R=10)

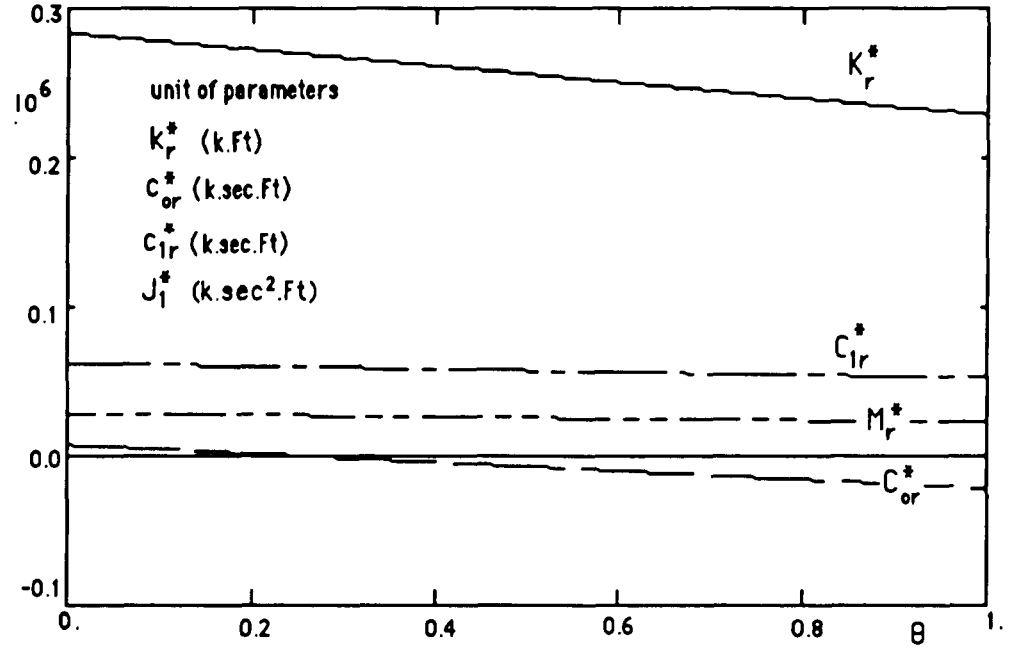

FIG (3.9) ROCKING CONCENTRATE PARAMETERS VARY WITH θ (X=0, R=10)

As shown in Fig (3.7), (3.8), and (3.9), all of the parameters for lift off model are positive when $\theta < 2.5$. Therefore valid values of θ are in the range of 0 to 0.25 . A comparison of the results from those two models will be made by calculating the acceleration spectra in following Chapter. It will be seen that the uniformly distributed model has been improved by the parabolic distributed model.

3.4 The Equations of Motion for Lift Off Model

During the response computation, the parameters of the model will be changed in each time step depending on whether lift off has occurred. The equations of motion (2.33) become nonlinear. The coefficient matrixes of this equation $[M]_L$, $[C]_L$, $[K]_L$ change with time. They can be modified from equations (2.34), (2.35), and (2.36) as follows:

$$[M]_L = \begin{bmatrix} M_h & Z_o M_h & & & & \\ Z_o M_h & J_o + Z_o^2 M_h & & & & \\ & & J_{1L} & & & \\ & & & M_v & & \\ & & & & M_{1L} & \end{bmatrix} \qquad (3.34)$$

$$[C]_L = \begin{bmatrix} C_h & F_c C_h & & & & \\ F_c C_h & C_{rL} & -C_{1L} & & & \\ & -C_{1L} & C_{1L} & & & \\ & & & C_{vL} & -C_L & \\ & & & -C_L & C_L & \end{bmatrix} \qquad (3.35)$$

$$[K]_L = \begin{bmatrix} K_h & F_k K_h & & & \\ F_k K_h & K_{rL} & & & \\ & & 0 & & \\ & & & K_{vL} & \\ & & & & 0 \end{bmatrix} \qquad (3.36)$$

in which, the elements of those matrixes are shown with " L " subscript and indicated as:

$$J_{1L} = J_1^* + \int_{A_e} x^2 \, \bar{m}_1 \, dA \qquad (3.37)$$

$$M_{1L} = M_1^* + \int_{A_e} \bar{m}_1 \, dA \qquad (3.38)$$

$$C_{rL} = C_{or}^* + C_{ir}^* + \int_{A_e} (\bar{C}_o + \bar{C}_1) x^2 \, dA \qquad (3.39)$$

$$C_{1L} = C_{1r}^* + \int_{A_e} \bar{C}_1 \, x^2 \, dA \qquad (3.40)$$

$$C_{vL} = C_{ov}^* + C_{1v}^* \int_{A_e} (\bar{C}_o + \bar{C}_1) \, dA \qquad (3.41)$$

$$C_L = C_{1v}^* + \int_{A_e} \bar{C}_1 \, dA \qquad (3.42)$$

$$K_{rL} = F_k^2 K_h + K_r^* + \int_{A_e} \bar{K} \, x^2 \, dA \qquad (3.43)$$

$$K_{vL} = K_v^* + \int_{A_e} \bar{K} \, dA \qquad (3.44)$$

where,

A_θ is the area of foundation base that contact with the soil ground during lift off.

3.5 Computer Solution

In this dissertation, the Wilson-θ direct integrating method (Appendix A) is used to solve the nonlinear equilibrium equation of motion (3.33). The foundation base will be divided into N strips before performing this direct time integration scheme. It is assumed that the stresses over each strip area at a special time step are constant. During an earthquake, the pressures σ acting on each strip are calculated and compared to the pressure σ_g caused by the gravity of the structure. If the pressure σ in a strip is in tension, ie, $\sigma > \sigma_g$, the portion of the structure will be separated from the soil, and the elements of the coefficient matrix of equation (3.33) must be modified. A flow chat of computer code that solves the equation (3.33) is shown in Fig (3.10).

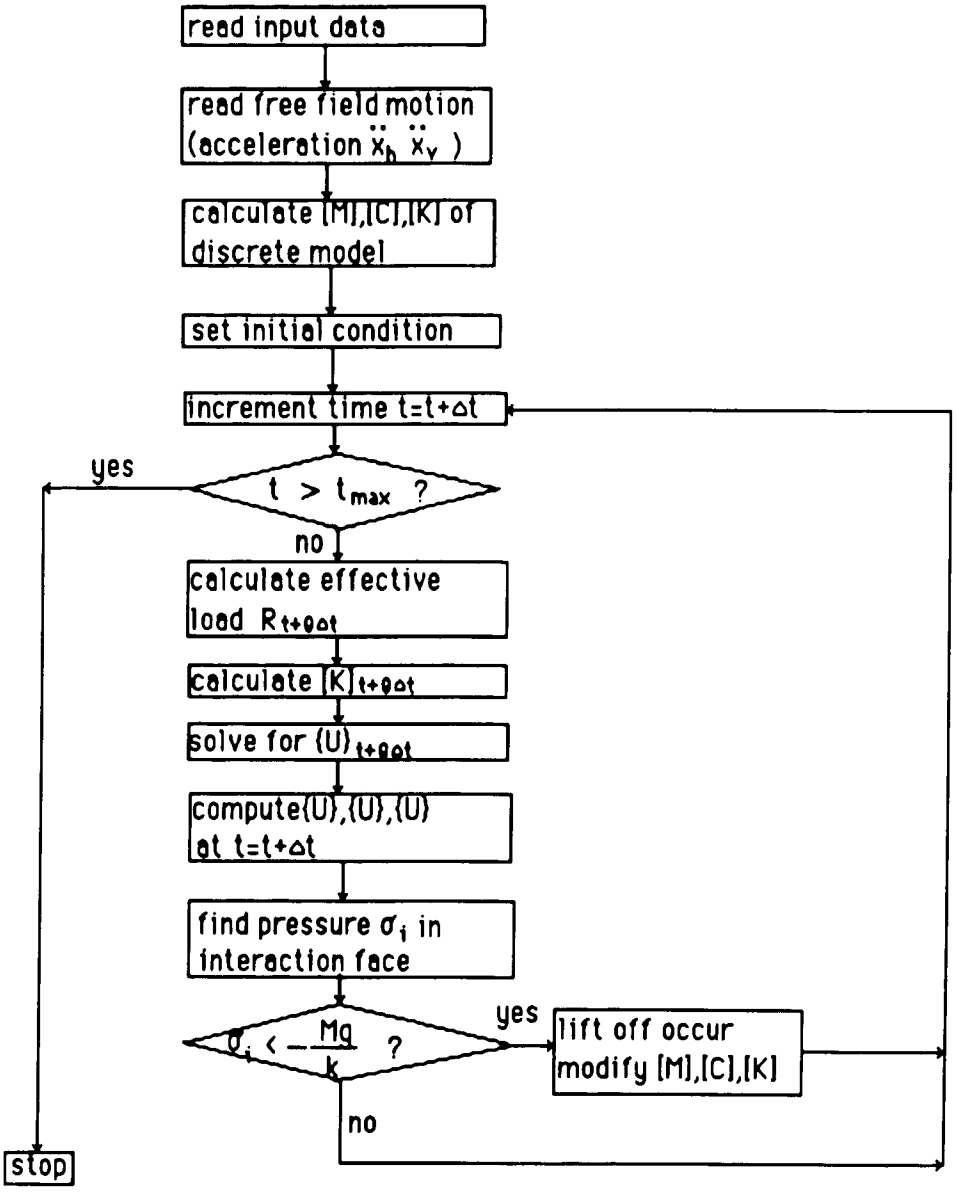

WHERE, k IS THE COEFFICIENT OF VERTICAL SPRING.

θ IS A CONSTANT FROM WILSON - θ METHOD

g IS THE CONSTANT OF GRAVITY

FIG (3.10) COMPUTER CODE FOR DISCRETE LIFT OFF MODEL

Chapter 4
Comparison of Discrete Model With Measured Data

In order to evaluate the validity of the discrete lift off model that was derived in Chapter 3, data obtained from two different experiments are used to compare with the results calculated from the model. The first data were measured during the SIMQUAKE II experiment [29]. The second is from the Taiwan SEISMIC experiment[30]. These experiments are described in Section 4.1 and Section 4.2, and comparisons are made between the measured data and that calculated with the discrete models. Comparisons are made between response spectra derived from the measured responses and spectra of the motions calculated with the discrete model. A final validation of the discrete model is given in Section 4.3. The dynamic stiffness and damping characteristics are computed from the discrete model and compared with a computation made directly from Wolf's model.

4.1 The SIMQUAKE II

The SIMQUAKE II [29] experiment was conducted on June 2, 1977 at the University of New Mexico's McCormick Ranch test site south of Albuquerque, New Mexico. The test was conducted by the Civil Engineering Research Facility of the University for the Electric Power Research Institute. Fig (4.1) and Fig (4.2) show a plan and elevation view taken through the experiment site. The loading was induced with two plane, high explosive arrays each covering a vertical plane about 200 feet wide and 75 feet deep (marked as Back and Front Arrays on Fig. 4.1). The top of the arrays were located about 25 feet below the surface, and separated from each other by 100 feet. The back array was detonated first with the front array detonated about 1.2 seconds later. The resulting free field motion consisted of two principal acceleration peaks with the first having a magnitude of 4 to 5 G's in the vicinity of the test structures.

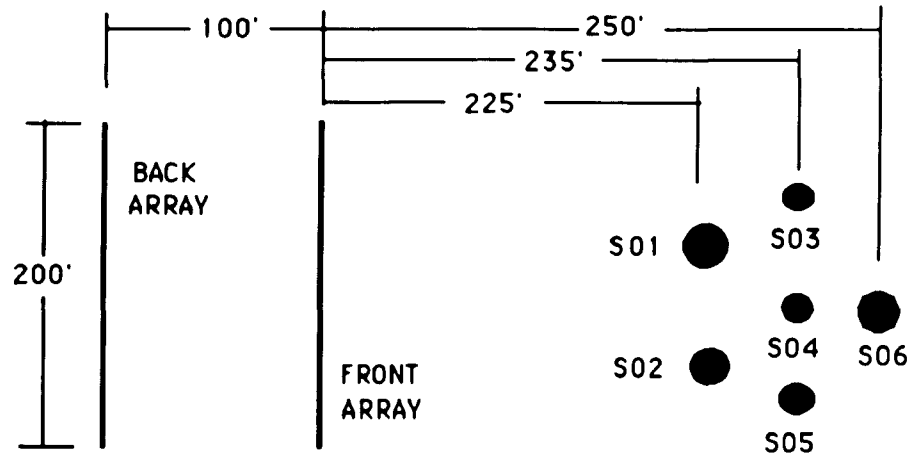

FIG (4.1) PLAN OF SIMQUAKE II EXPERIMENT

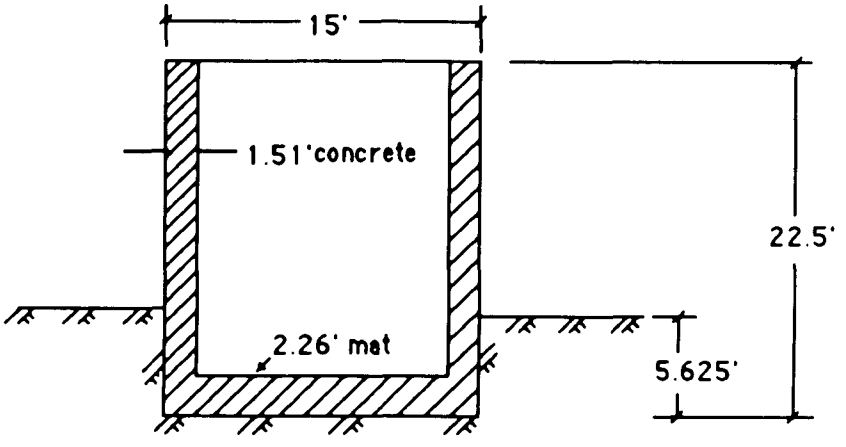

FIG (4.2) SECSION OF STRUCTURE S01

The test area containing the structural models were located about a line normal to the plane of the arrays and originating at the center of the arrays. The closest structure was 225 feet from the front array while the farthest structure was located 250 feet from the front array. Six structures were placed in thetest area. The structures consisted of a concrete cylinder founded on a concrete slab. Steel plates were placed on the surface of the concrete to simulate the reinforcement. Structural frequency of these structures were all over 40 cps. The structures were scale models of reactor containment buildings.

Structure S01 is used for this study and its dimensions are shown as in Fig (4.2). It is a 1/8 scale model and was located at 225 feet from the front array. At this range the peak free field acceleration was 5 G's. The structure may be shown to be rigid so that the only significant flexibilities were associated with the soil structure interaction process. It has a weight of 253.31 kips and the following interaction properties:

Horizontal Frequency	= 25.5 cps
Rocking Frequency	= 10.6 cps
Vertical Frequency	= 20.9 cps
Horizontal Damping	= 37.5 %
Rocking Damping	= 6.8%
Vertical Damping	= 44.1%

There were extensive free field and in - structure measurements taken during the experiments. Vertical free field accelerograms were obtained immediately below the level of the structure. These are used as input to the lift off model. It should be noted that there was relatively little variation of the free field pulse as one moves away from the structure. Horizontal structure acceleration measurements were obtained at the top and bottom of the structure. These are used to valuate the rigid body horizontal and rotational components of the structure response. Vertical base mat measured accelerations are used to obtain the vertical response of the structure.

The response spectra for the horizontal motion at top of structure S01 (include rocking effects), the horizontal motion at the foundation, and the vertical motion, are calculated by using the discrete lift off model that was developed in Chapter 3. The uniform distribution set of parameters is used. Two percent of critical equipment damping is used for all response spectra. The free field motion in the vertical and horizontal direction near the foundation base are used as the input data. In this dissertation, the kinetic interaction part is neglected according to the assumptions in Chapter 2. It should be noted that the input motion is about twelve times that required to cause liftoff so that these effects can be expected to be significant.

Comparisons are made in terms of the three response spectra described above (horizontal at the base, horizontal at the top of the structure, and vertical), as shown in Figure (4.5) through (5.7). Spectra are obtained for the measured data, data generated including liftoff effects, and data generated using Wolf's model but neglecting liftoff effects. For all three spectra the spectra generated from the liftoff model agrees well with the spectra of the measured data. When liftoff is neglected in the model the calculated horizontal spectra at the top of the structure and the vertical spectra do not agree well with the spectra of the measured data indicating that the inclusion of liftoff effects are important.

4.2 Taiwan Seismic Experiment

A large scale soil structure interaction experiment[30] was sponsored by the Electric Power Research Institute (EPRI) and the Taiwan Power Company (Taipower).

A 1/4-scale model containment structure was constructed in Lotung,Taiwan. The structural configuration is shown on Fig.4.3.

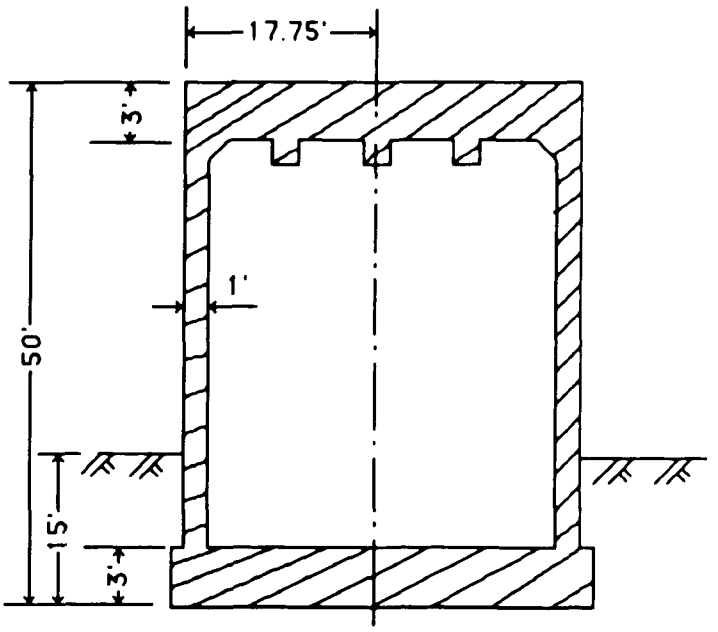

FIG (4.3) THE 1/4-SCALE CONTAINMENT MODEL

Strong motion monitoring instruments were installed in the free field near the model. The free field instrumentation has three linear arrays radiating out approximately 4-1/2 diameters from the 1/4 scale model and two downhole arrays to a depth of approximately 4-1/2 diameters. One of the downhole arrays is adjacent to the model and the other is in line with the outer edge of the surface arrays. Strong motion accelerometers were installed on the bottom and near the top of the 1/4 scale models to record the foundation base mat motion and dynamic structural amplification. As shown in Fig(4.3), the size of the 1/4 scale structure and soil properties are

Weight of the structure	= 1693 kips
Radius of the structure	= 17.75ft
Soil wet density	= 110 pcf
Soil Poisson's ratio	= 0.35

Rigid body SSI frequency:

Rocking	= 6.9 HZ
Horizontal	= 11.4 HZ
Vertical	= 10.7 HZ

The construction of the model structure was completed and data collection began in September 1985. By July 1986, twelve strong earthquakes ranging from Richter magnitude 5.3 to 6.5 had been recorded. The maximum peak ground acceleration of the record used for this study was 0.18 G.

Comparisons of spectra computed from predicted and measured and measured accelerations are made for a gage location at the top of the structure (F4U) and the bottom of the structure. The spectra, in each of three directions, for the upper location are shown on Figs. 4.8 through 4.10. The comparisons for the lower gage are shown on Figs. 4.11 through 4.13. As may be seen the predicted spectra agree well with the measured data.

4.3 Comparison of The Dynamic Stiffness and Damper

As mentioned in Chapter 3, the parameters of the spring/damper model used in the lift off model are modified from Wolf's discrete model. When liftoff is neglected, the dynamic stiffness and damper coefficients of the liftoff model must be matched with that from Wolf's model. From Wolf's model [1], the dynamic stiffness and damper K and C are obtained in the frequency domain.

As shown in Fig (4.4), a rigid cylinder is embedded into an elastic half space. If a vertical force acting on the cylinder is in the form of

$$P_0(\omega t)=P_c(\omega)\cos(\omega t) + P_s(\omega)\sin(\omega t)\ , \qquad (4.1)$$

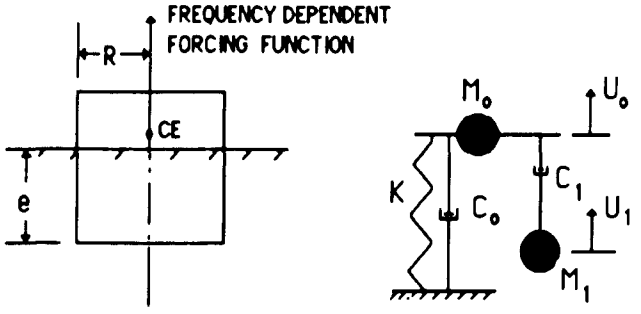

FIG (4.4) AN EMBEDDED CYLINDER IN VERTICAL MOTION

the equations of motion for the system are

$$M_o\ddot{U}_o + (C_o + C_1)\dot{U}_o - C_1\dot{U}_1 + KU_o = P_c(\omega)\cos(\omega t) + P_s(\omega)\sin(\omega t) \quad (4.2)$$

$$M_1\ddot{U}_1 + C_1(\dot{U}_1 - \dot{U}_o) = 0 \quad (4.3)$$

The displacement U_o and U_1 must be in form of

$$U_o = A_o\cos(\omega t) + B_o\sin(\omega t) \quad (4.4)$$

$$U_1 = A_1\cos(\omega t) + B_1\sin(\omega t) \quad (4.5)$$

Solving for the above equations in the steady state vibration case, the frequency dependent forcing functions, P_C and P_S, can be obtained as:

$$P_c(\omega) = (K - \omega^2 M_o - \frac{C_1^2\,\omega^2 M_1}{\omega^2 M_1^2 + C_1^2})A_o + (C_o + C_1 - \frac{C_1^3}{\omega^2 M_1^2 + C_1^2})\omega B_o \quad (4.6)$$

$$P_s(\omega) = -(C_o + C_1 - \frac{C_1^3}{\omega^2 M_1^2 + C_1^2})\omega A_o + (K - \omega^2 M_o - \frac{C_1^2\,\omega^2 M_1}{\omega^2 M_1^2 + C_1^2})B_o \quad (4.7)$$

If a vertical displacement is imposed on the mass M_0,i.e., let A_0=1 and B_0=0 in equation (4.5) and (4.6), the dynamic stiffness in the vertical motion can be obtained as follows:

$$K_v(\omega)=P_c(\omega)= K -\omega^2 M_0 - \frac{C_1^2\,\omega^2 M_1}{\omega^2 M_1^2 + C_1^2} \tag{4.8}$$

$$C_v(\omega)=-P_s(\omega)=\left(C_0+ C_1-\frac{C_1^3}{\omega^2 M_1^2 + C_1^2}\right)\omega \tag{4.9}$$

The values M_0, M_1, C_0, C_1 and K are obtained from Chapter 2; and ω is the frequency. The values $K_v(\omega)$ and $C_v(\omega)$ are dynamic-stiffness coefficients for the spring and damper respectively.

The lift off model is used to generate a solution of for a forcing function P(t) in the time domain by imposing the vertical displacement,$U_0=\cos(\omega t)$, on the cylinder. In order to obtain the frequency dependent forcing function the numerical solution P(t) is expanded in a Fourier series as follows:

$$P(t)= A_0 + \sum_{n=1}^{\infty} A_n \cos(\Omega_n t) + \sum_{n=1}^{\infty} B_n \sin(\Omega_n t) \tag{4.10}$$

The force P(t) must have the form,

$$P(t)=P_C(\omega)\cos(\omega t) + P_S(\omega)\sin(\omega t) \tag{4.11}$$

Comparing Equation (4.10) to (4.11) only two terms remain in Eq.(4.9) when $\Omega_n=\omega$, and the terms P_C and P_S can be obtained as

$$P_c = A_n = \frac{\omega}{\pi}\int_{-\frac{\pi}{\omega}}^{\frac{\pi}{\omega}} P(t)\cos(\omega t)dt \qquad (4.12)$$

$$P_s = B_n = \frac{\omega}{\pi}\int_{-\frac{\pi}{\omega}}^{\frac{\pi}{\omega}} P(t)\sin(\omega t)dt \qquad (4.13)$$

According to the equation (4.2),(4.8), and (4.9), the dynamic stiffness coefficients from the liftoff model should be:

$$K_V(\omega)=P_C(\omega) \qquad (4.14)$$

$$C_V(\omega)=-P_S(\omega) \qquad (4.15)$$

The $K_V(\omega)$ and $C_V(\omega)$ values as function of frequency (ω) when Poisson's ratio is 0.25 and embedment is 0.5 are plotted in Fig (4.15).Similarly, the coefficients for the horizontal and rocking motion varying with frequency (ω) are illustrated in Fig(4.14) and Fig(4.16). It can be seen that the values from the liftoff model are in good agreement with the values of Wolf's model.

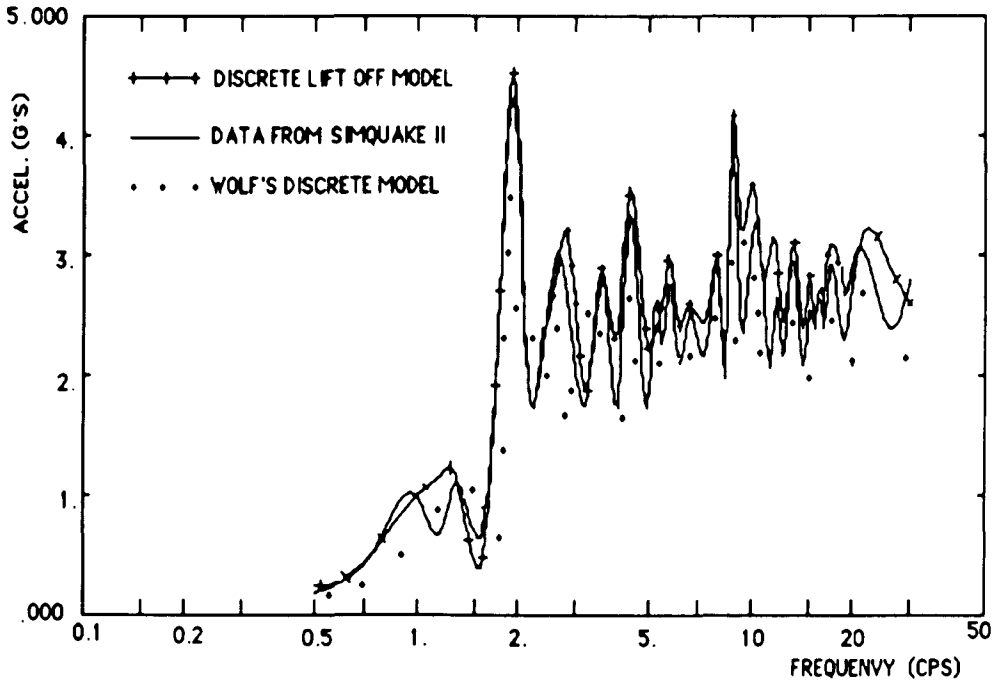

FIG (4.5) HORIZONTAL ACCELERATION SPECTRA AT BASE OF FOUNDATION

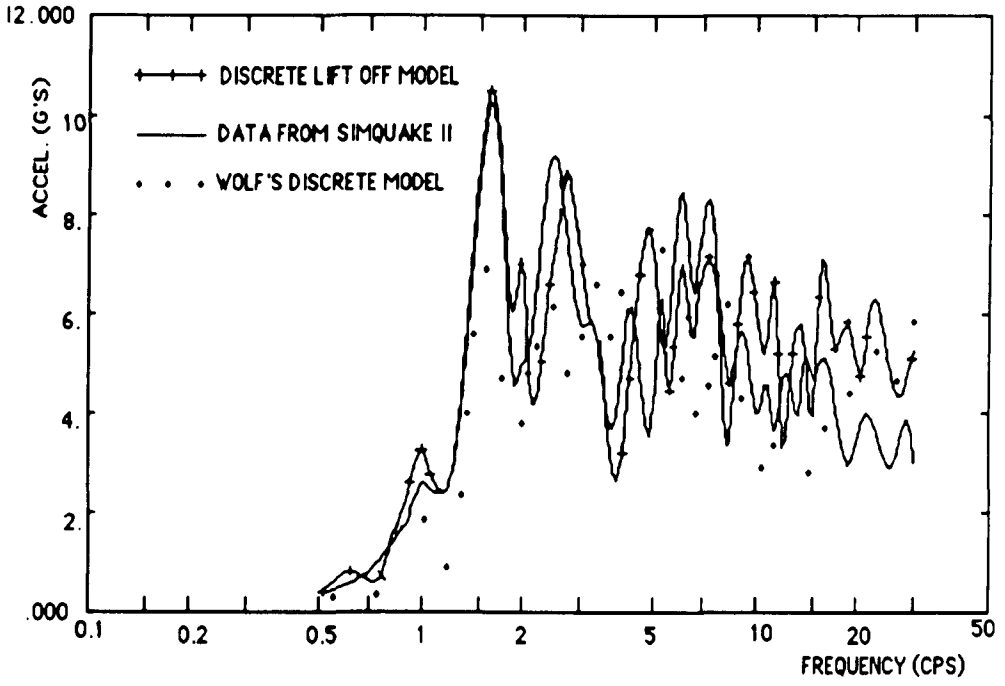

FIG (4.6) HORIZONTAL ACCELERATION SPECTRA AT TOP OF STRUCTURE

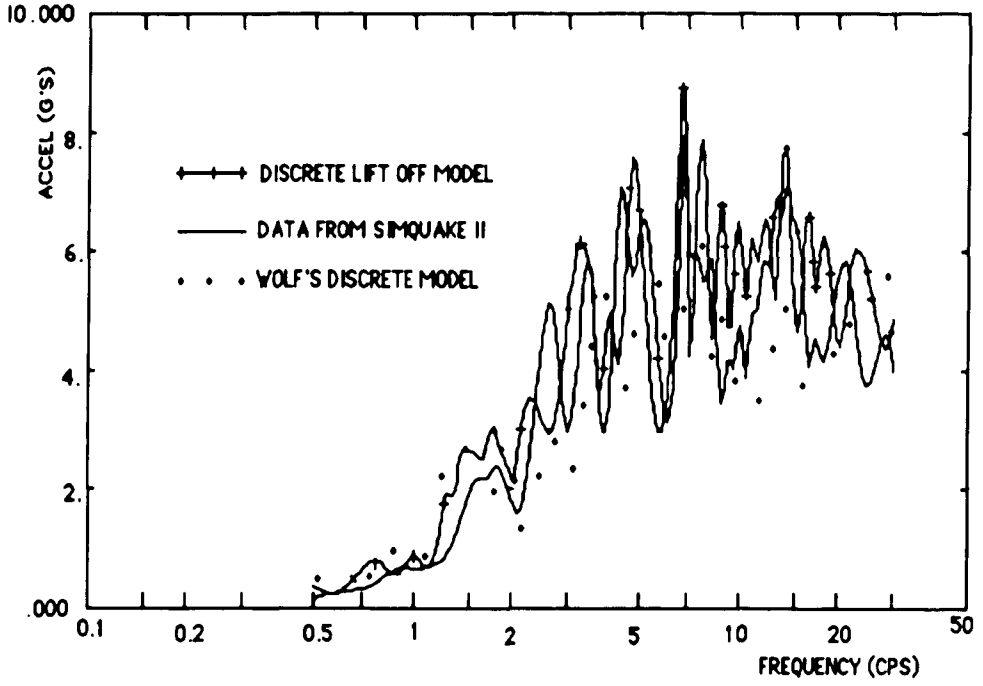

FIG(4.7) VERTICAL ACCELERATION SPECTRA OF STRUCTURE

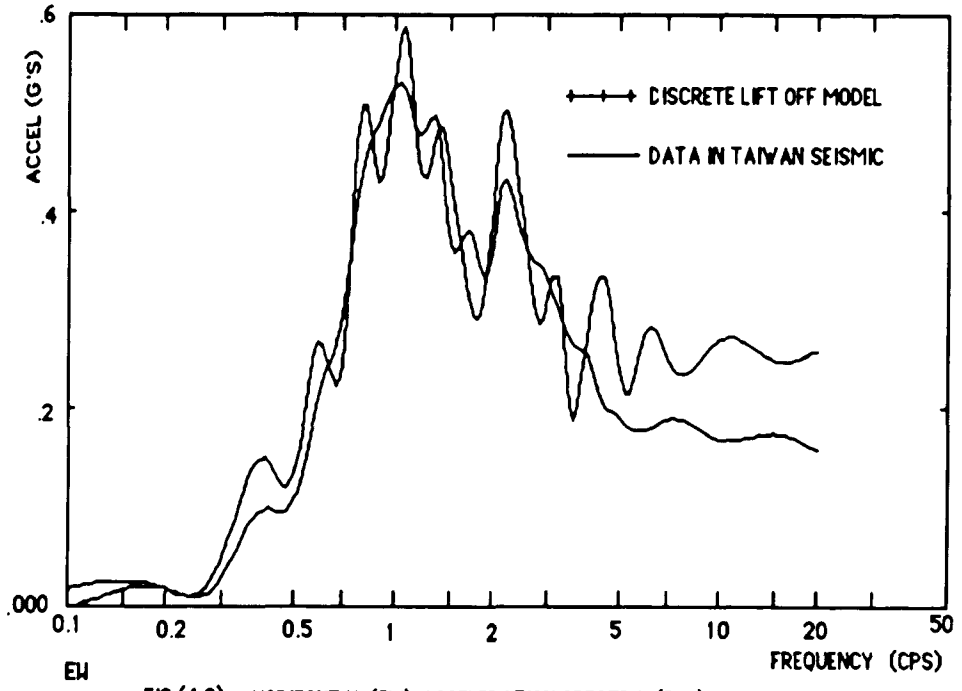

EW

FIG (4.8) HORIZONTAL (EW) ACCELERATION SPECTRA (F4U)

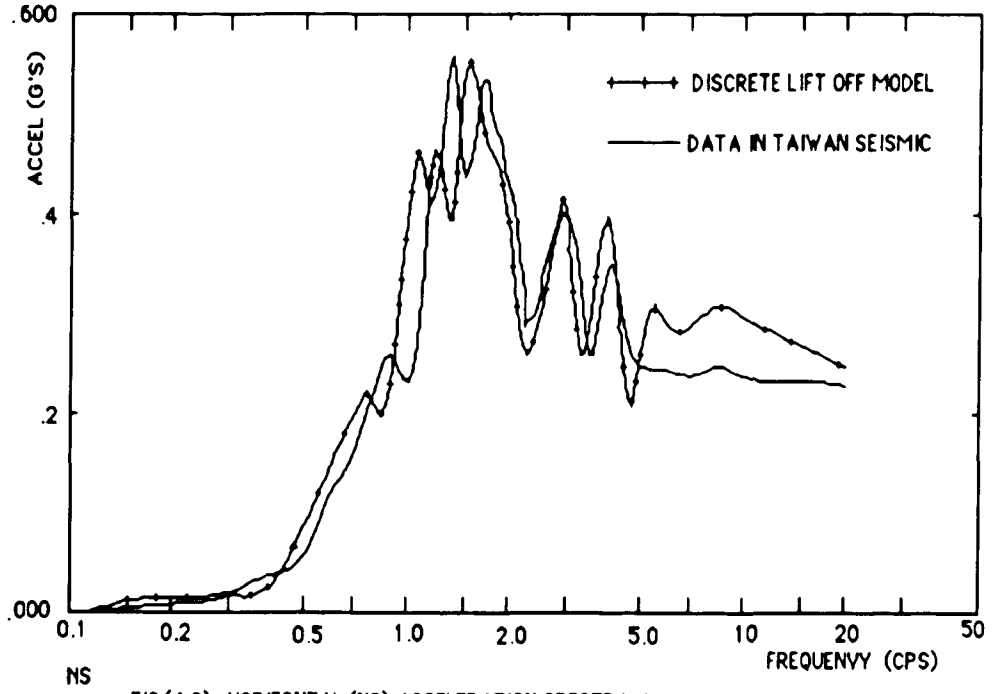

FIG(4.9) HORIZONTAL (NS) ACCELERATION SPECTRA (F4U)

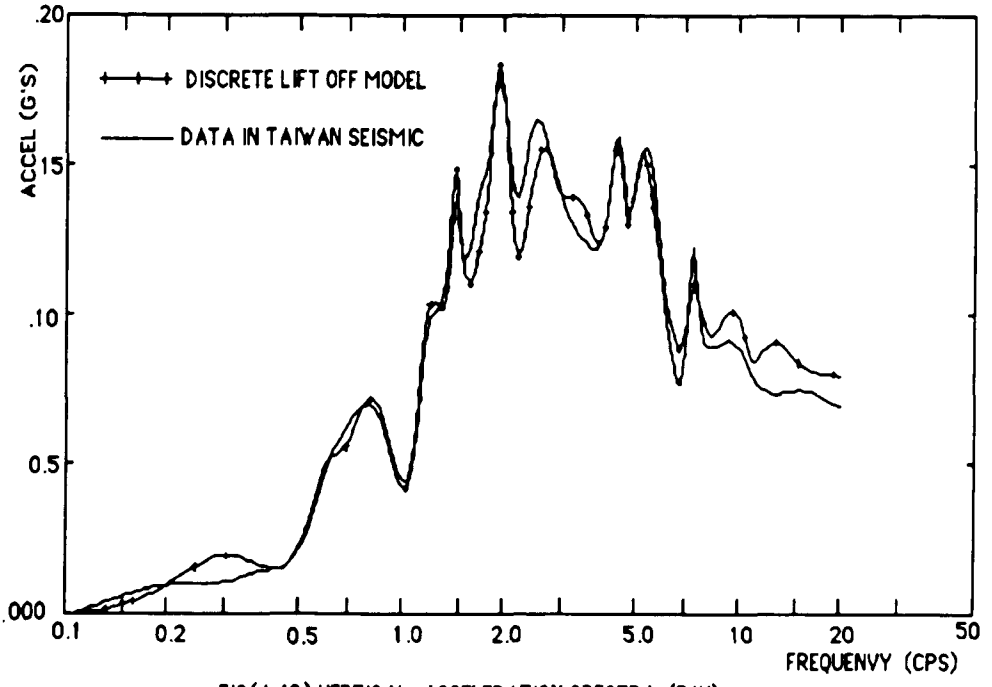

FIG(4.10) VERTICAL ACCELERATION SPECTRA (F4U)

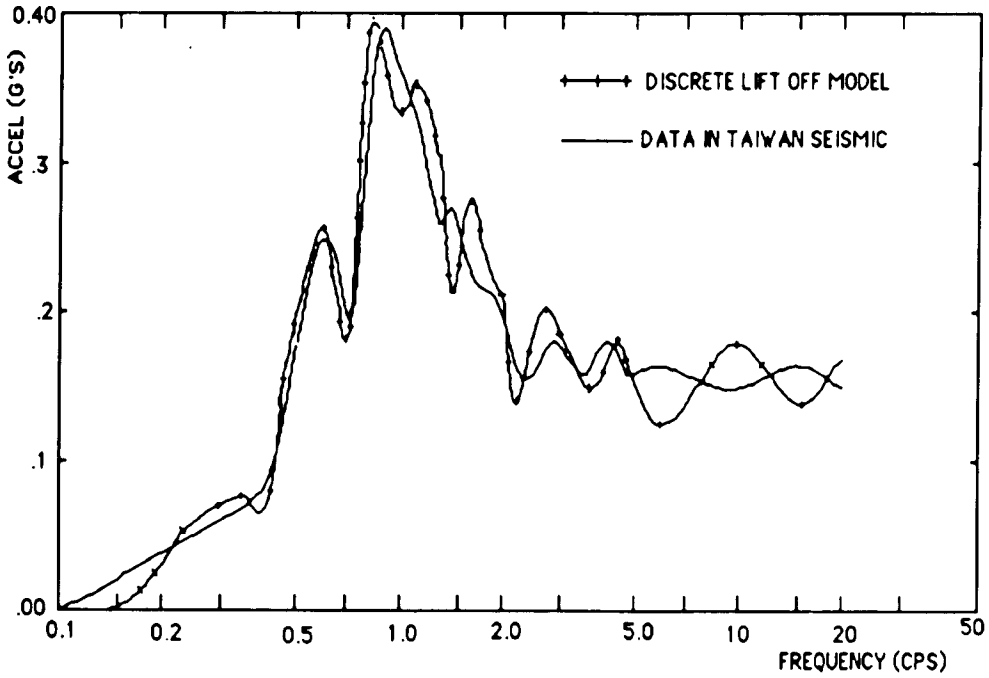

FIG (4.11) HORIZONTAL (EW) ACCELERATION SPECTRA (F4L)

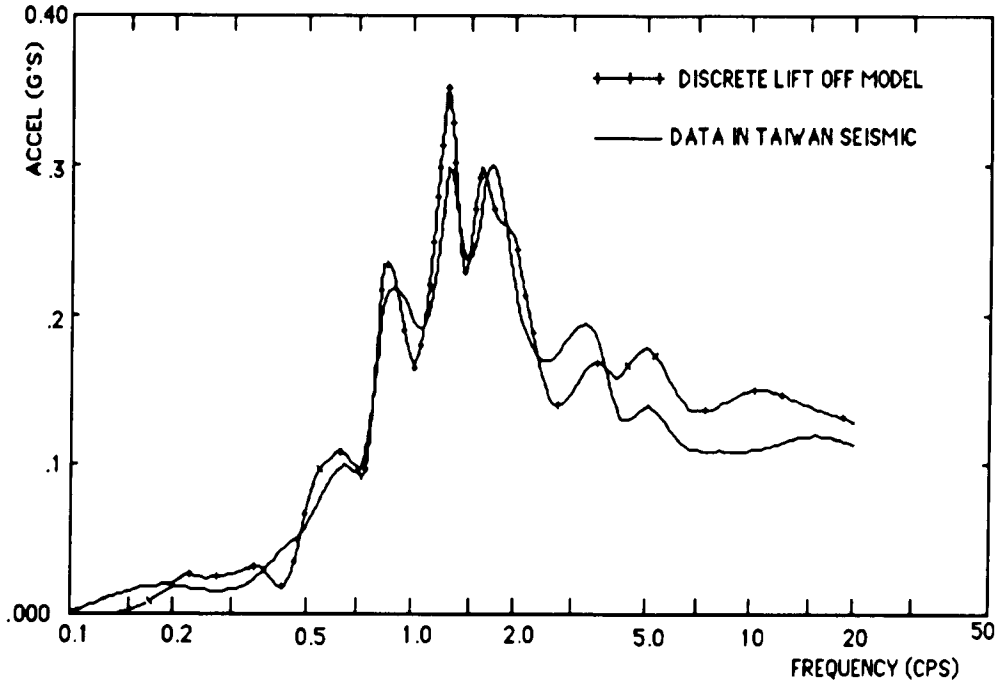

FIG (4.12) HORIZONTAL (NS) ACCELERATION SPECTRA (F4L)

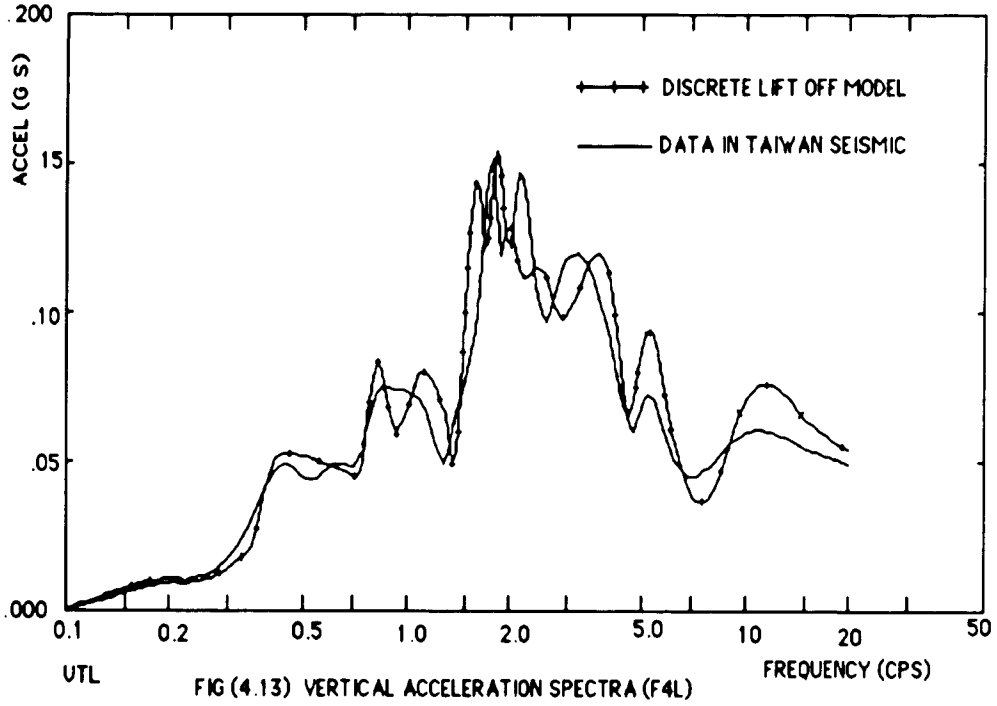

FIG (4.13) VERTICAL ACCELERATION SPECTRA (F4L)

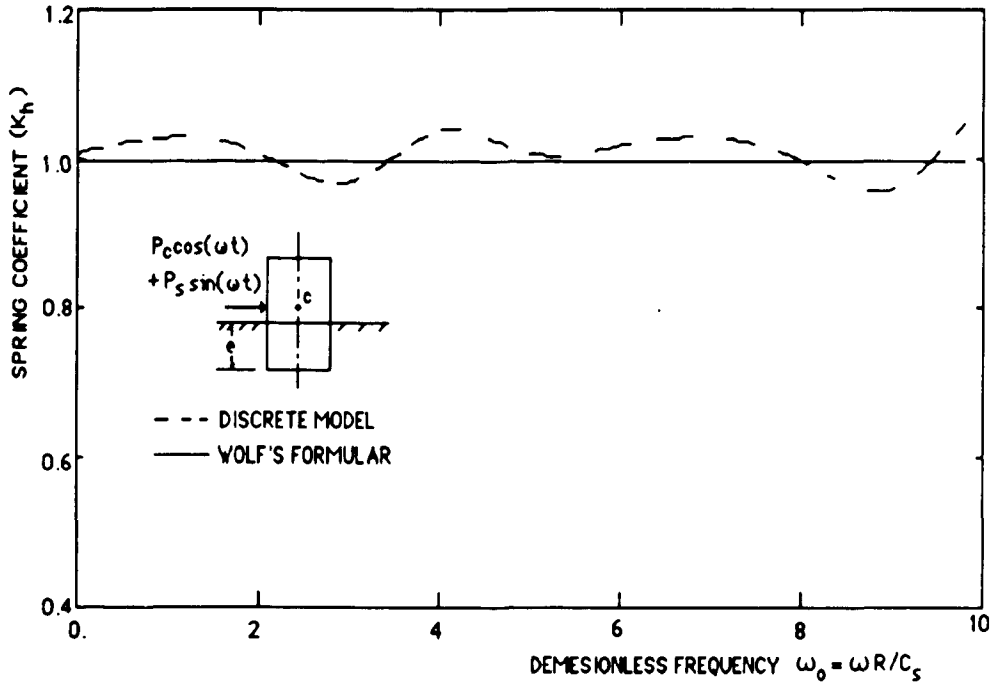

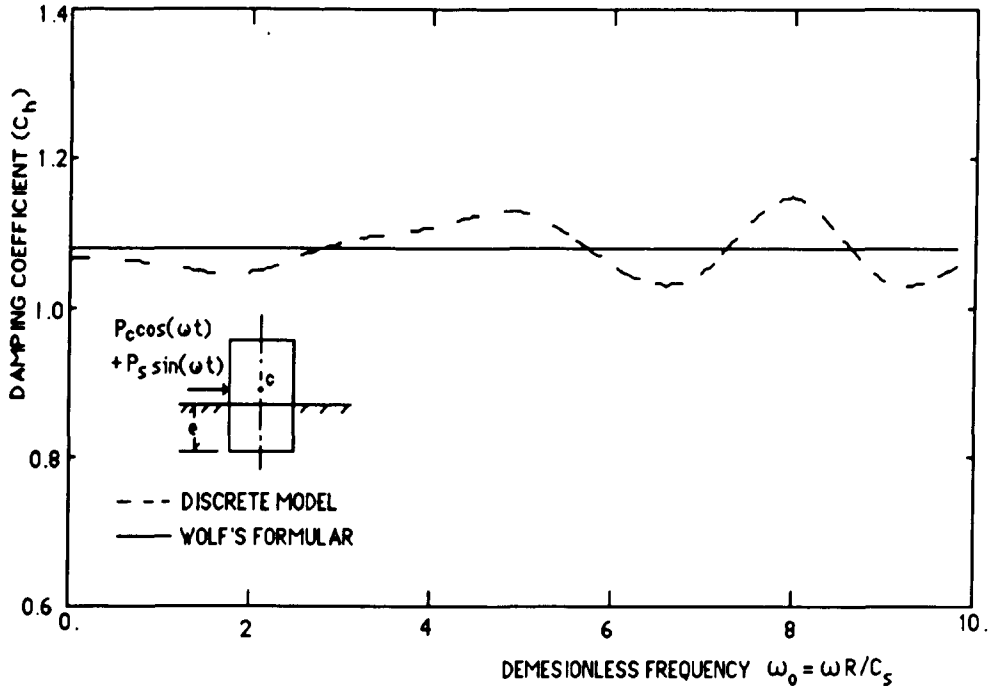

FIG (4.14) DYNAMIC STIFFNESS COEFFICIENT FOR HORIZONTAL MOTION

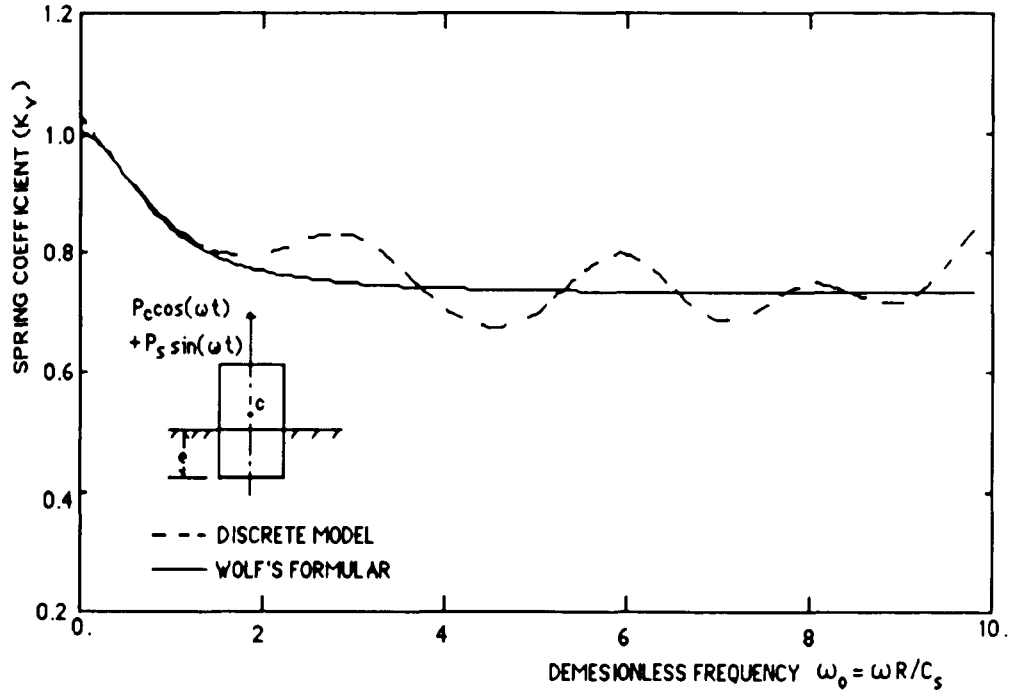

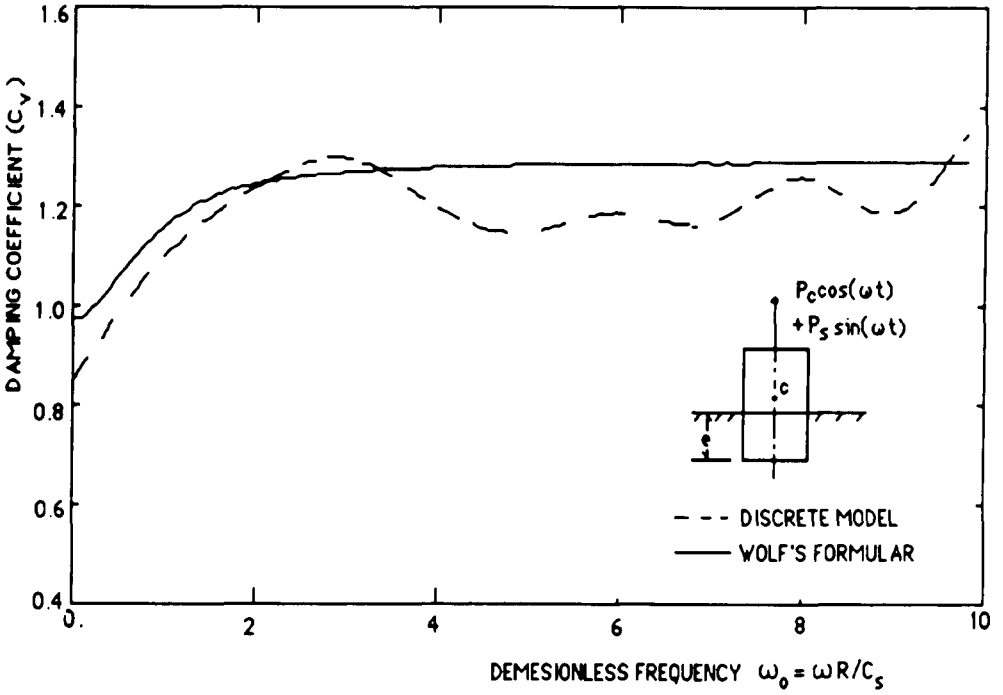

FIG (4.15) DYNAMIC STIFFNESS COEFFICIENT FOR VERTICAL MOTION

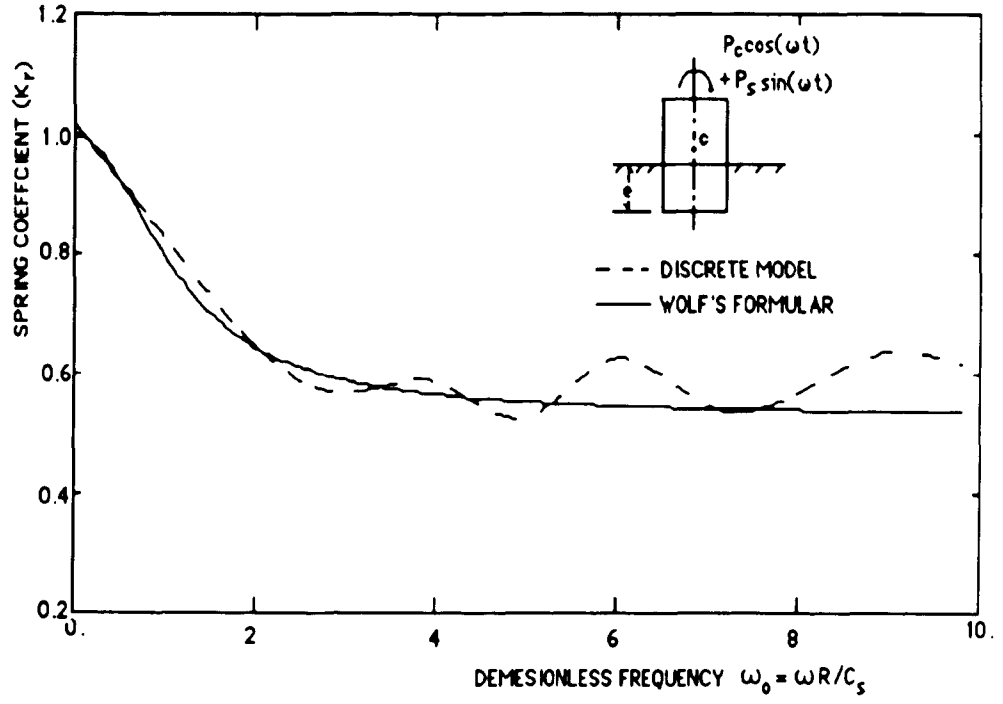

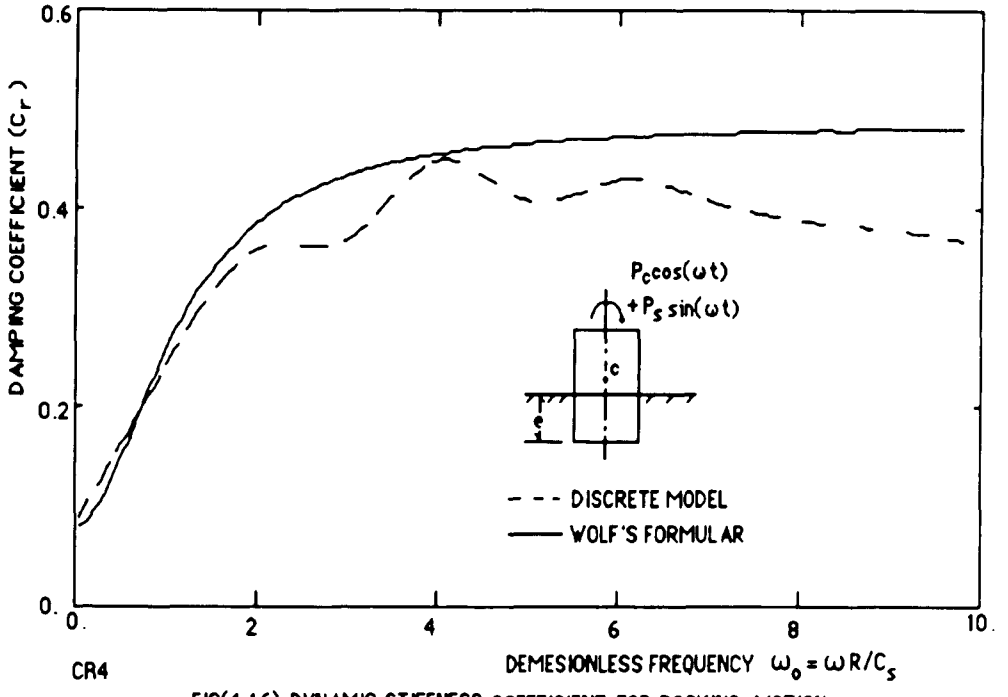

CR4

FIG(4.16) DYNAMIC STIFFNESS COEFFICIENT FOR ROCKING MOTION

Chapter 5
The Effects of Lift Off

The seismic response of most structures, including nuclear power plant structures is calculated neglecting the effects of liftoff. Therefore, it is important to investigate effects of neglecting liftoff when it occurs. a variation of parameter study is presented in this Chapter which determines the acceleration level required to cause liftoff, and the consequences of neglecting liftoff effects if liftoff occurs. The peak free field accelerations required to cause liftoff to occur is first investigated. The consequences of neglecting liftoff are investigated by generating floor response spectra for cases where liftoff is both included and neglected.

The parameters which effect this problem are: the depth of the structure's embedment; the SSI frequencies; the damping ratio of the interaction system; the position of the center of gravity of structure; and the mass characteristics of the structure. These parameters are varied in the following Sections. The horizontal and vertical time histories measured at Taiwan [30] are used as input to the models. These accelerations are scaled up to modify the severity of the input.

5.1 The Peak Acceleration Required to Cause Liftoff

The following nondimensional parameters are used to define the characteristics of the structure and the interaction process:

$$\lambda = e/R \tag{5.1}$$

$$\xi = Zo/R \tag{5.2}$$

$$\varepsilon = \sqrt{\rho G}\ R^2/Ms \tag{5.3}$$

$$\gamma = GR/M_s \tag{5.4}$$

$$\delta = GR^3/J_s \tag{5.5}$$

where,

λ - embedment of structure

ξ - ratio for the height of structure center of gravity to the radius.

ε - the interaction damping ratio

R, Z_o, e, V_s, M_s, and J_s have the same meaning as in Chapter 3

The SSI frequencies related to these parameters are:

$$f_h=\frac{1}{2\pi}\left[\frac{8\gamma}{2-\mu}(1+\lambda)\right]^{1/2} \tag{5.6}$$

$$f_\theta=\frac{1}{2\pi}\left[\frac{8\delta}{3(1-\mu)}(1+1.3\lambda+\lambda^3)+\frac{8\delta}{2-\mu}\frac{F_k^2}{R^2}(1+\lambda)\right]^{1/2} \tag{5.7}$$

$$f_v=\frac{1}{2\pi}\left[\frac{4\gamma}{1-\mu}(1+0.54\lambda)\right]^{1/2} \tag{5.8}$$

The interaction damping parameters become:

$$\overline{C}_h=\frac{8\gamma}{(2-\mu)\varepsilon}(0.68+0.57\sqrt{\lambda})(1+\lambda) \tag{5.9}$$

$$\overline{C}_{0r}=\frac{8\delta}{3(1-\mu)\varepsilon}(1+1.3\lambda+\lambda^3)(1+1.46\lambda+\lambda^3) \tag{5.10}$$

$$\overline{C}_{1r}=\frac{8\delta}{3(1-\mu)\varepsilon}(1+1.3\lambda+\lambda^3)(0.4+0.03\lambda^2) \tag{5.11}$$

$$\overline{C}_{0v}=\frac{4\gamma}{(1-\mu)\varepsilon}(1+0.54\lambda)(1.85+0.89\lambda) \tag{5.12}$$

$$\overline{C}_{1v}=\frac{4\gamma}{(1-\mu)\varepsilon}(1+0.54\lambda)(0.32-0.001\lambda) \tag{5.13}$$

The peak accelerations required to cause lift off are calculated in this section. The Ref. 30 input is used to calculate the response of the structure, and the peak acceleration scaled up until there is a tendency for a tensile stress to develop at the foundation/soil interface. Solutions are obtained as the above parameters are varied to determine the effect of the five nondimensional parameters on the acceleration required to cause liftoff.

The effect of the SSI frequencies on the liftoff acceleration are presented in Figs. 5.1 through 5.12. There is only a slight dependence of the liftoff acceleration on the rocking frequency except when the rocking frequency is less than 3 cps. the liftoff acceleration increases sharply as the rocking SSI frequency decreases below 3 cps. The acceleration required to cause lift off increases as the vertical interaction frequency decreases. It follows that the tendency for lift off to occur increases with a stiffer horizontal interaction frequency and with a softer vertical interaction frequency.

The peak acceleration required to cause lift off vary with other three parameters of the interaction system. Fig.(5.13) to Fig.(5.15) show the effect of these parameters on the peak acceleration required to cause liftoff. As would be expected, the accelerations decrease with the height (ξ) of the structure's center of gravity above the base; increase as the interaction damping (ε) increases; and increase as the depth (λ) of embedment of the structure increases.

5.2 Effects of Neglecting Lift Off

The effects of neglecting liftoff are evaluated by generating floor response spectra for cases when liftoff is included and neglected. The structural and SSI characteristics used for these comparisons are:

Rocking frequency	= 5 cps
Vertical frequency	= 20 cps
Horizontal frequency	= 13.5 cps
Rocking damping	= 1% (ε = 10)

Vertical damping	= 15.1%
Horizontal damping	= 21.1%
Embedment (e/R)	= 1.0*R (λ = 1.0)
Height of CG (h/R)	= 1.0*R(ξ = 1.0)

From the results of the previous section lift off will occur at a peak acceleration of (0.23 G's) as shown in Fig. (5.10). Comparisons are made for accelerograms having peak amplitudes of 1.33, 1.67, and 2.00 times the accelerogram required to cause liftoff. Two percent equipment damping is used to calculate the spectra in the horizontal , rocking, and vertical directions. Solutions are obtained including liftoff effects and neglecting liftoff effects. The results are presented by dividing the liftoff spectra by the no liftoff spectra, so that a ratio of unity indicates no liftoff effects. The results are shown on Figs. 5.16 through 5.18.

As shown in Fig (5.16) lift off has no effect on the horizontal spectra at the bottom of the foundation. This result is expected because the horizontal interaction parameters are not effected by foundation/base mat separation. Liftoff effects are significant for the horizontal spectra at the top of structure since this includes rocking effects. The effect is significant when the input data is larger than 1.33 times the acceleration required to cause liftoff. The spectra peaks when lift off is considered exceed the no liftoff spectra by factors of 1.5 and 3.2 for the input of 1.67 and 2.00 times the lift off acceleration. It should also be noted that the liftoff spectra exceeds the no lift off spectra over a wide frequency range. This Frequency range (1 to 4 cps) is important for the seismic design of equipment and buildings. It can be concluded that it is important to consider liftoff for those problems where rocking motion is significant.

The effect of lift off on the vertical motion is shown in Fig (5.18). It can be seen that lift off has a significant effect for frequencies higher than 10 cps.

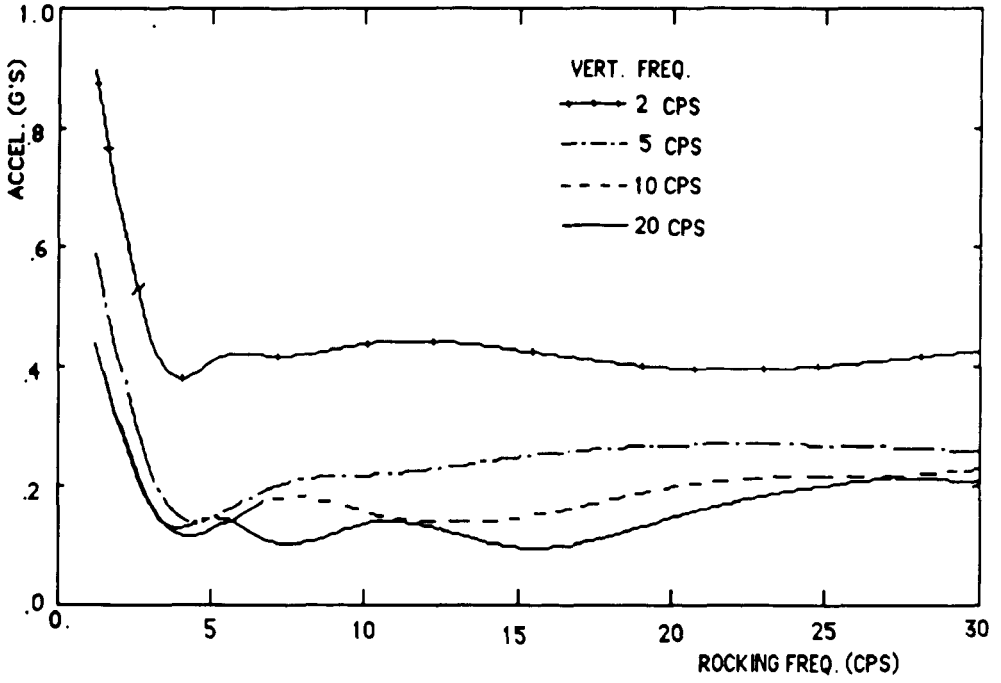

FIG (5.1) PEAK ACCEL. TO CAUSE LIFT OFF ($\xi = 0.5$, $\varepsilon = 1$, $\lambda = 0$)

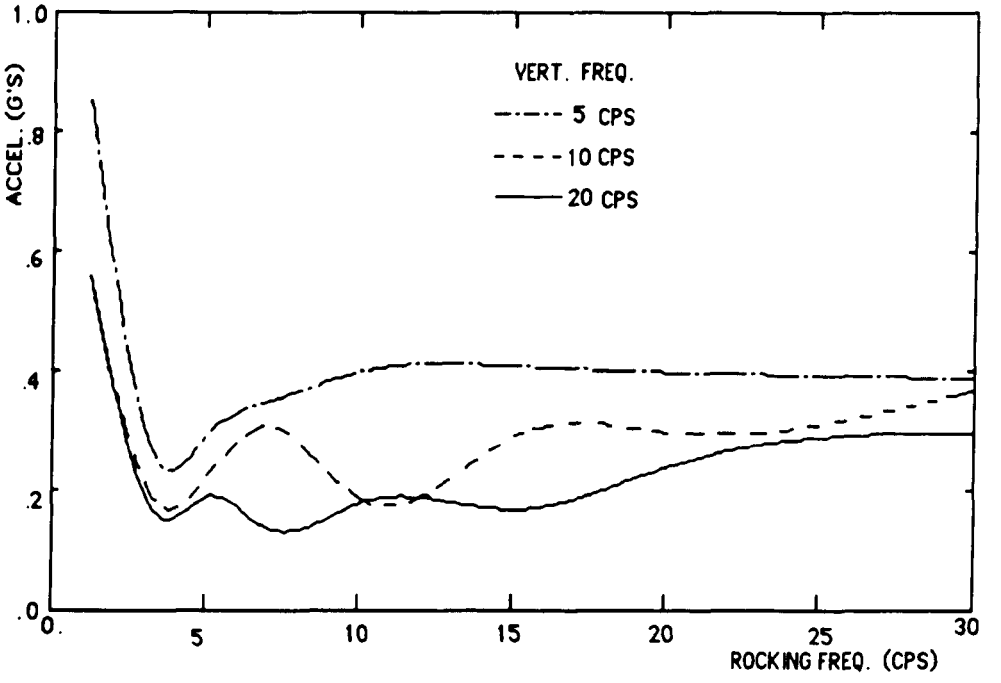

FIG(5.2) PEAK ACCEL. TO CAUSE LIFT OFF ($\xi = 0.5$, $\varepsilon = 1$, $\lambda = 0.5$)

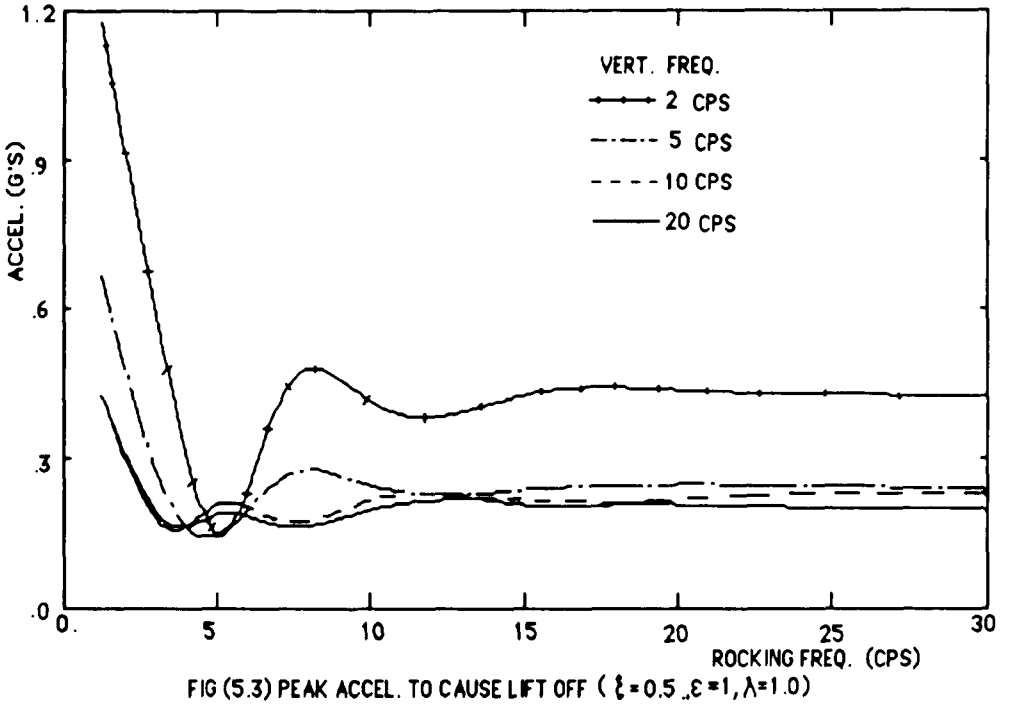

FIG (5.3) PEAK ACCEL. TO CAUSE LIFT OFF ($\xi = 0.5$, $\varepsilon = 1$, $\lambda = 1.0$)

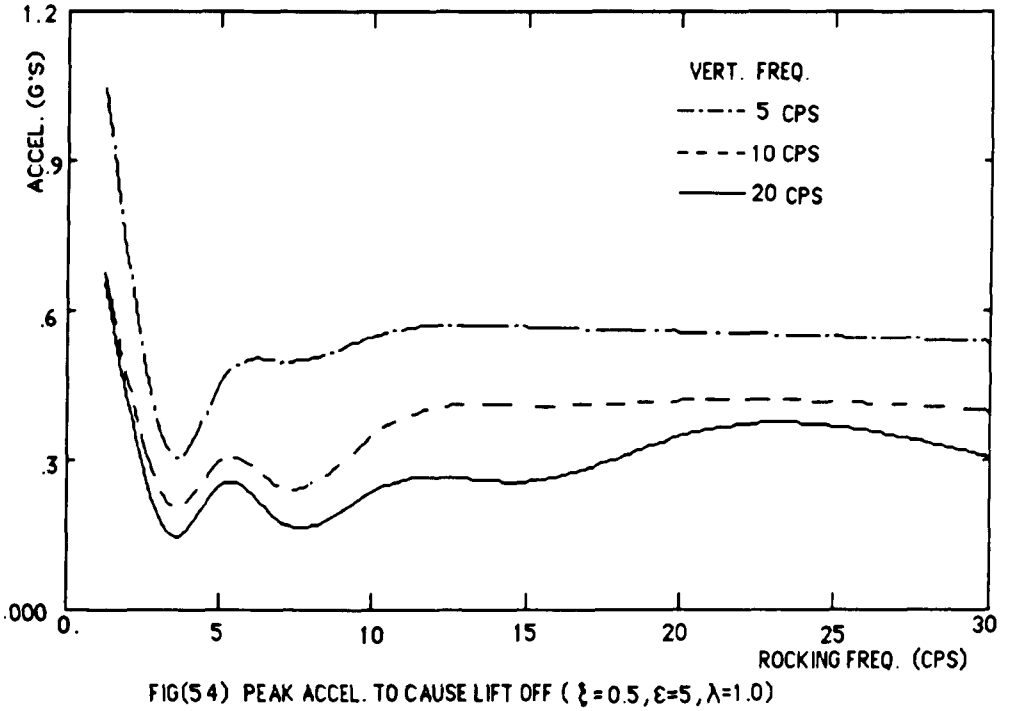

FIG(5.4) PEAK ACCEL. TO CAUSE LIFT OFF ($\xi = 0.5$, $\varepsilon = 5$, $\lambda = 1.0$)

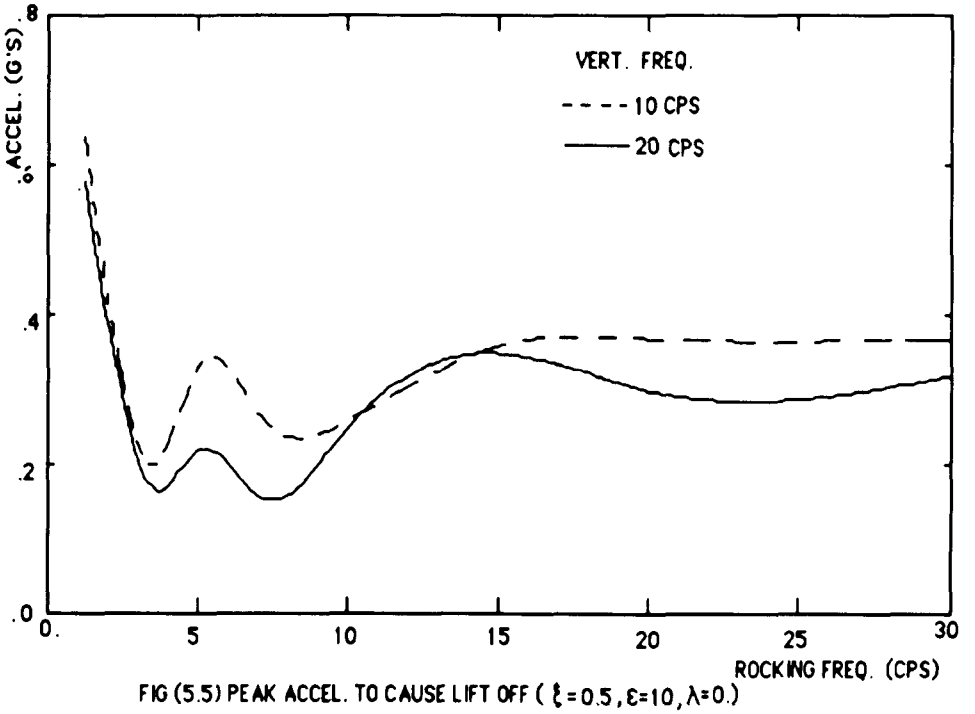

FIG (5.5) PEAK ACCEL. TO CAUSE LIFT OFF (ξ=0.5, ε=10, λ=0.)

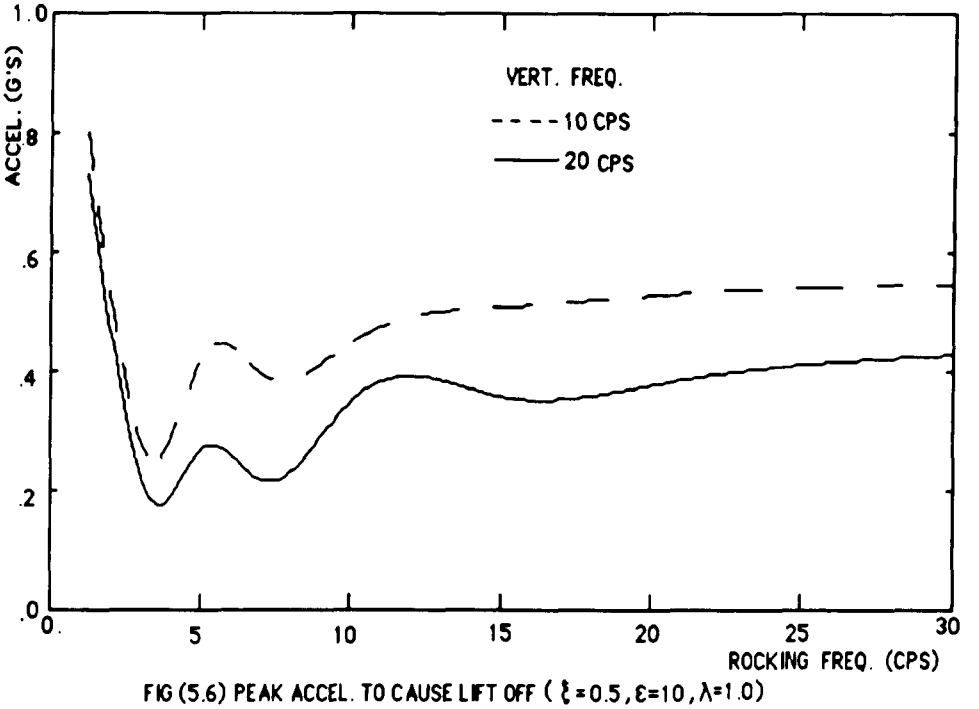

FIG (5.6) PEAK ACCEL. TO CAUSE LIFT OFF (ξ=0.5, ε=10, λ=1.0)

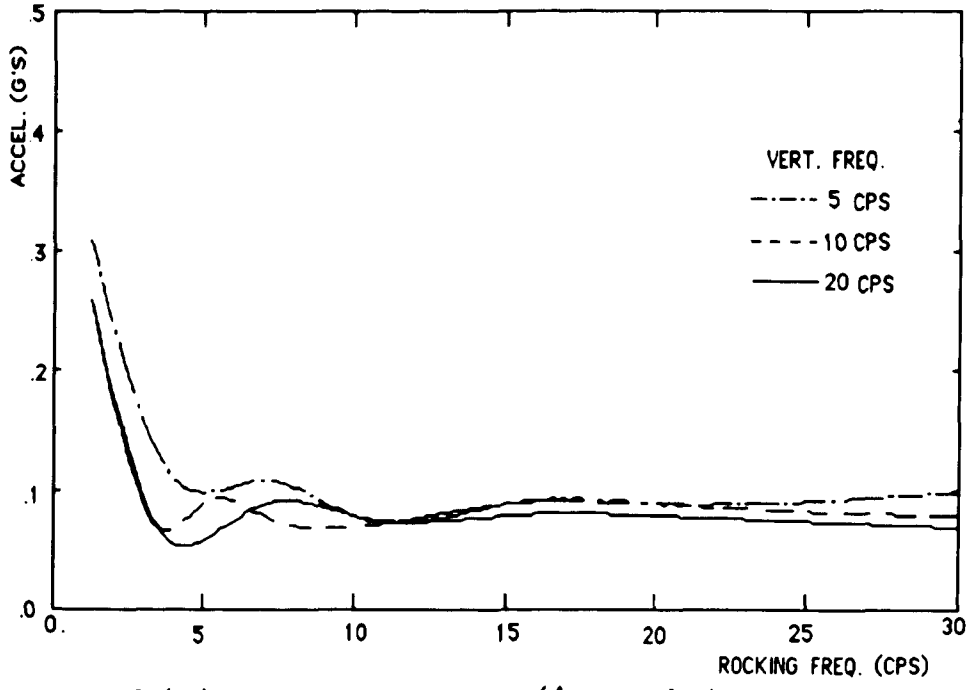

FIG(5.7) PEAK ACCEL. TO CAUSE LIFT OFF (ξ=1., ε=1 , λ=0)

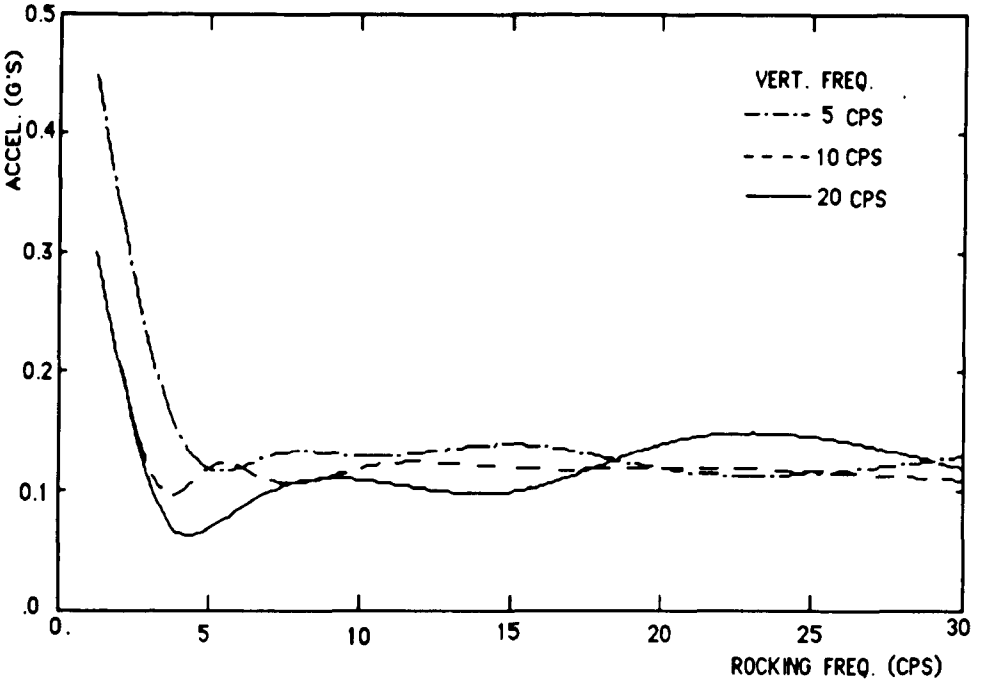

FIG (5.8) PEAK ACCEL. TO CAUSE LIFT OFF (ξ=1 , ε=5 , λ=.0)

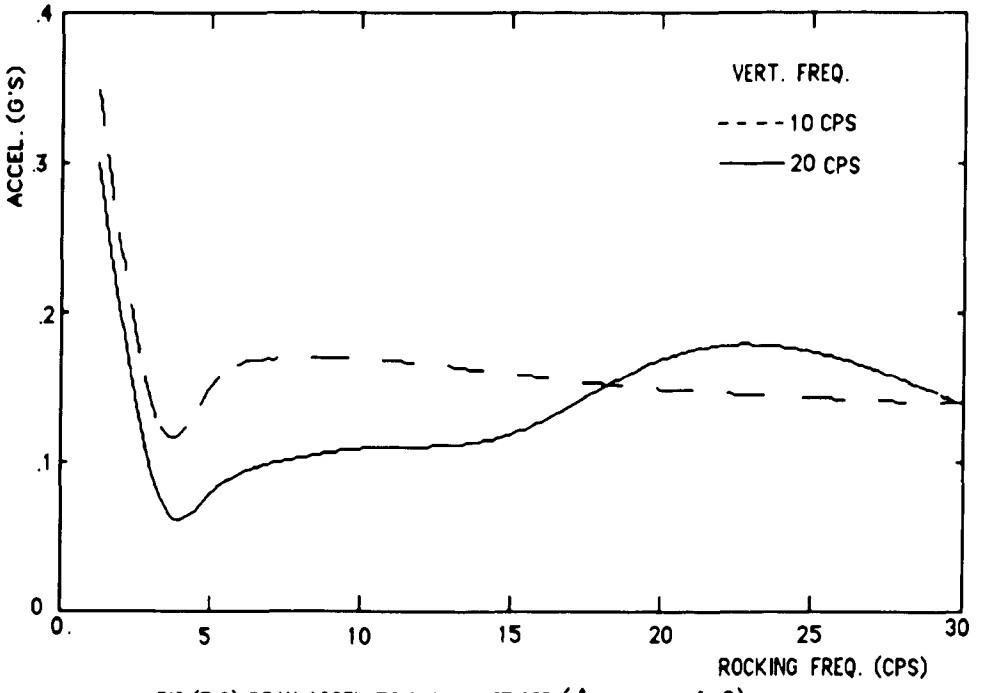

FIG (5.9) PEAK ACCEL. TO CAUSE LIFT OFF (ξ=1 , ε=10 , λ=0)

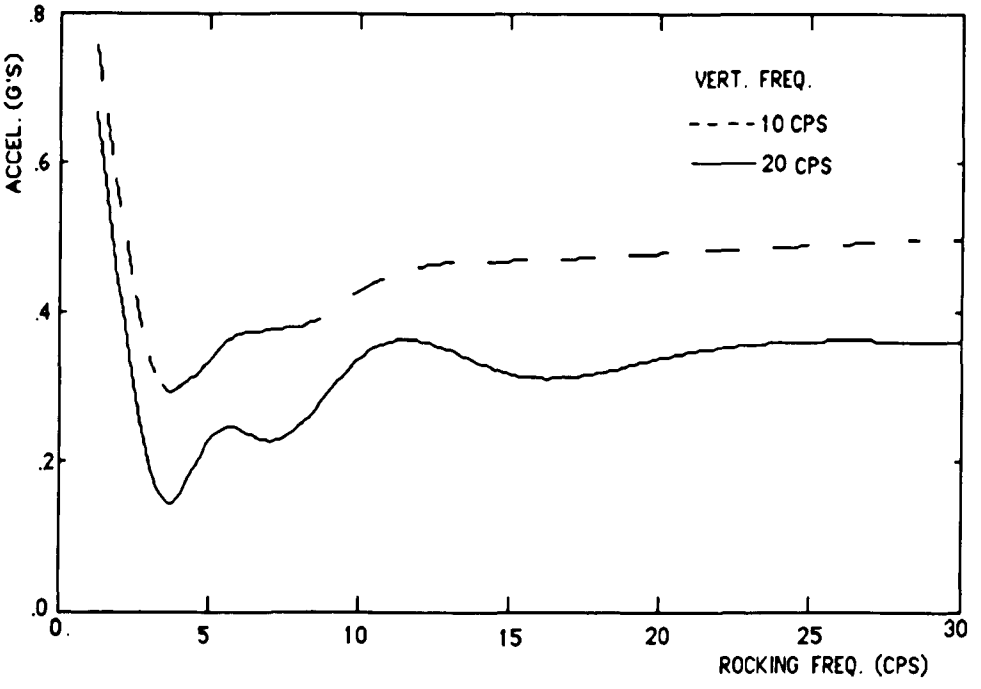

FIG (5.10) PEAK ACCEL. TO CAUSE LIFT OFF (ξ=1 , ε=10 , λ=1.0)

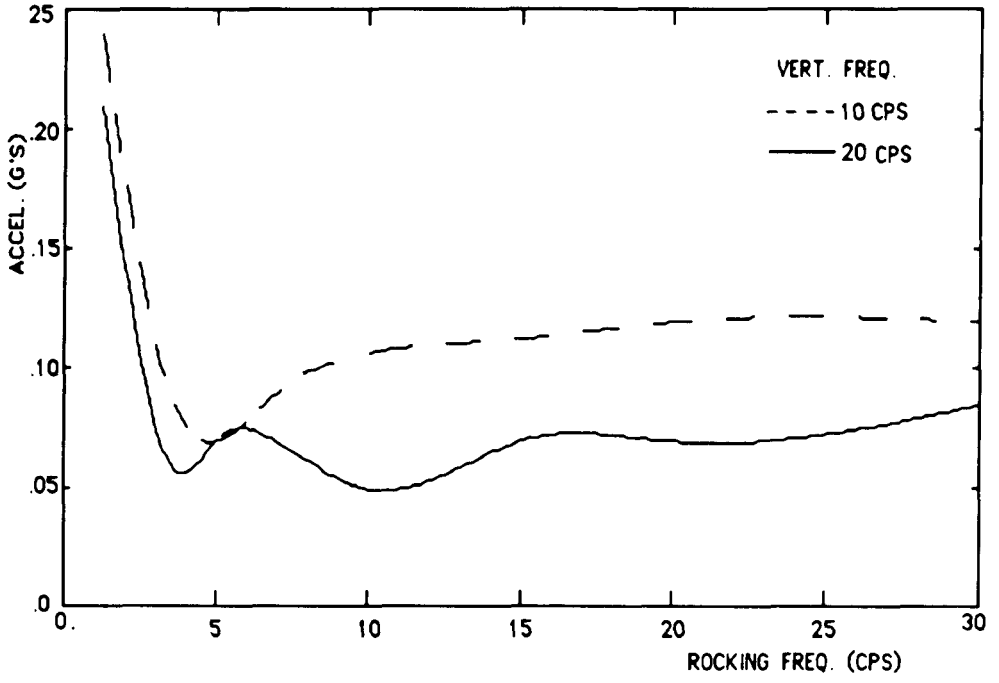

FIG (5.11) PEAK ACCEL. TO CAUSE LIFT OFF (ξ=1.5, ε=10, λ=0.0)

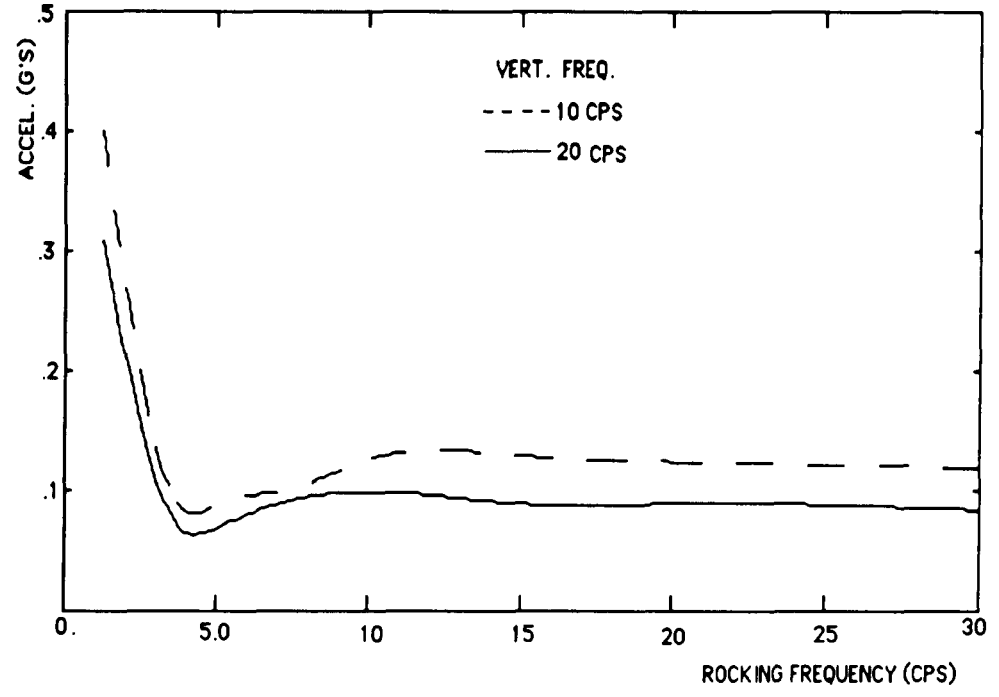

FIG (5.12) PEAK ACCELI TO CAUSED LIFT OFF (ξ = 1.5, ε = 10, λ = 1)

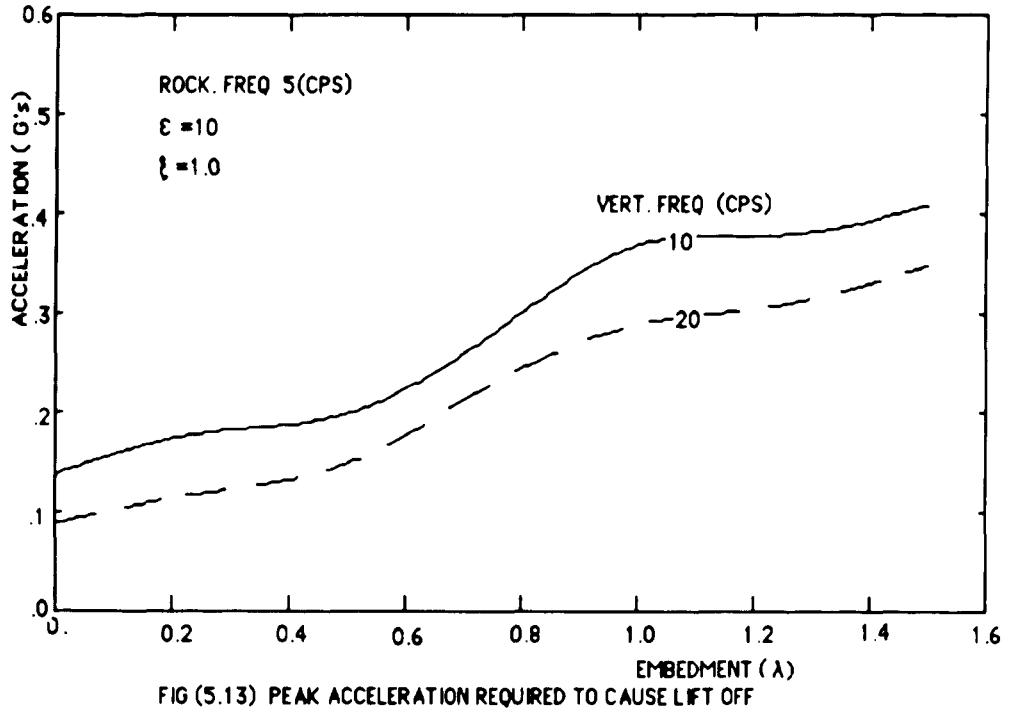

FIG (5.13) PEAK ACCELERATION REQUIRED TO CAUSE LIFT OFF VARYING WITH EMBEDMENT

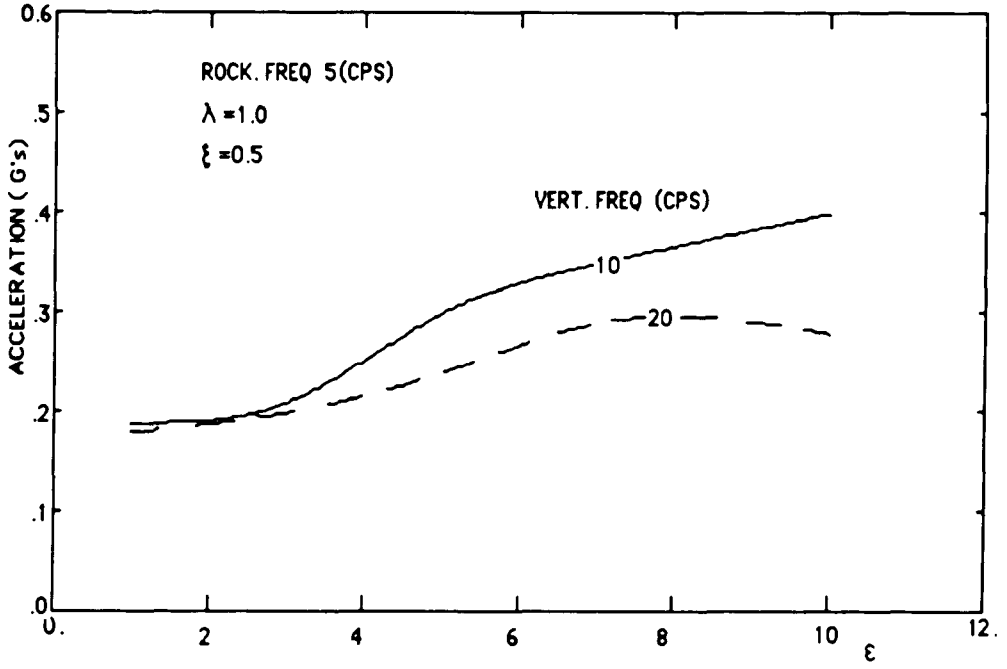

FIG (5.14) PEAK ACCELERATION REQUIRED TO CAUSE LIFT OFF VARYING WITH INTERACTION DAMPING

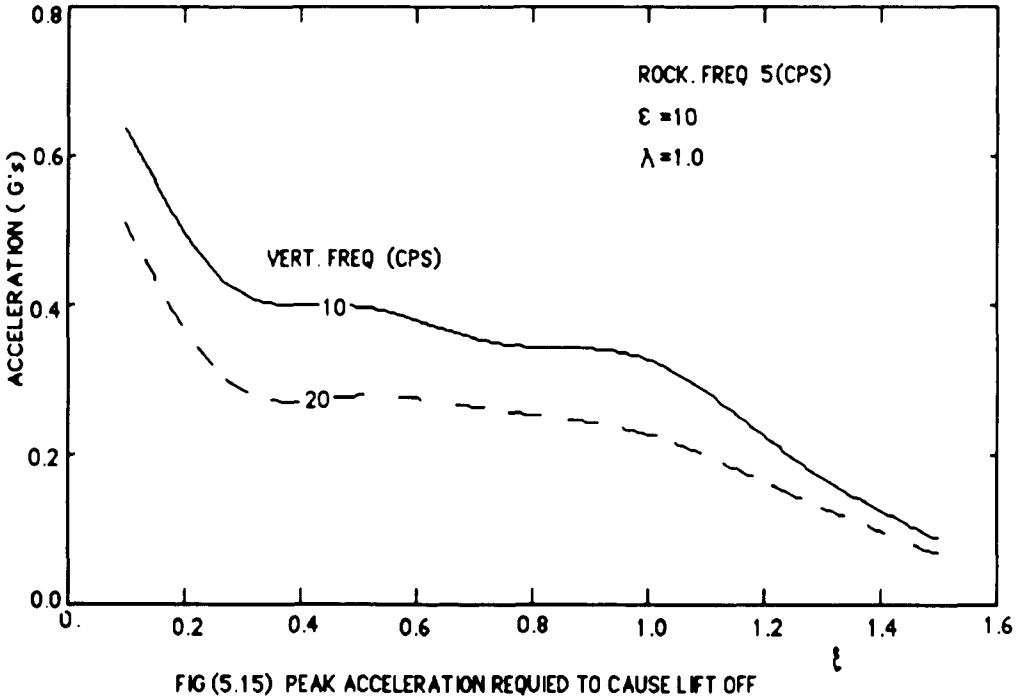

FIG (5.15) PEAK ACCELERATION REQUIED TO CAUSE LIFT OFF
VARYING WITH HEIGHT OF CENTER OF GRAVITY

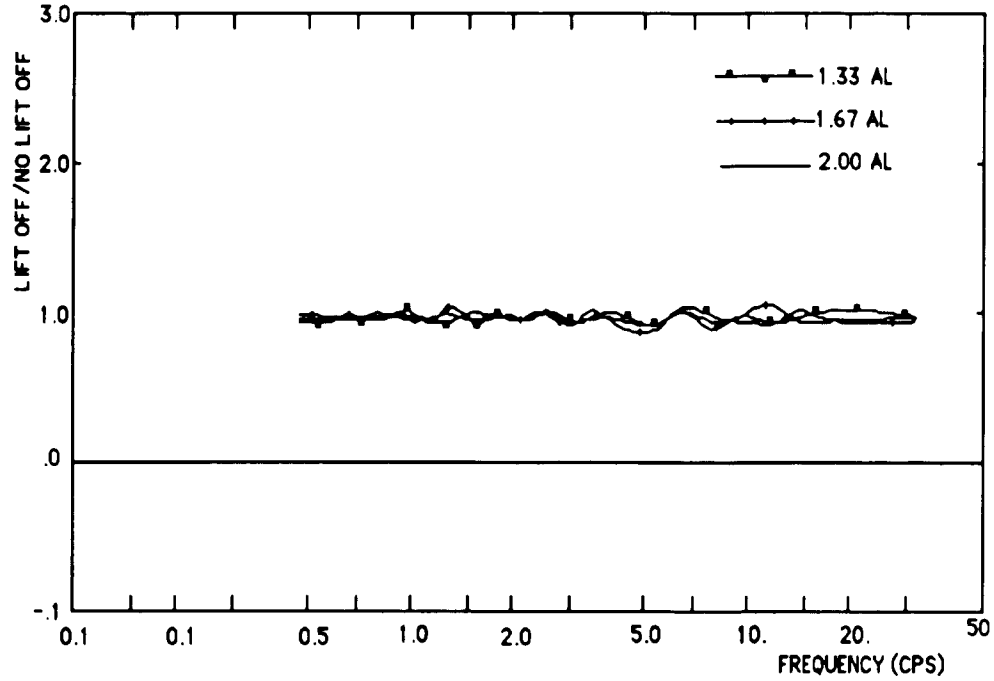

FIG(5.16) RATIO HORIZONTAL LIFT OFF /NO LIFT OFF SPECTRA

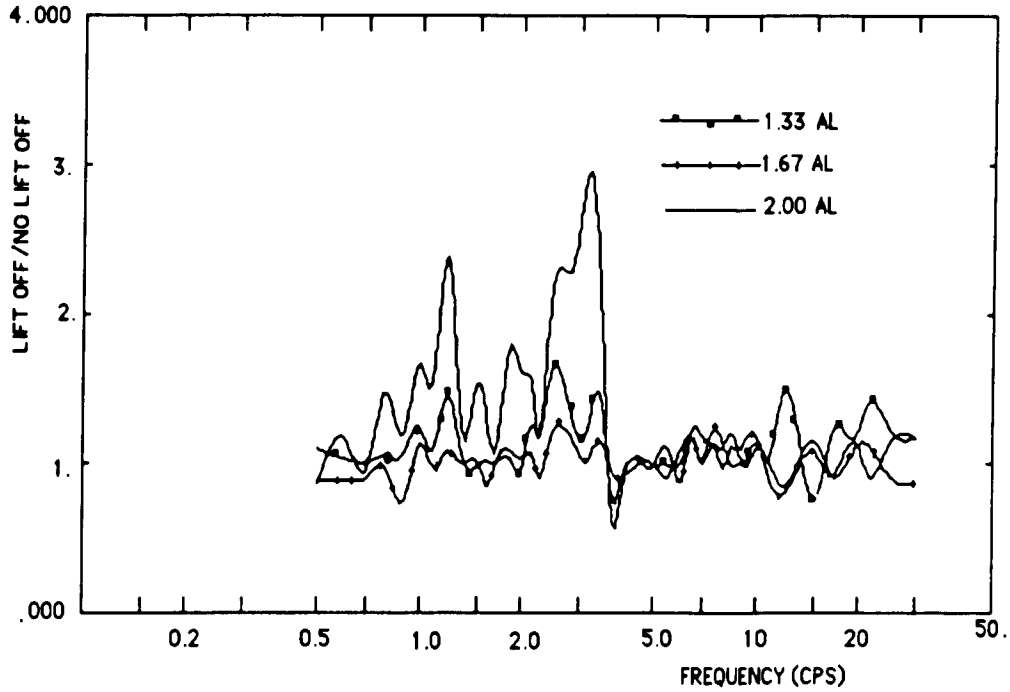

FIG (5.17) RATIO OF ROCKING AT TOP/NO LIFT OFF SPECTRA

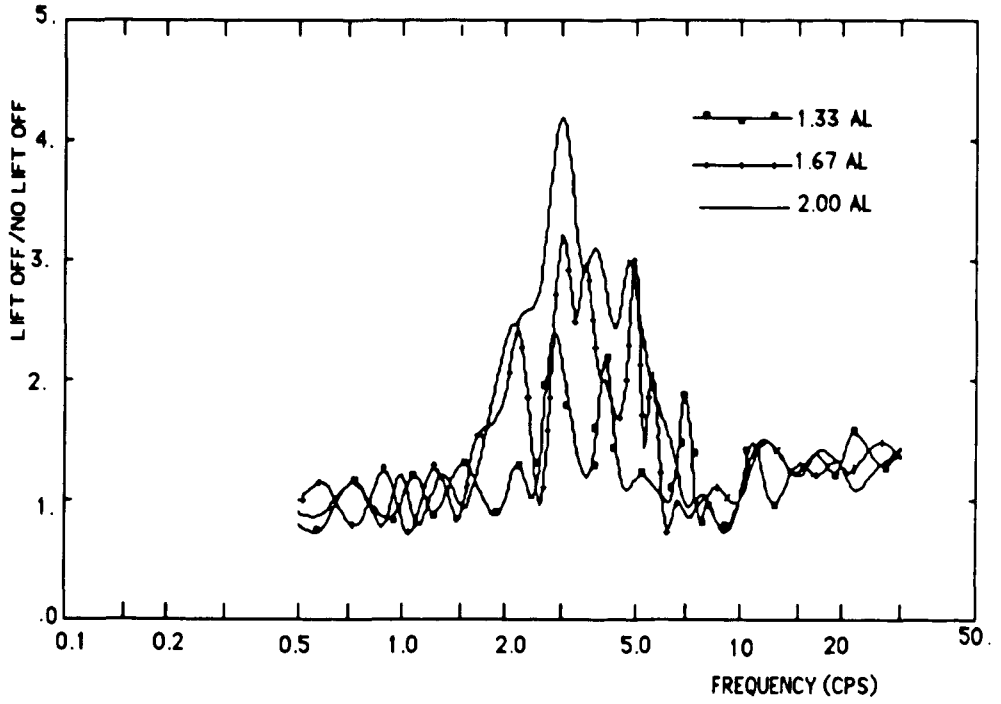

FIG(5.18)RATIO VERTICAL LIFT OFF /NO LIFT OFF SPECTRA

Chapter 6
Basic Equations For The Continuum Mechanics Method

As described in Chapter 3, the discrete model embodies several assumptions which lead to questions regarding the reliability of the model. First, the effects of the structural motion on the free field is embodied in two masses (M_0 and M_1) attached to the foundation through discrete dampers. Second, the parameters of the discrete model are developed by "curve fitting" the response of the model to that derived by more rigorous methods. Third, the assumption for the distribution of the discrete parameters over the foundation required for lift off calculation is some what arbitrary.

In this Chapter, an alternative method is developed which resolves these uncertainties. The foundation area is divided into segments and the interaction force histories acting on each segment are established as the unknowns. The force time histories are divided into a series of pulses. At any time (t), the unknowns are the magnitudes of the pulses applied to each of segment. The response of the free field under the foundation is the free field input motion plus the local effects of the interaction forces. Unit pulse solutions are used as influence functions to represent the effect of the interaction pulses on the free field. The equations of motion of the structures are used to evaluated the structural response. Compatibility of displacements between the structure and free field develop the equations required to solve for the unknown pulses.

In section 6.1 several assumptions are made for the simplification of the system. The compatibility condition on the interface is established in section 6.2 . Section 6.3 gives the ground motion expression due to the interaction forces, and in section 6.4, the general governing equations of the method are developed.

6.1 Assumptions

The analysis is based on the following assumptions:

1) The structure and foundation is a rigid cylinder that is sitting on the surface of an elastic half space.

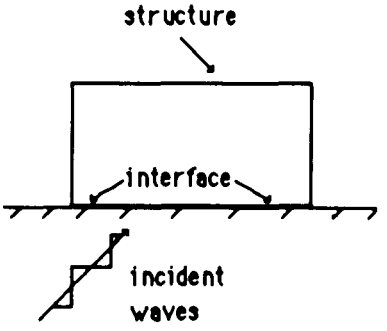

Fig (6.1) Rigid structure on the Surface of ground

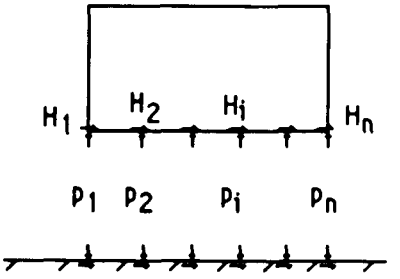

Fig(6.2) interaction forces at the interface

2) The base of foundation is divided into N strips as shown in Fig. 6.3. The vertical and horizontal forces at the center of each strip are established as the unknown variables for the problem.

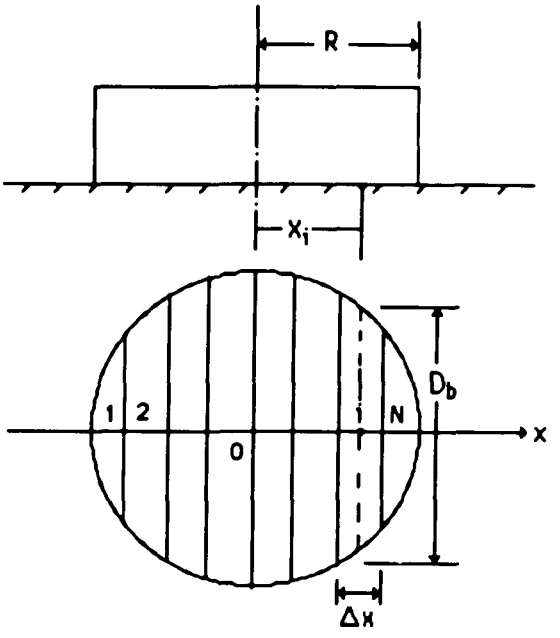

FIG (6.3) THE FOUNDATION BASE DIVIDED INTO N STRIPS

3) The pressures acting over each strip are constant during the time step Δt_M. The force history of each node is ,therefore, made by of a series of pulses, acting during a time step $\Delta t_M = t_M - t_{M-1}$ as shown in Fig. 6.4.

4) The free field motion at the interface is used as the input data. For each node (center of the strip), the value of the foundational motion is assumed to be the input motion plus the effect of the pulses.

5) The foundation is "welded" to the soil for the non-liftoff condition.

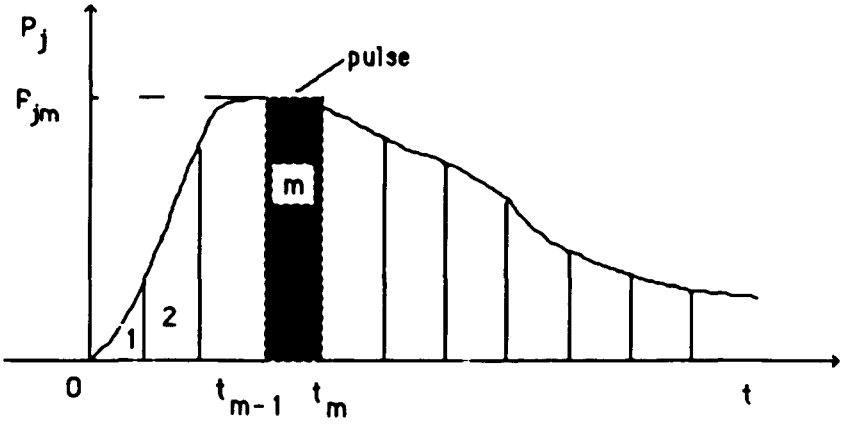

Fig (6.4) presssure history at interface

6.2 Compatibility Condition on the Interface

At any time t_k, the deformation of the ground media under the foundation base must be identical to the motion of the foundation. The foundation base mat is divided into N segments (strips) as shown in Fig (6.3). For a strip i, the width is Δx and the length is D_b. If a node i is the point at the center of a strip i, the displacement of the foundation at node i must be equal to the summation of the ground motion due to interaction forces plus the free field motion at the same node. The relationship of these displacements can be expressed as following:

$$V_{gi}(t_k)+V_{fi}(t_k)=V_{si}(t_k) \tag{6.1}$$

$$U_{gi}(t_k)+U_{fi}(t_k)=U_{si}(t_k) \tag{6.2}$$

in which,

$V_{gi}(t_k)$ the vertical ground motion in node (strip) i at $t=t_k$ due to the interaction forces.

$U_{gi}(t_k)$ the horizontal ground motion in node (strip) i at $t=t_k$ due to the interaction forces.

$V_{si}(t_k)$ structure vertical displacement in node i at $t=t_k$

$U_{si}(t_k)$ structure horizontal displacement in node i at $t=t_k$

$V_{fi}(t_k)$ the vertical free field motion in node i at $t=t_k$

$U_{fi}(t_k)$ the horizontal free field motion in node i at $t=t_k$

Since the structure foundation base is assumed to be rigid , the values $V_{si}(t_k)$, and $U_{si}(t_k)$ can be expressed as a function of the displacement at the center of gravity of the structure in the vertical, horizontal and rocking directions as shown in Fig 6.5 and 6.6.

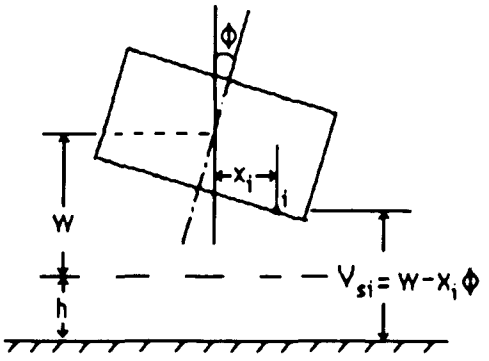

FIG (6.5) vertical displacement of structure

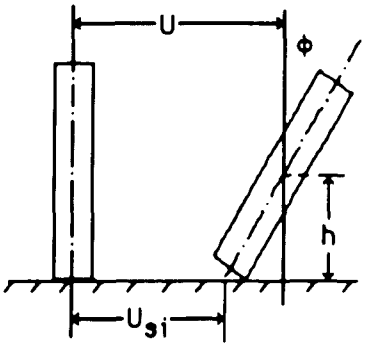

FIG (6.6) horizontal displacement of structure

$$V_{si}(t_k)=w(t_k)-x_i \cdot \Phi(t_k) \qquad (6.3)$$

$$U_{si}(t_k)=U(t_k)-h \cdot \Phi(t_k) \qquad (6.4)$$

in equation (6.3) and (6.4),

$W(t_k)$ the vertical displacement at center of gravity of structure.

x_i the distance from node i to center of base.

$\Phi(t_k)$ the rotation of rigid foundation at $t=t_k$

$U(t_k)$ the horizontal displacement at center of gravity of the structure at $t=t_k$

h the height of the center of gravity for the structure

6.3 Ground Motion Due to The Interaction Forces

Influence functions are developed in Chapter 7 giving the displacement in strip (i) due to a unit pulse applied to strip (j). For example, $VP_{ij}(t_k-t_m)$ is the vertical displacement of strip (i) at time (t_k) caused by a unit vertical pulse applied to

strip (j) at time (t_m). The displacements of ground due to the interaction forces are equal to the summation of the displacement caused by the individual pulse effects, which can be expressed as follows:

$$V_{gi} = \sum_{j=1}^{N} \sum_{m=1}^{k} P_{jm} V_{ij}^{p} (t_k - t_m) + \sum_{j=1}^{N} \sum_{m=1}^{k} H_{jm} V_{ij}^{c} (t_k - t_m) \qquad 6.5$$

$$U_{gi} = \sum_{j=1}^{N} \sum_{m=1}^{k} H_{jm} U_{ij}^{c} (t_k - t_m) + \sum_{j=1}^{N} \sum_{m=1}^{k} P_{jm} U_{ij}^{p} (t_k - t_m) \qquad 6.6$$

in which,

P_{jm} the magnitude of an uniform vertical pulse acting on strip j during the time step Δt_m

H_{jm} the magnitude of an uniform horizontal pulse acting on strip j during the time step Δt_m

$VP_{ij}(t_k-t_m)$, $UP_{ij}(t_k-t_m)$ are vertical and horizontal displacements at surface of an elastic half space due to a vertical unit uniform pulse in a strip.

$VC_{ij}(t_k-t_m)$, $UC_{ij}(t_k-t_m)$ are vertical and horizontal displacements at surface of an elastic half space due to a horizontal unit uniform pulse in a strip.

6.4 General Governing Equations

Substituting equations 6.3 through 6.6 into the equations 6.1 and 6.2, the compatibility equations become:

1) Final compatibility equations

$$\sum_{j=1}^{N}\sum_{m=1}^{k} P_{jm}\, V_{ij}^{p}\,(t_k - t_m) + \sum_{j=1}^{N}\sum_{m=1}^{k} H_{jm}\, V_{ij}^{c}\,(t_k - t_m)$$

$$= W(t_k) - X_i\,\phi(t_k) - V_{fi}(t_k) \qquad (6.7)$$

$$\sum_{j=1}^{N}\sum_{m=1}^{k} H_{jm}\, U_{ij}^{c}\,(t_k - t_m) + \sum_{j=1}^{N}\sum_{m=1}^{k} P_{jm}\, U_{ij}^{p}\,(t_k - t_m)$$

$$= U(t_k) - h\,\phi(t_k) - U_{fi}(t_k) \qquad (6.8)$$

2) Equilibrium Equations of Motion

Since there are 2N+3 unknowns [P_{jk}, H_{jk}, (j=1,..,n), W,ϕ,U] from Eq. (6.7) to (6.8),and only 2N equations, three additional equations are needed to complete the system. The remaining three equations come consideration of the equilibrium of all of forces in three directions (vertical,horizontal, and rocking). The resulting equations are:

$$M \cdot \ddot{W} = \sum_{i=1}^{N} P_{ik} - M \cdot G \qquad (6.9)$$

$$M \cdot \ddot{U} = \sum_{i=1}^{N} H_{ik} \qquad (6.10)$$

$$J \cdot \ddot{\phi} = -\sum_{i=1}^{N} P_{ik} \cdot X_i + M \cdot h \cdot \ddot{U} \qquad (6.11)$$

where,

M ,J the mass and moment of inertia of the structure

$\ddot{W}$, $\ddot{U}$, $\ddot{\phi}$ three accelerations at center of gravity of the structure

G acceleration constant of gravity

h the height of structure center of gravity

Equations (6.7) to (6.11), represent 2 N+3 equations that can be solved for the 2N+3 unknowns.

6.5 Lift Off Model

The structure foundation is assumed to be "welded" to the ground until the structural accelerations become sufficiently large so that the pressures in some strips of foundation tend to be be tensile. The part of foundation with tensile forces will separate from the soil,or "lift off", since soil cannot carry tensile forces.

In order to evaluate the effect of lift off equations (6.9) through (6.11) must be modified. The required modification is relatively simple. During the solution of equations (6.9) to (6.11), the terms needed to be changed is only the P_{im} and H_{im}. If lift off occurs, the pulse term P_{im} must be less than the pressure due to the gravity of structure, and H_{im} should be zero. After lift off the foundation will be back to contact with soil in whole area.

Chapter 7
Displacement Due To Uniform Pulses In A Strip

As Shown in Fig 6.3, the foundation mat is divided into (N) strips to facilitate a numerical solution. The compatibility equations given in Chapter 6 require influence functions giving the displacements (horizontal and vertical) in a strip due to unit pulses (horizontal and vertical) acting in another strip and at some given time after the pulse was applied. These influence functions are developed in This Chapter.

The solutions for the vertically applied pulses are developed from a solution obtained by Pekeris [6] in 1955, and the solution for the horizontally applied pulses are developed from the work of Chao [7] in 1960. In each case the solutions give the displacement at the surface of a half space at a time (t) after point pulse load is applied to the half space at a distance (r) from the point of interest (see Fig 7.1). Each of these basic solutions are given in Appendix B.

The time detail of the load is first converted (in Section 7.1) from the step load form given in the Pekeris and Chao solution to the point pulse (i.e., unity between t_{m-1} and t_m, and zero elsewhere) form required in this study. The effect of a unit point pulse is then (Section 7.2) integrated over the area of a strip (i) to obtain the displacement of any point in strip (j). Finally, an average displacement in strip (j) is obtained (Section 7.3) and this data is used in the compatibility equation of Chapter 6

7.1 Displacements Due to Point Pulse

1). Displacement Due to Unit Step load

As shown in Fig (7.1), points a and b are on the surface of an elastic half space, and the distances to the axis Z are r_1 and r respectively. If a unit vertical step load is applied to point b at time ($t=t_m$), the solution for the vertical displacement, $V_p(r-r_1, t_k-t_M)$, and horizontal displacement, $U_p(r-r_1, t_k-t_M)$, at the surface was derived by Pekeris [6] in 1955.

Similarly, from Chao's solution [7] in 1960, the horizontal and vertical displacement due to a unit horizontal step load are $U_c(r-r_1, t_k-t_M)$ and $U_c(r-r_1, t_k-t_M)$ respectively. These two set of solutions are given in Appendix B1 and B2.

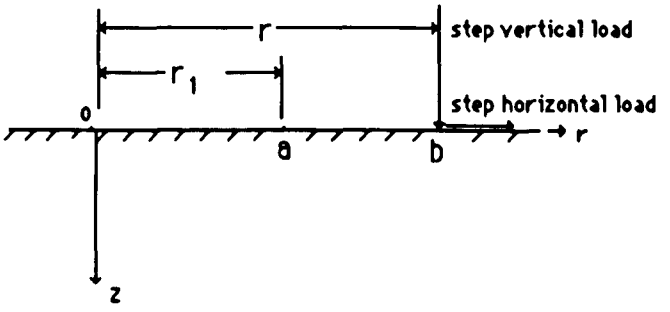

FIG(7.1) AN STEP LOAD APPLIED ON AN ELASTIC HALF SPACE

2). The Definition of The Unit Point Pulse

A unit point pulse is defined as a force of unit magnitude when $t_{M-1} \le t \le t_M$ and zero at other time. By using the Pekeris solution, the displacements (ground motion) due to a vertical point pulse acting on the elastic half space during a time step $\Delta t=t_m-t_{m-1}$ can be defined as follows:

a) In the vertical direction

$$V_f^p(r-r_1, t_k-t_M) = V_p(r-r_1, t_k-t_{M-1}) - V_p(r-r_1, t_k-t_M) \qquad (7.1)$$

b) In the horizontal direction

$$U_f^p(r-r_1, t_k-t_M) = U_p(r-r_1, t_k-t_{M-1}) - U_p(r-r_1, t_k-t_M) \qquad (7.2)$$

Similarly, by using Chao's solution, the displacements (ground motion) due to horizontal point pulse acting on the elastic half space during a time step $\Delta t = t_m - t_{m-1}$ can be obtained as:

a) In the vertical direction

$$V_f^c(\, r-r_1, t_k-t_M) = V_c(\, r-r_1, t_k-t_{M-1}) - V_c(\, r-r_1, t_k-t_M) \qquad (7.3)$$

b) In the horizontal direction

$$U_f^c(\, r-r_1, t_k-t_M) = U_c(\, r-r_1, t_k-t_{M-1}) - U_c(\, r-r_1, t_k-t_M) \qquad (7.4)$$

in which,

$V_f^p(\, r-r_1, t_k-t_M)$ and $V_f^c(\, r-r_1, t_k-t_M)$ are the vertical displacement at the surface of an elastic half space caused by a unit point pulse during time step t_{m-1} to t_m.

$U_f^p(\, r-r_1, t_k-t_M)$ and $U_f^c(\, r-r_1, t_k-t_M)$ are the horizontal displacement at the surface of an elastic half space caused by a unit point pulse during time step t_{m-1} to t_m.

7.2 Displacement at Any Point (x_1, y_1) in strip (j) Due to The Total Unit Uniform Pulse Acting on Strip (i)

The foundation is divided into N strips. The displacement at the interface of the ground caused by the total pulse that is uniformly distributed over a strip (i) can be obtained as follows:

a) When i is different from j

$$V^{p}_{ij}(x_1, y_1, t_k - t_m) = \int_{-b}^{b} \int_{x_0 - \frac{\Delta}{2}}^{x_0 + \frac{\Delta}{2}} V^{p}_{f}(|r - r_1|, t_k - t_m)\, dx\, dy \qquad (7.5)$$

$$U^{p}_{ij}(x_1, y_1, t_k - t_m) = \int_{-b}^{b} \int_{x_0 - \frac{\Delta}{2}}^{x_0 + \frac{\Delta}{2}} U^{p}_{f}(|r - r_1|, t_k - t_m)\, dx\, dy \qquad (7.6)$$

$$V^{c}_{ij}(x_1, y_1, t_k - t_m) = \int_{-b}^{b} \int_{x_0 - \frac{\Delta}{2}}^{x_0 + \frac{\Delta}{2}} V^{c}_{f}(|r - r_1|, t_k - t_m)\, dx\, dy \qquad (7.7)$$

$$U^{c}_{ij}(x_1, y_1, t_k - t_m) = \int_{-b}^{b} \int_{x_0 - \frac{\Delta}{2}}^{x_0 + \frac{\Delta}{2}} U^{c}_{f}(|r - r_1|, t_k - t_m)\, dx\, dy \qquad (7.8)$$

$$|r - r_1| = \sqrt{(x - x)^2 + (y - y_1)^2}$$

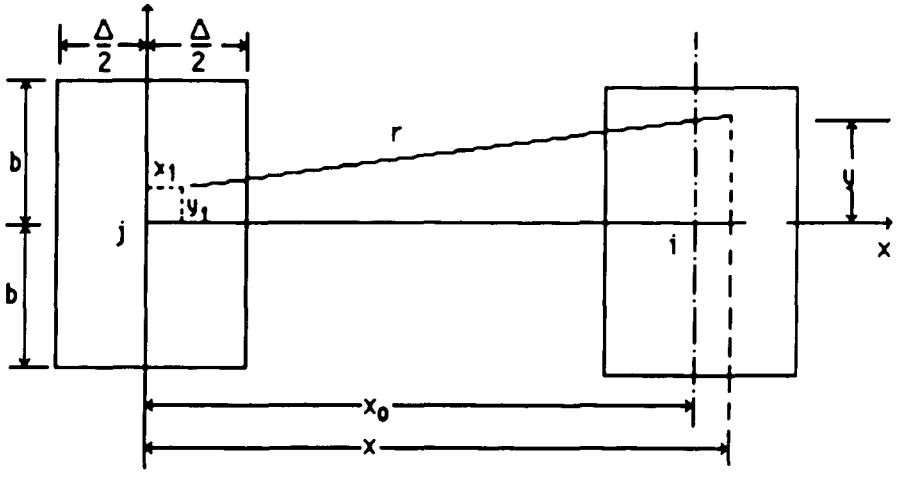

Fig (7.2) displacement at point (X_1, Y_1) in strip i due to the pulse over strip j

b) When i is the same as j

$$V^{p}_{ij}(x_1, y_1, t_k - t_m) = \int_{-b}^{b} \int_{-\frac{a}{2}}^{+\frac{a}{2}} V^{p}_{f}(|r - r_1|, t_k - t_m)\, dx\, dy \qquad (7.9)$$

$$U^{p}_{ij}(x_1, y_1, t_k - t_m) = \int_{-b}^{b} \int_{-\frac{a}{2}}^{+\frac{a}{2}} U^{p}_{f}(|r - r_1|, t_k - t_m)\, dx\, dy \qquad (7.10)$$

$$V^{c}_{ij}(x_1, y_1, t_k - t_m) = \int_{-b}^{b} \int_{-\frac{a}{2}}^{+\frac{a}{2}} V^{c}_{f}(|r - r_1|, t_k - t_m)\, dx\, dy \qquad (7.11)$$

$$U^{c}_{ij}(x_1, y_1, t_k - t_m) = \int_{-b}^{b} \int_{-\frac{a}{2}}^{+\frac{a}{2}} U^{c}_{f}(|r - r_1|, t_k - t_m)\, dx\, dy \qquad (7.12)$$

$$|r - r_1| = \sqrt{(x - x_1)^2 + (y - y_1)^2}$$

here,

$V^{p}_{ij}(x_1, y_1, t_k - t_M)$ is the vertical displacement of any point within strip i caused by the vertical unit uniform pulse over the strip j

$U^{p}_{ij}(x_1, y_1, t_k - t_M)$ is the horizontal displacement of any point within strip i caused by the vertical unit uniform pulse over the strip j

$V^{c}_{ij}(x_1, y_1, t_k - t_M)$ is the vertical displacement of any point within strip i caused by the horizontal unit uniform pulse over the strip j

$U^{c}_{ij}(x_1, y_1, t_k - t_M)$ is the horizontal displacement of any point within strip i caused by the horizontal unit uniform pulse over the strip j

The integration regions are shown on Fig 7.2 or Fig 7.3.In order to illustrate how the displacements described above vary throughout the strip, some values of those displacements are calculated and plotted. All results are based on a unit uniform pulse applied during the time step (t=0.000-0.002).

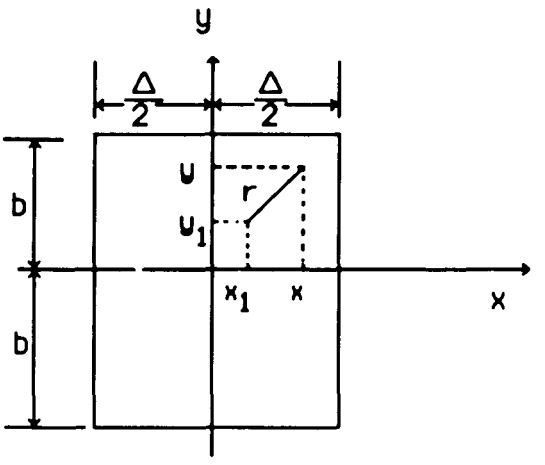

Fig (7.3) displacement at point (X_1, Y_1) in strip i due to the pulse over strip i

Figs. 7.4 and 7.5 illustrate the variation of the three displacements, V^P_{ij},(V^C_{ij} or U^P_{ij}), U^C_{ij}, along the y direction, when the pulse is applied in its own strip. These displacements occur at the end of the point pulse (i.e., t=0.002 sec.). Figs. 7.6 and 7.7 illustrate the variation of the displacements with y caused by a unit uniform pulse acting in other strips. Again, the displacements are at t=0.002 sec. The shapes of these curves are similar. The peak values of displacement are concentrated in the middle region of the strip. It can be seen that the peak values are much greater than the others along the y direction.

Fig 7.8 gives the three displacements varying along the width (x direction) of strip 1 when the unit uniform pulse is applied in strip 1. Similar to Fig 7.8, a displacement caused by an unit uniform pulse applied in strip 2 is shown in Fig 7.9. Since the width of a strip is relatively small, the values of displacements along the width are not so different.

In this dissertation the foundation base is only divided in one direction (x), and the displacement of a strip is computed by taking the average for the whole strip as determined in the following section.

7.3 Average Displacement Over A Strip.

The average displacement over a strip due to a unit uniform pulse can be obtained by integrating the displacements from equations (7.5) to (7.12), and then dividing by the area of the strip.

a) in vertical direction

$$V^{p}_{ij}(t_k - t_m) = \frac{1}{A}\int_{-b}^{b}\int_{-\frac{a}{2}}^{+\frac{a}{2}} V^{p}_{ij}(x_1, y_1, t_k - t_m)\, dx\, dy \qquad (7.13)$$

$$V^{c}_{ij}(t_k - t_m) = \frac{1}{A}\int_{-b}^{b}\int_{-\frac{a}{2}}^{+\frac{a}{2}} V^{c}_{ij}(x_1, y_1, t_k - t_m)\, dx\, dy \qquad (7.14)$$

b) in horizontal direction

$$U^{c}_{ij}(t_k - t_m) = \frac{1}{A}\int_{-b}^{b}\int_{-\frac{a}{2}}^{+\frac{a}{2}} U^{c}_{ij}(x_1, y_1, t_k - t_m)\, dx\, dy \qquad (7.15)$$

$$U^{p}_{ij}(t_k - t_m) = \frac{1}{A}\int_{-b}^{b}\int_{-\frac{a}{2}}^{+\frac{a}{2}} U^{p}_{ij}(x_1, y_1, t_k - t_m)\, dx\, dy \qquad (7.16)$$

where,

$VP_{ij}(t_k - t_m)$ is the average vertical displacement of soil in strip i at $t = t_k - t_m$ caused by a vertical unit uniform pulse ($P_{jm} = 1$) applied over strip j

$UP_{ij}(t_k - t_m)$ is the average horizontal displacement of soil in strip i at $t = t_k - t_m$ caused by a vertical unit uniform pulse acting over strip j

$VC_{ij}(t_k - t_m)$ is the average vertical displacement of soil in strip i at $t = t_k - t_m$ caused by a horizontal unit uniform pulse ($P_{jm} = 1$) acting over strip j

$UC_{ij}(t_k - t_m)$ is the average horizontal displacement of soil in strip i at $t = t_k - t_m$ caused by a horizontal unit uniform pulse acting over strip j.

The coefficients in equations (6.5) and (6.6), $VP_{ij}(t_k-t_m)$, $UP_{ij}(t_k-t_m)$, $VC_{ij}(t_k-t_m)$, and $UC_{ij}(t_k-t_m)$ are the average displacements due to a unit uniform pulse applied to a strip.

The average displacement in strip i due to unit uniform pulse acting on a strip has been calculated and plotted in Figs. 7.10 to 7.18. Fig 7.10 through 7.14 show the displacement of a strip center varying along the X axis. Since the waves are mixed together the mixed wave shape is propagating from left edge (x=o) to the right edge (x=30) of the foundation base when time increases. It can be seen that the mixed wave shape travels rather fast so that the displacements vanish rapidly as the distance from the center of that strip to point of interest increases. Figs. 7.15 to 7.18 illustrate the variations of displacement with time. It can be seen that displacements are concentrated in a small time region. Beyond this region, the values of displacement vanish.

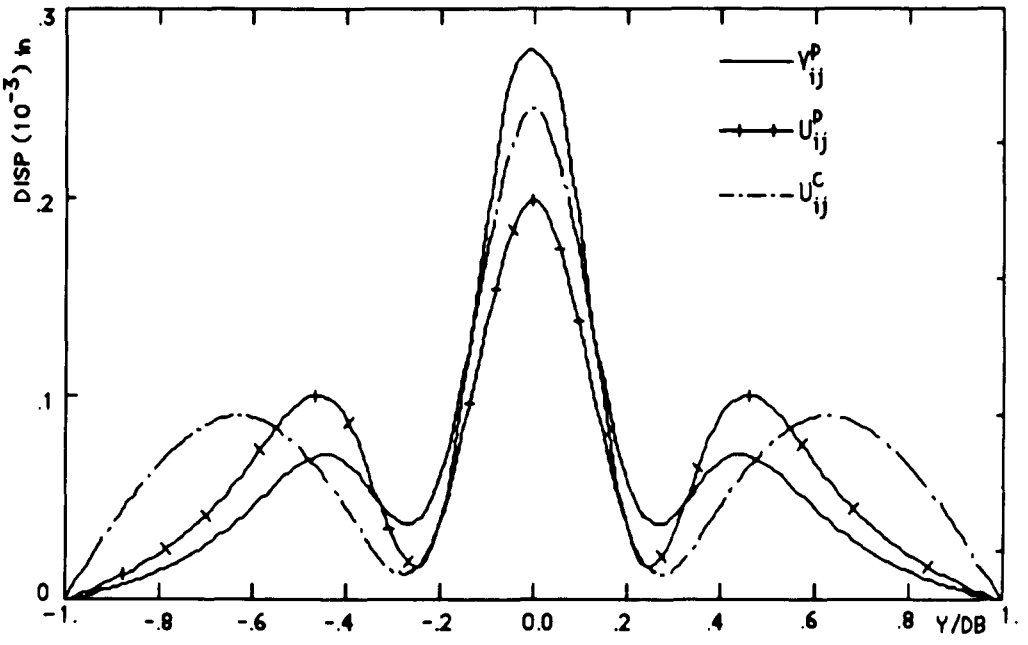

FIG(7.4) DISP IN STRIP 1 VARYING WITH Y CAUSED BY A UNIT UNIFORM PULSE ACTING IN STRIP 1 T=(0.000-0.002)

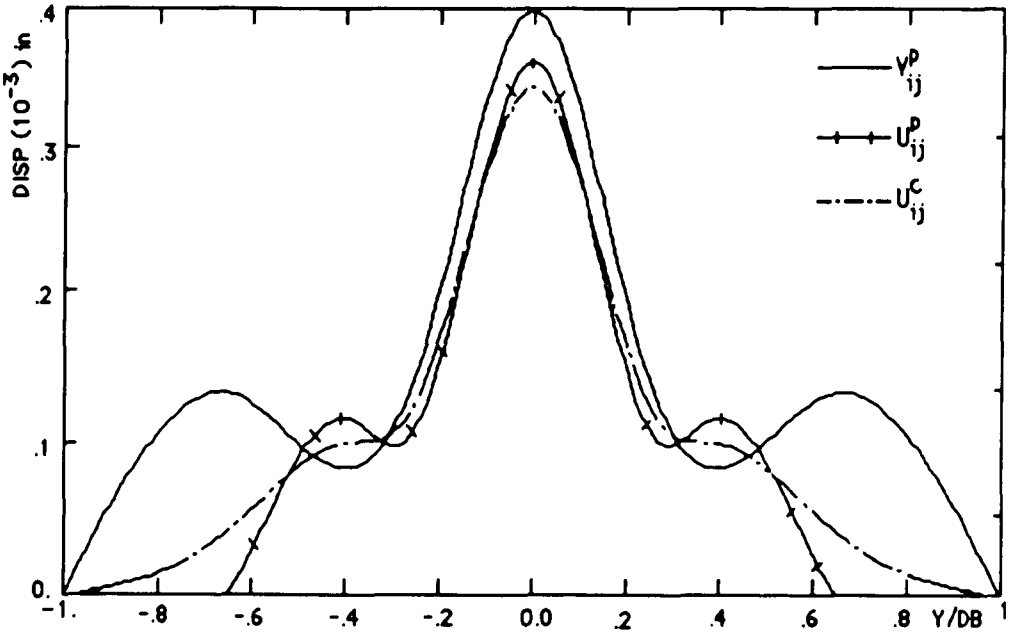

FIG(7.5) DISP. IN STRIP 7 VARYING WITH Y CAUSED BY A UINT UNIFORM PULSE ACTING IN STRIP 7 T=(0.000-0.002)

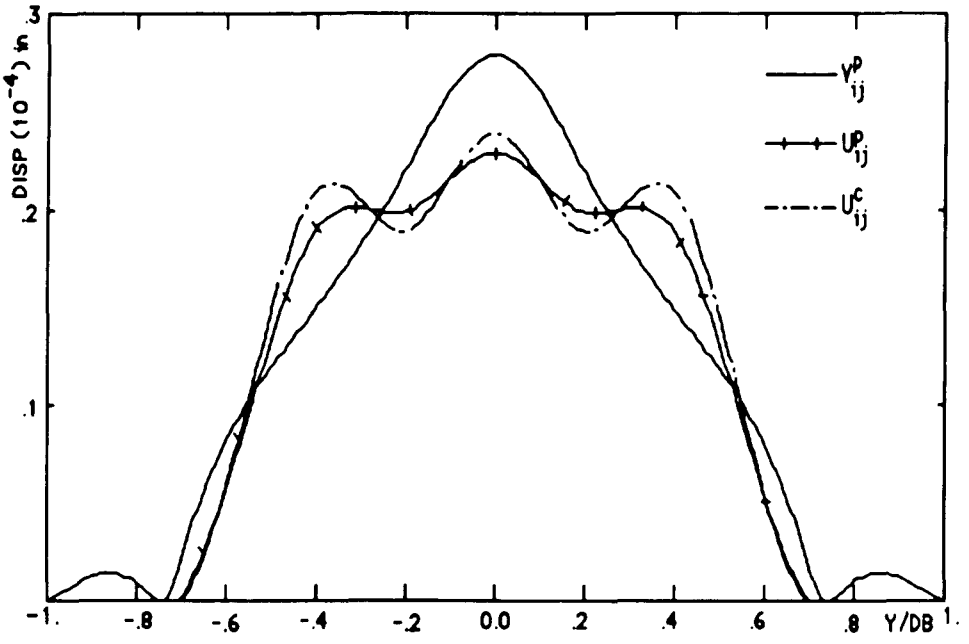

FIG(7.6) DISP. IN STRIP 2 VARYING WITH Y CAUSED BY A UNIT UNIFORM PULSE ACTING IN STRIP 1 T=(0.000-0.002)

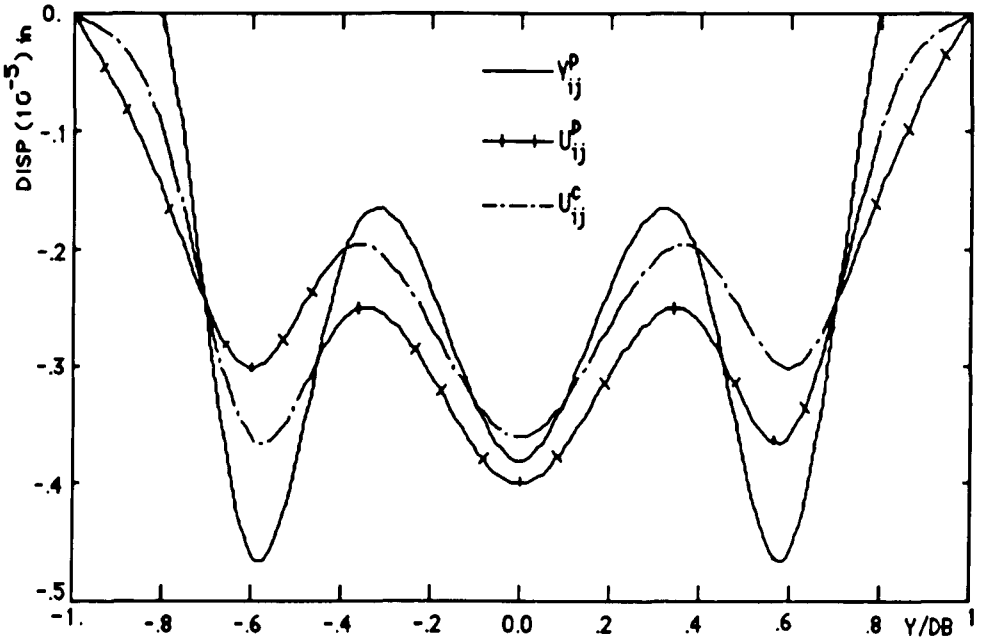

FIG(7.7) DISP. IN STRIP 3 VARYING WITH Y CAUSED BY A UNIT UNIFORM PULSE IN STRIP 1 T=(0.000-0.002)

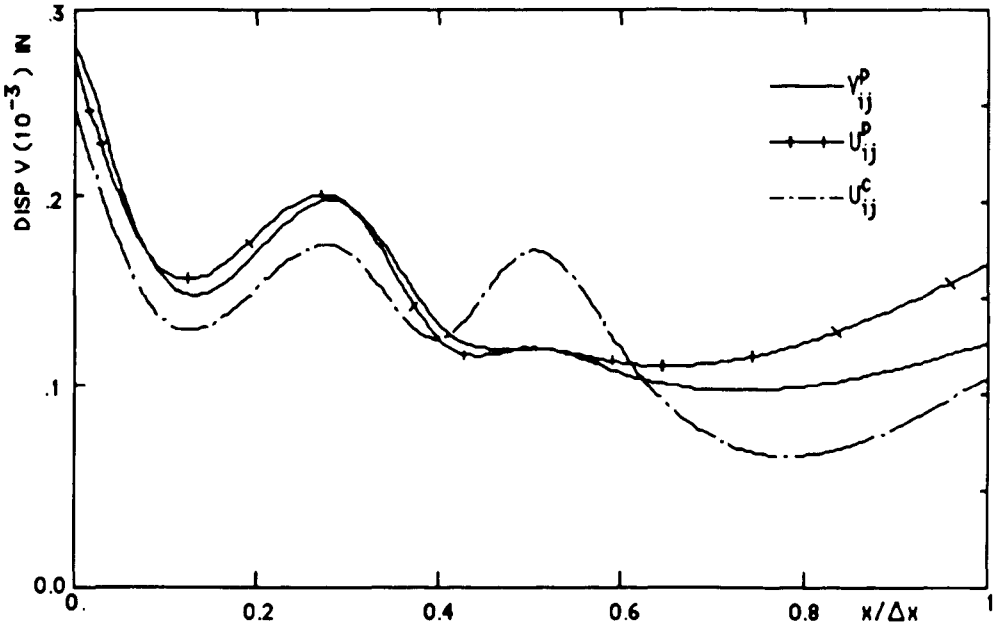

FIG(7.8) DISP. OF STRIP 1 VARYING WIDTH Δx CAUSED BY A UNIT UNIFORM PULSE IN STRIP 1 T=(0.000-0.002)

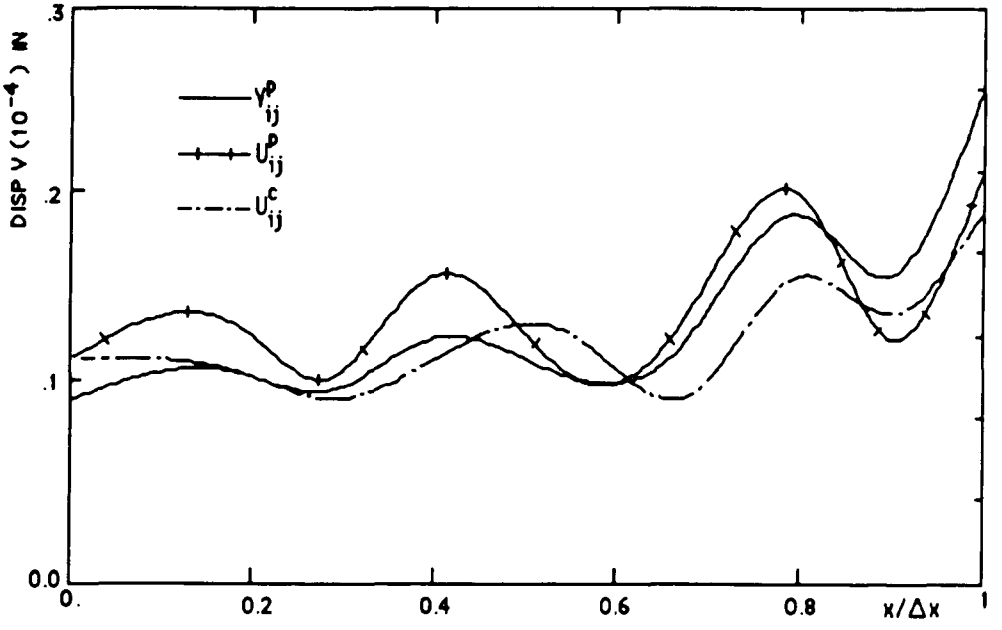

FIG(7.9) DISP. OF STRIP 1 VARYING WIDTH Δx CAUSED BY A UNIT UNIFORM PULSE IN STRIP 2. T=(0.000-0.002)

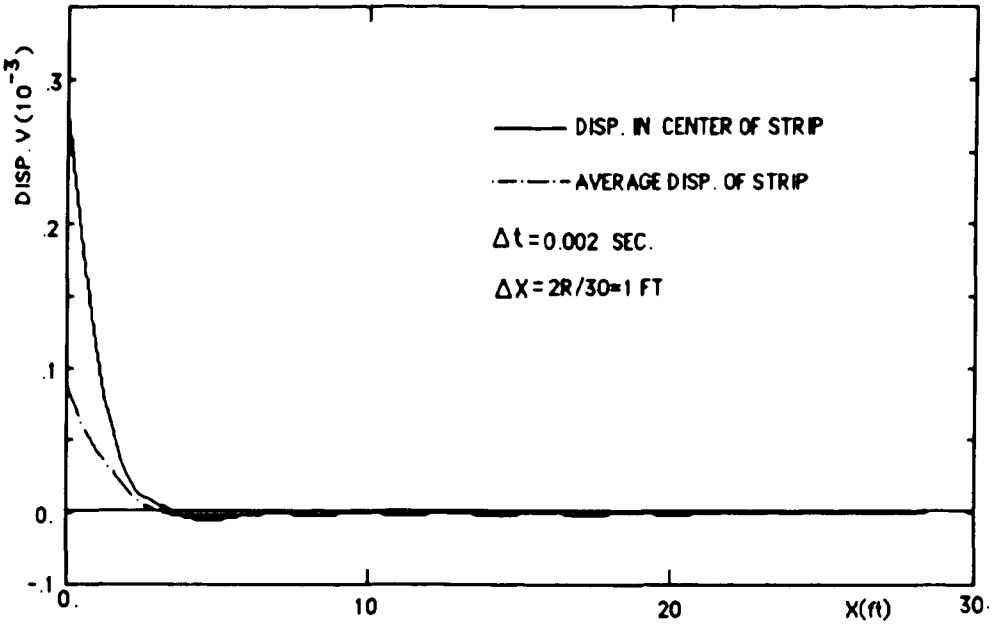

FIG (7.10) DISP. IN STRIP 1 DUE TO UNIT UNIFORM PULSE ACTING OVER STRIP i AT TIME STEP 1 T=(0.000-0.002)

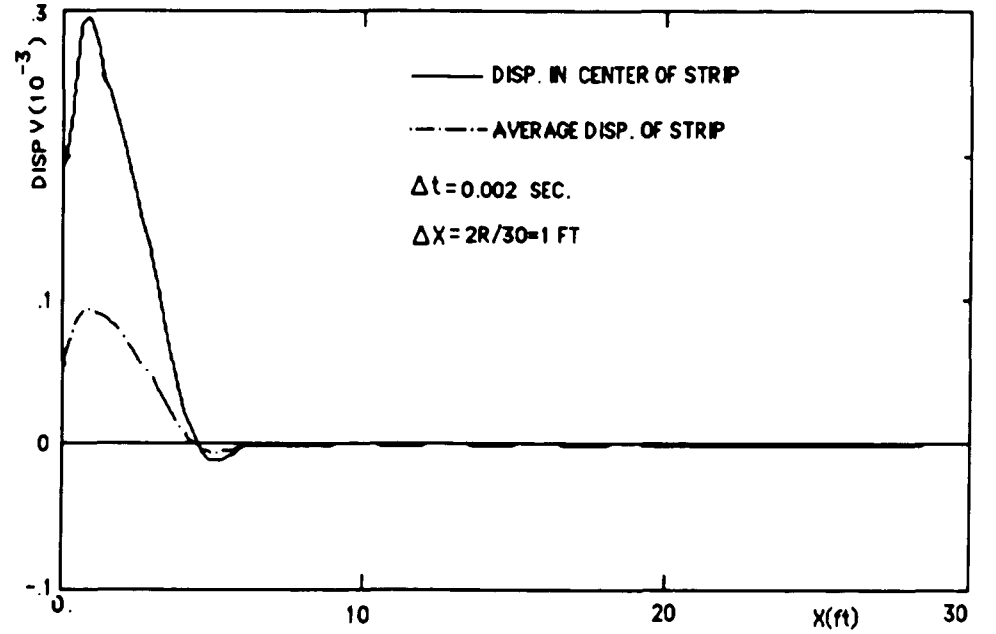

FIG (7.11) DISP. IN STRIP 2 DUE TO UNIT UNIFORM PULSE ACTING OVER STRIP i AT TIME STEP 1 T=(0.000-0.002)

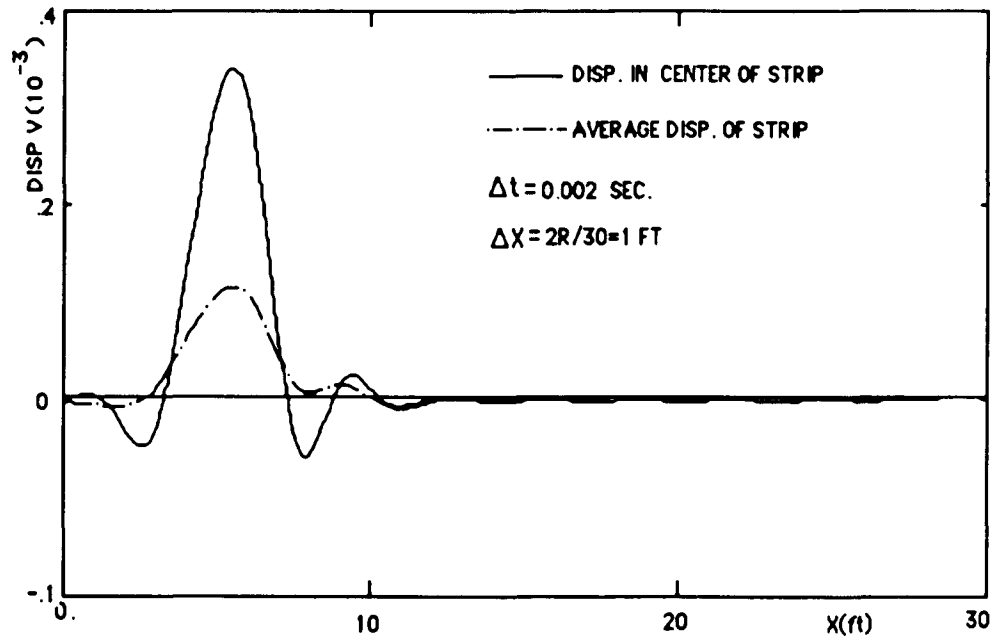

FIG (7.12) DISP. IN STRIP 5 DUE TO UNIT UNIFORM PULSE ACTING OVER STRIP i AT TIME STEP 1 T=(0.000-0.002)

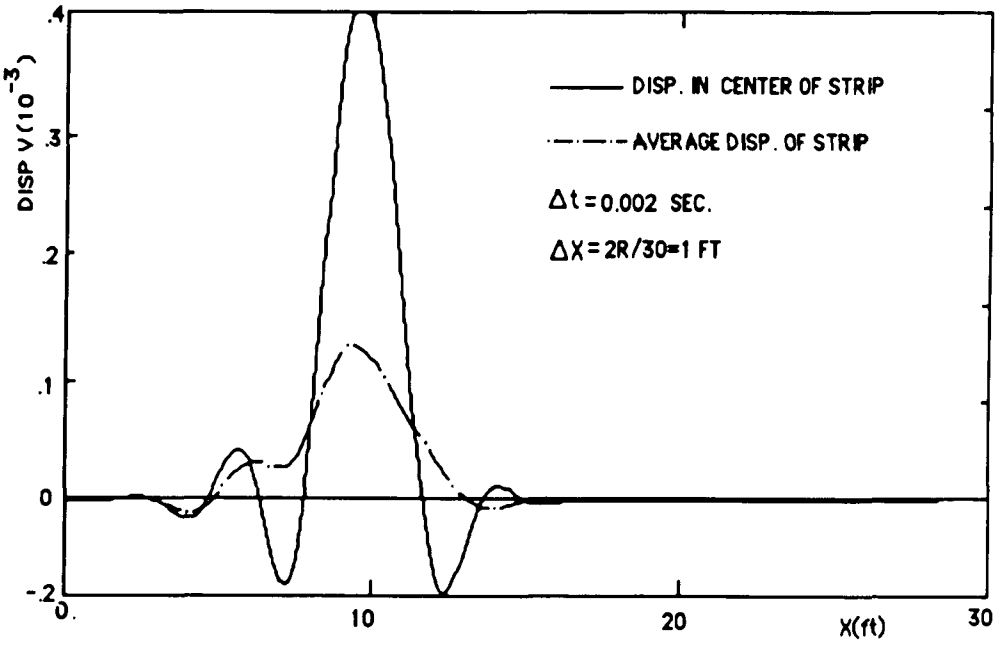

FIG (7.13) DISP. IN STRIP 10 DUE TO UNIT UNIFORM PULSE ACTING OVER STRIP i AT TIME STEP 1 T=(0.000-0.002)

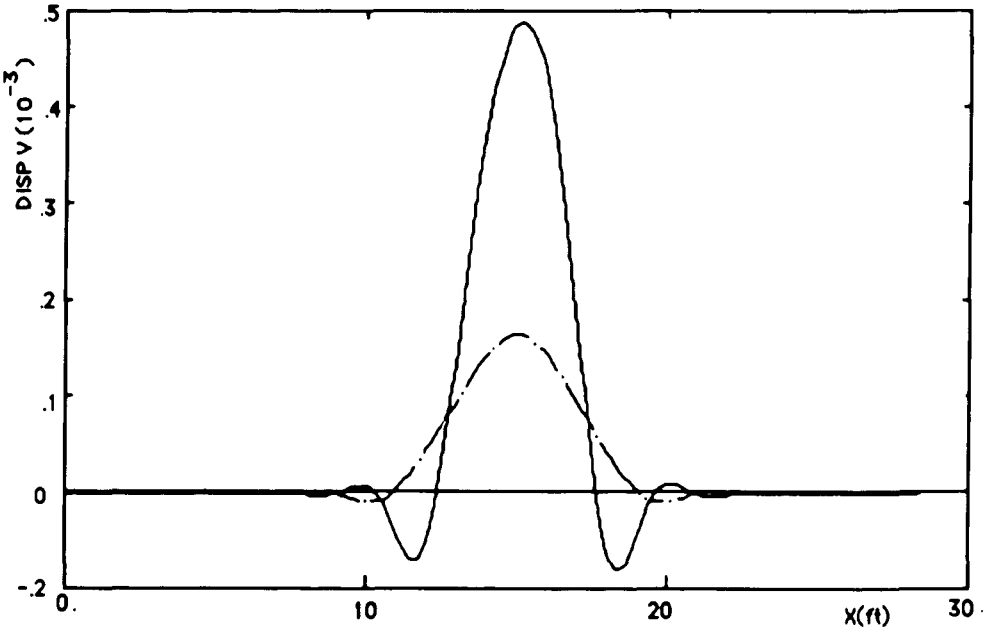

FIG (7.14) DISP. IN STRIP 15 DUE TO UNIT UNIFORM PULSE ACTING OVER STRIP i AT TIME STEP 1 T=(0.000-0.002)

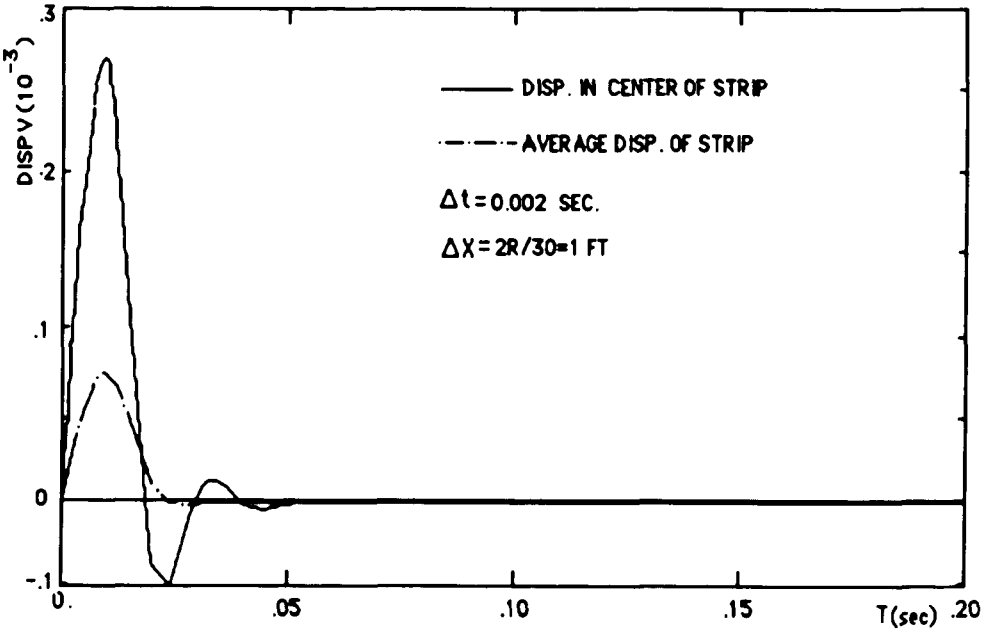

FIG (7.15) DISP. IN STRIP 1 DUE TO UNIT UNIFORM PULSE ACTING OVER STRIP 1 VARYING WITH TIME

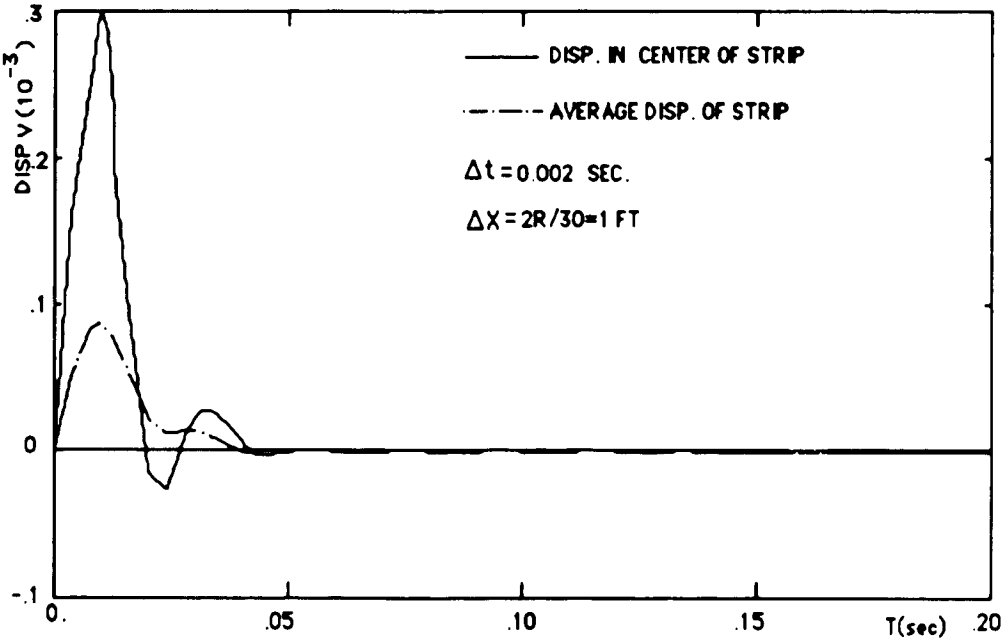

FIG (7.16) DISP. IN STRIP 2 DUE TO UNIT UNIFORM PULSE ACTING OVER STRIP 2 VARYING WITH TIME

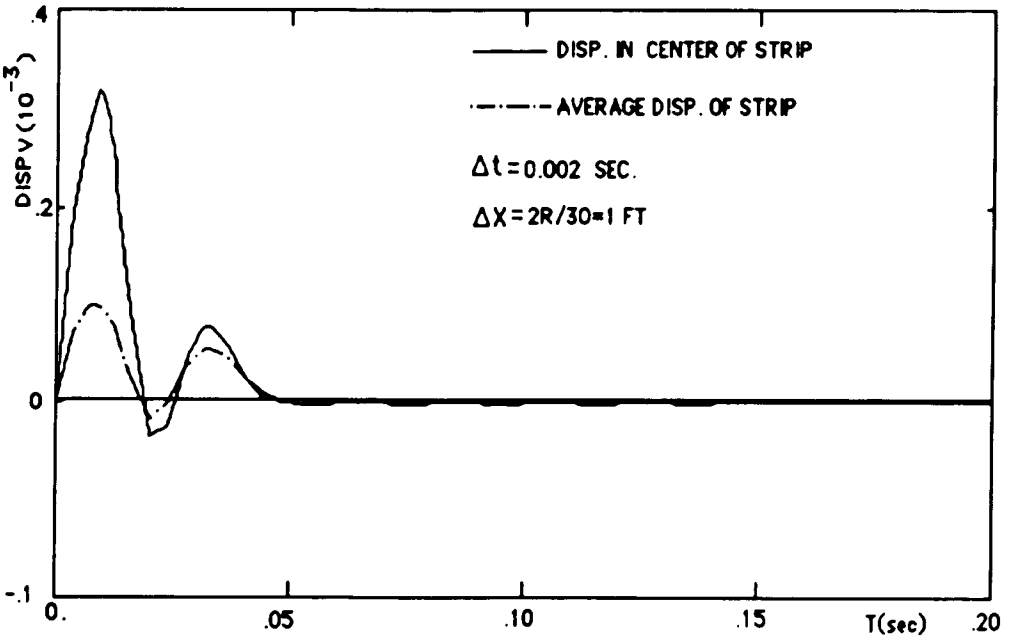

FIG(7.17) DISP. IN STRIP 5 DUE TO UNIT UNIFORM PULSE ACTING OVER STRIP 5 VARYING WITH TIME

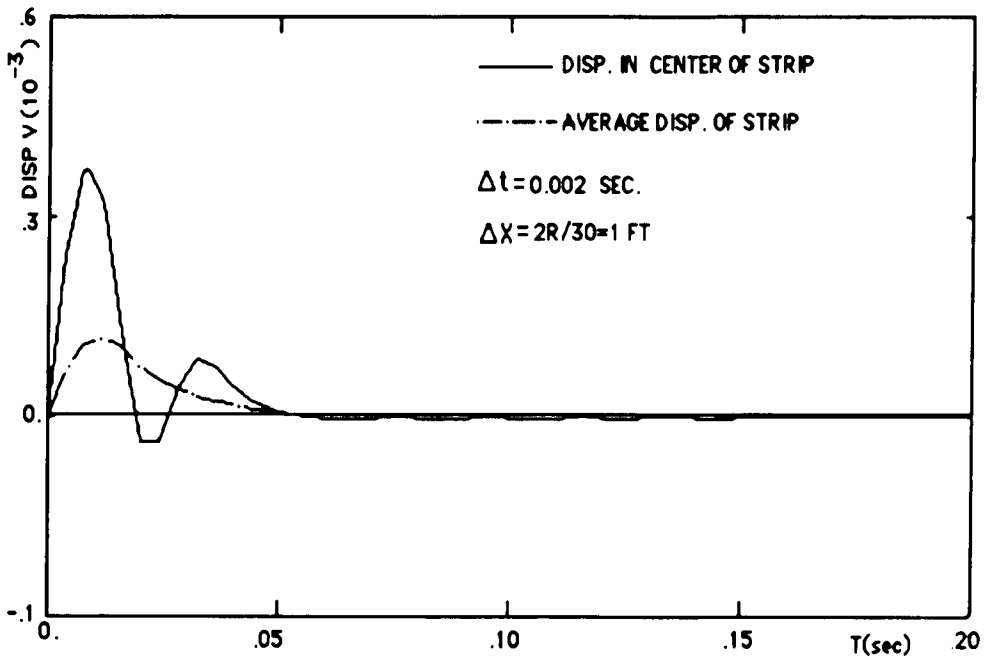

FIG (7.18) DISP. IN STRIP 7 DUE TO UNIT UNIFORM PULSE ACTING OVER STRIP 7 VARYING WITH TIME

Chapter 8
Numerical Techniques

8.1 Introduction

The numerical method used to solve the equations are developed in this Chapter. A Runge-Kutta fourth order integration method is used to solve the equations from (6.7) to (6.11). First two of these equations,(6.7)and (6.8), are solved for the vertical and horizontal pulses that are applied in each strip in terms of the center gravity displacement and rotation of the foundation at time ($t=t_k$). Since uniform pulses applied at times far removed from (t_k) do not contribute to the deformation at (t_k) as described in Chapter 7, one only needs to consider the effects of forces applied near the time $t=t_k$. Therefore the problem becomes simple. Second, a computer code for this method is developed. Finally in order to illustrate the sensitivity of the solution to equations (6.7) through (6.11) to variation in the width of strip Δx,and time increment Δt, the pressures in a strip are computed. The results indicate that the pressure in a strip converges to a constant value when Δx and Δt become smaller.

8.2 The Uniform Pulse In A Strip

It is of special interest to examine the terms in equations(6.7) to (6.8) when m=k. Due to the finite time required for a disturbance to travel across the ground and according to the solutions of Pekeris and Chao, if i is not equal j, we know that,

$$V_{ij}^{p}(0)=0; \qquad V_{ij}^{c}(0)=U_{ij}^{p}(0)=0; \qquad U_{ij}^{c}(0)=0$$

If we substitute above conditions into equations (6.7) and (6.8) , and rewrite them as:

$$P_{ik}\ V^{p}_{ii}(o) + H_{ik}\ V^{c}_{ii}(o) = W(t_k) - X_i\,\phi(t_k) - V_{fi}(t_k)$$

$$-\sum_{j=1}^{NK-1}\sum_{m=1} P_{jm}\,V^{p}_{ij}(t_k - t_m) - \sum_{j=1}^{NK-1}\sum_{m=1} H_{jm}\,V^{c}_{ij}(t_k - t_m) \qquad (8.1)$$

$$P_{ik}\ U^{c}_{ii}(o) + H_{ik}\ U^{p}_{ii}(o) = U(t_k) - h\,\phi(t_k) - U_{fi}(t_k)$$

$$-\sum_{j=1}^{NK-1}\sum_{m=1} P_{jm}\,U^{p}_{ij}(t_k - t_m) - \sum_{j=1}^{NK-1}\sum_{m=1} H_{jm}\,U^{c}_{ij}(t_k - t_m) \qquad (8.2)$$

$$(i \neq j)$$

If we set

$$R_v = W(t_k) - X_i\,\phi(t_k) - V_{fi}(t_k)$$

$$-\sum_{j=1}^{NK-1}\sum_{m=1} P_{jm}\,V^{p}_{ij}(t_k - t_m) - \sum_{j=1}^{NK-1}\sum_{m=1} H_{jm}\,V^{c}_{ij}(t_k - t_m) \qquad (8.3)$$

$$R_H = U(t_k) - h\,\phi(t_k) - U_{fi}(t_k)$$

$$-\sum_{j=1}^{NK-1}\sum_{m=1} P_{jm}\,U^{p}_{ij}(t_k - t_m) - \sum_{j=1}^{NK-1}\sum_{m=1} H_{jm}\,U^{c}_{ij}(t_k - t_m) \qquad (8.4)$$

$$(i \neq j)$$

and notice $V^{c}_{ii}(o) = U^{p}_{ii}(o)$ the equations (8.1) and(8.2) become

$$P_{ik}\ V^{p}_{ii}(o) + H_{ik}\ V^{c}_{ii}(o) = R_V \qquad (8.5)$$

$$P_{ik}\ V^{c}_{ii}(o) + H_{ik}\ U^{c}_{ii}(o) = R_H \qquad (8.6)$$

Solve for P_{ik} and H_{ik}.

$$P_{ik} = \frac{R_v U_{ii}^c(o) - R_H V_{ii}^c(o)}{V_{ii}^p(o)U_{ii}^c(o) - [V_{ii}^c(o)]^2} \tag{8.7}$$

$$H_{ik} = \frac{R_H V_{ii}^p(o) - R_v V_{ii}^c(o)}{V_{ii}^p(o)U_{ii}^c(o) - [V_{ii}^c(o)]^2} \tag{8.8}$$

in which, i=1,2,3,.....,N; j=1,2,3,.....,N (i=j)

Equations (8.7) and (8.8) can then be used to compute the uniform pulse applied to each strip in the foundation. Since P_{ik} and H_{ik} are functions of W,U and ϕ, these two values must then be determined with equations (6.9) through (6.11) simultaneously.

8.3 Numerical Technique

The Runge-Kutta fourth order integration method is used to solve the three second order differential equations (6.9) to (6.11) that were developed in Chapter 6.

Assuming the right hand of those equations are

$$f_1(t_k,W,U,\phi) = \frac{1}{M}\sum_{i=1}^{N} P_{ik} - G \tag{8.9}$$

$$f_2(t_k,W,U,\phi) = \frac{1}{M}\sum_{i=1}^{N} H_{ik} \tag{8.10}$$

$$f_3(t_k,W,U,\phi) = -\frac{1}{J}\sum_{i=1}^{N} P_{ik}\cdot X_i + \frac{M}{J}h\ddot{U} \tag{8.11}$$

$y_1 = U; \qquad \dot{y}_1 = \ddot{U};$

$y_2 = \phi; \qquad \dot{y}_2 = \ddot{\phi}$

$y_3 = W; \qquad \dot{y}_3 = \dot{W};$

The equations (7.9) to (7.11) can simply be written as

$$\dot{y}_i = f_i\,(t_k, y_1, y_2, y_3) \tag{8.12}$$

If we set

$$\dot{y}_i = Q_i\,(t_k) \tag{8.13}$$

$$\dot{Q}_i = f_i\,(t_k, y_1, y_2, y_3) \tag{8.14}$$

the Runge-Kutta integration method formula must be

$$y_{k+1,i} = y_{k,i} + \frac{\Delta t}{6}\left(\alpha_{i1} + 2\alpha_{i2} + 2\alpha_{i3} + \alpha_{i4}\right) \tag{8.15}$$

$$Q_{k+1,i} = Q_{k,i} + \frac{\Delta t}{6}\left(\beta_{i1} + 2\beta_{i2} + 2\beta_{i3} + \beta_{i4}\right) \tag{8.16}$$

where,

$$\alpha_{i1} = f_i\,(t_k, y_{k1}, y_{k2}, y_{k3}) \tag{8.17}$$

$$\alpha_{i2} = f_i\left(t_k + \frac{\Delta t}{2},\ y_{k1} + \frac{\Delta t}{2}\alpha_{11},\ y_{k2} + \frac{\Delta t}{2}\alpha_{21} + y_{k3} + \frac{\Delta t}{2}\alpha_{31}\right) \tag{8.18}$$

$$\alpha_{i3} = f_i\left(t_k + \frac{\Delta t}{2},\ y_{k1} + \frac{\Delta t}{2}\alpha_{12},\ y_{k2} + \frac{\Delta t}{2}\alpha_{22} + y_{k3} + \frac{\Delta t}{2}\alpha_{32}\right) \tag{8.19}$$

$$\alpha_{i4} = f_i\left(t_k + \Delta t,\ y_{k1} + \Delta t\,\alpha_{12},\ y_{k2} + \Delta t\,\alpha_{22} + y_{k3} + \Delta t\,\alpha_{32}\right) \tag{8.20}$$

$$\beta_{i1} = Q_i(t_k) \tag{8.21}$$

$$\beta_{i2} = Q_i(t_k + \frac{\Delta t}{2}) \tag{8.22}$$

$$\beta_{i3} = Q_i(t_k + \frac{\Delta t}{2}) \tag{8.23}$$

$$\beta_{i4} = Q_i(t_k + \Delta t) \tag{8.24}$$

in which,

Δt, time increment

i=1,2,3; k=1,2,3,...k_t

8.4 Computer Code

A computer program has been prepared to carry out the above analysis and a flow chart for this code is shown in Fig (8.1). In the beginning of this code,the displacement $VP_{ij}(t_k-t_m)$, $V^C_{ij}(t_k-t_m)$,or $UP_{ij}(t_k-t_m)$, and $U^C_{ij}(t_k-t_m)$ due to unit uniform pulse are computed and stored in the array PET(m,i,j),where i and j are the index number referring to the range between two segments i and j, and the index (m) refers to the number of time increments. A sufficient number of time steps are stored to reach the time when the values of those displacements can be neglected. An outline of the computer code scheme is described as following:

1) Set initial conditions

When t=0 (k=1)

$$y_i(0)=0$$

$$\dot{y}_i(0)=0$$

$$\ddot{y}_1(0)=\ddot{U}(0)=0$$

$$\ddot{y}_2(0)=\ddot{V}(0)-G$$

$$\ddot{y}_3(0)=\ddot{\phi}(0)=0$$

2) Compute the uniform pulse, P_{im} and H_{im},over the strip i at a special time step Δt_m.

3) Solving equations (8.15) through (8.24), the displacements $y_i(t_{k+1})$ are obtained by means of the Runge-Kutta integration method.

4) Repeat over the procedures 2) and (3) until to end of the time.

8.5 Effect of Strip Width ΔX And Time Step Δt

This Section will give some results to illustrate the dependence of the solution on the strip width Δx and time step Δt . All results in this section are based on the soil structure interaction system that consists of a rigid cylinder and an elastic half space (soil ground). The structure with radius (R=20 ft) sits on the surface of the soil ground. The properties of the structure and soil are

weight of structure	M= 1628 kips
shear modulus of soil	G=980 ksf
soil density	γ_s=0.11 kcf
Poisson's ratio	μ=0.25

The time increment Δt varies from 0.001 to 0.01 sec; and the width of strip $\Delta x = 2R/N$ varies from 8 to 0.4 ft. The earthquake motion described in Section 4.2 is used as input. The pressures acting on different strips at a time $t_k = 0.01$ sec. are computed and illustrated in Fig (8.2) to (8.12).

It is follows that a value of N approaching 60 is required to have good data regarding the pressure distribution under the foundation. Undoubtedly much smaller values of N could be used if the response of the structure was of primary interest rather than a detailed evaluation of the pressure distribution under the foundation. The results for the time increment lead to the conclusion that a value of $\Delta t = 0.003$ sec leads to good predictions of pressure.

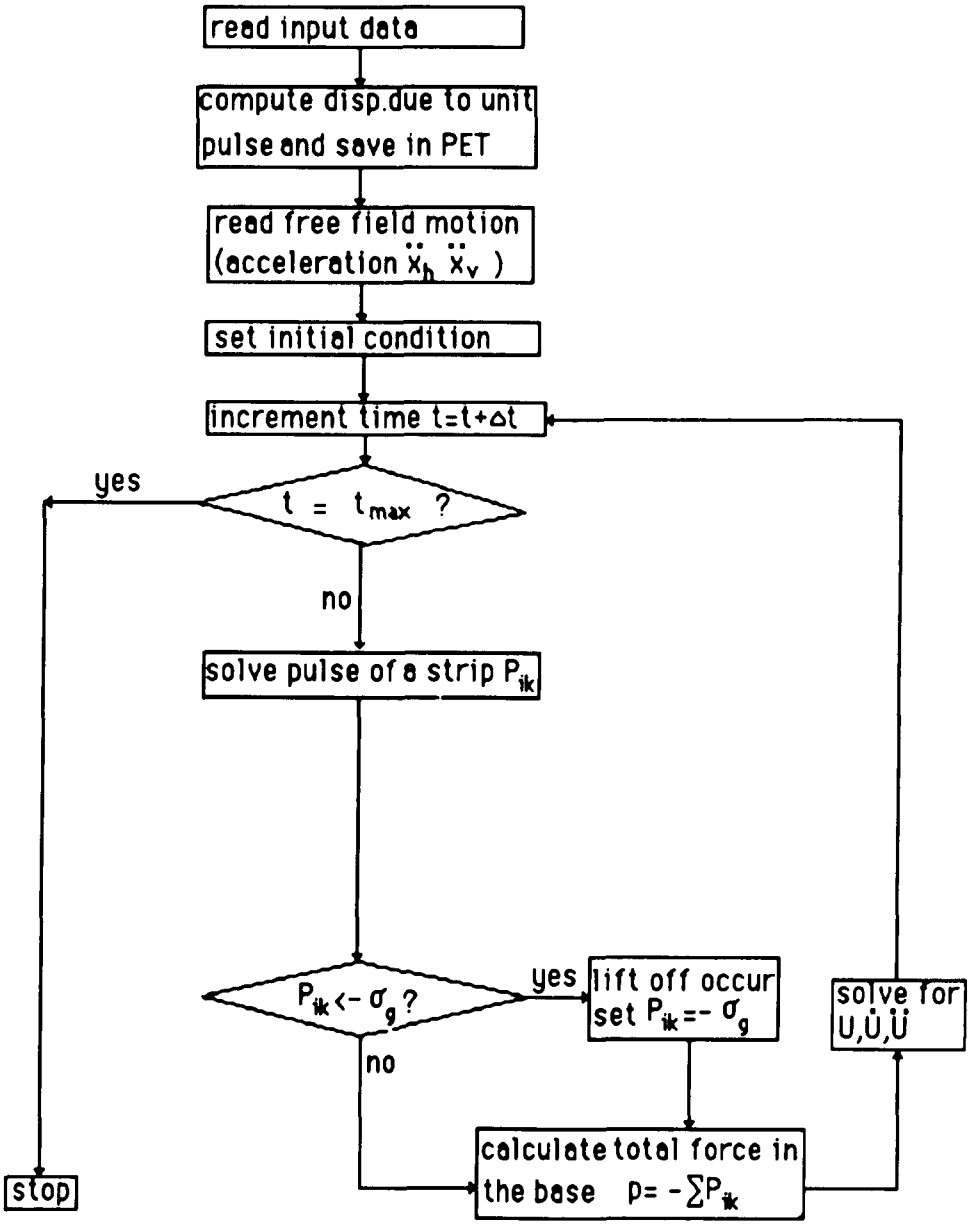

σ_g = PRESSURE CAUSED BY THE WEIGHT OF STRUCTURE

FIG (8.1) COMPUTER CODE OF CONTINUUM MECHANIC METHOD

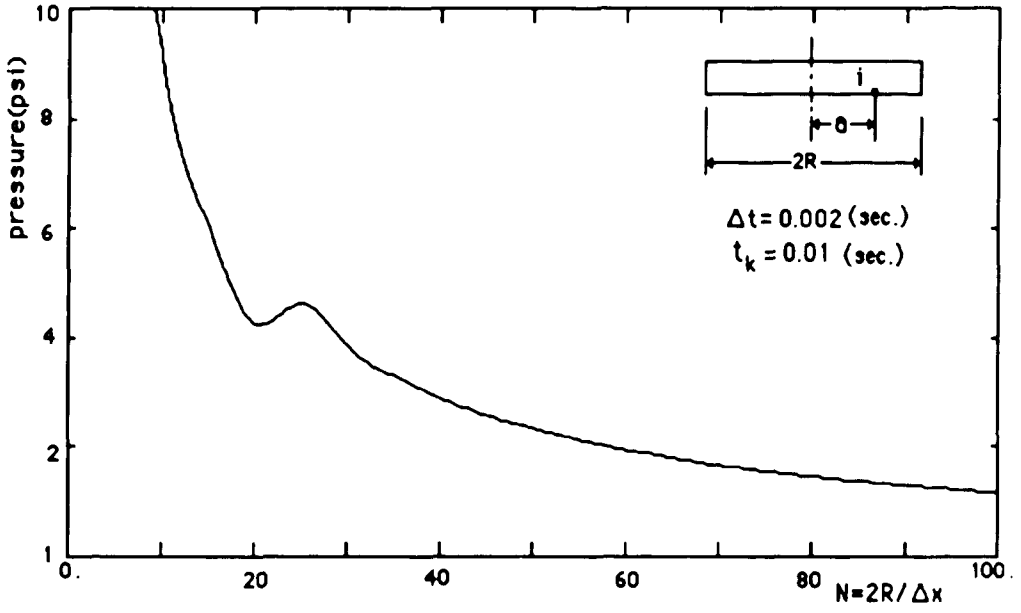

Fig.(8.2) The Pressure Applied in Strip i (a/R=1.0)
Versus Width of Strip Δx at Time (t=0.01sec.)

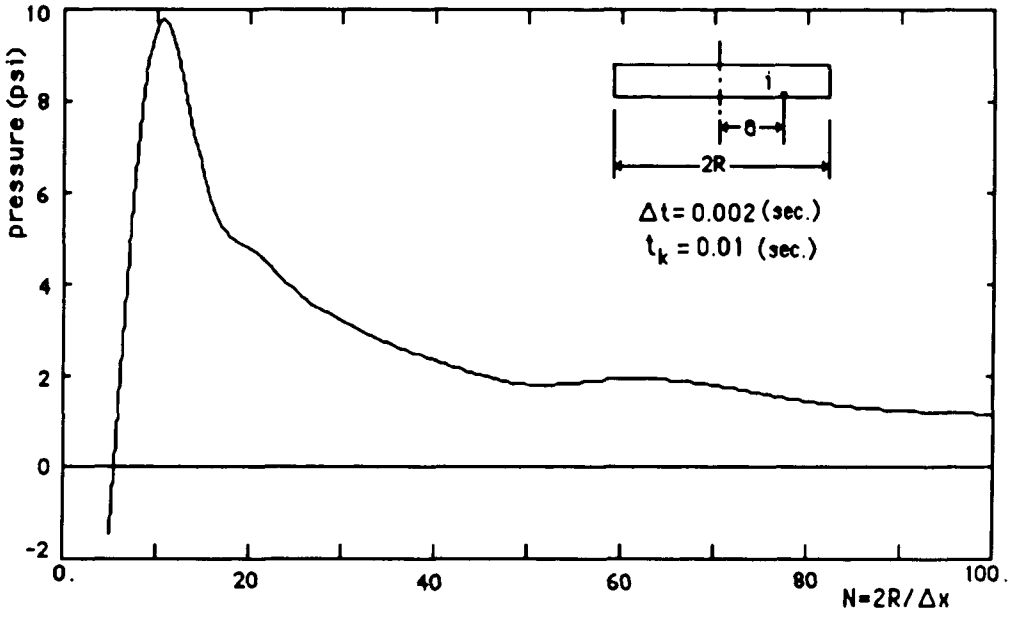

Fig.(8.3) The Pressure Applied in Strip i (a/R=0.8)
Versus Width of Strip Δx at Time (t=0.01sec.)

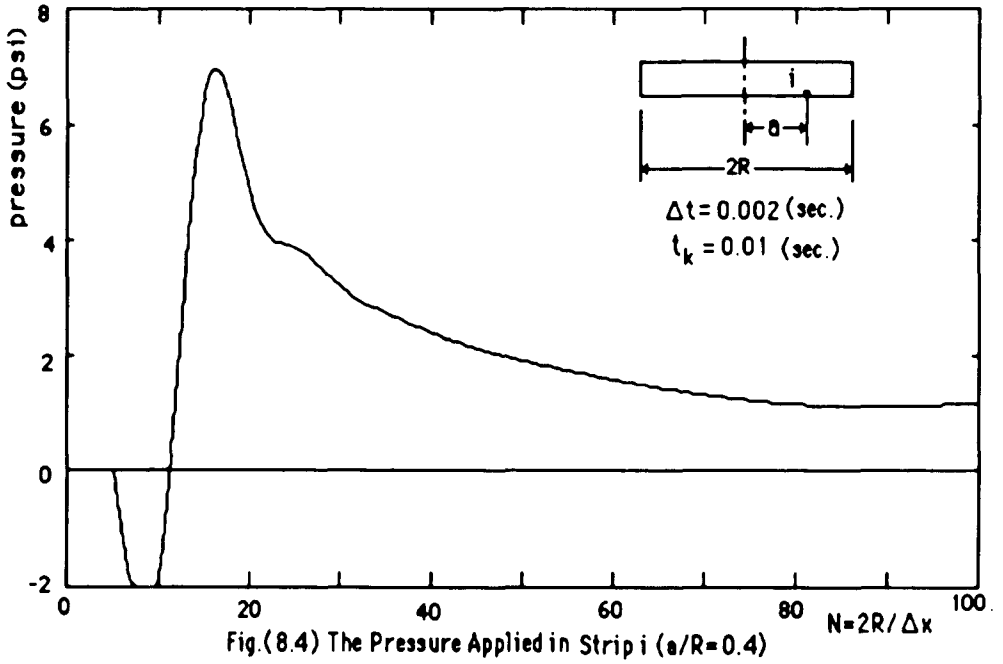

Fig.(8.4) The Pressure Applied in Strip i (a/R=0.4)
Versus Width of Strip Δx at Time (t=0.01sec.)

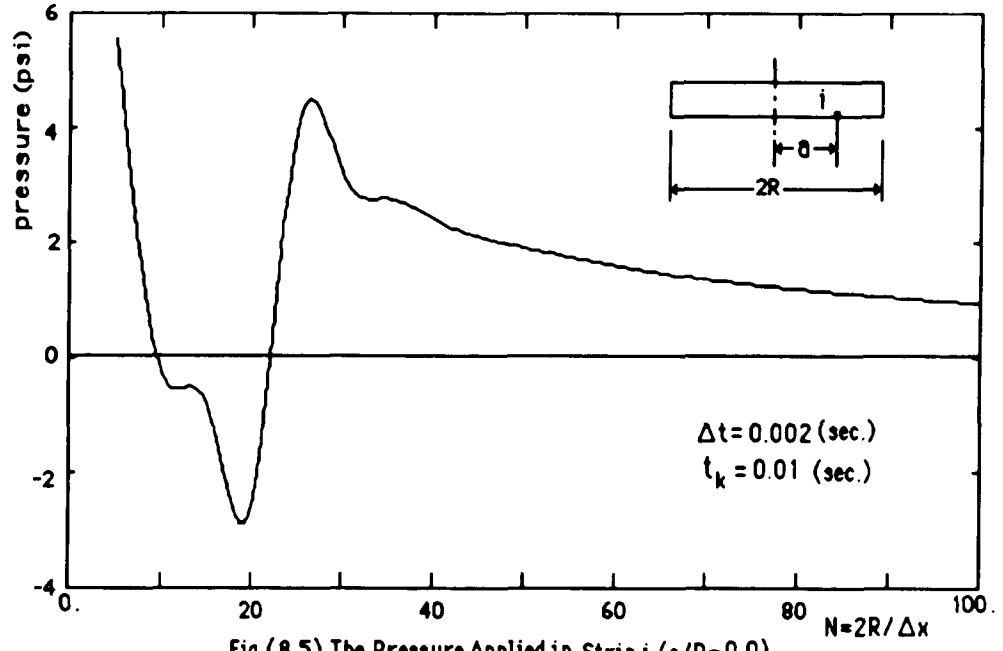

Fig.(8.5) The Pressure Applied in Strip i (a/R=0.0)
Versus Width of Strip Δx at Time (t=0.01sec.)

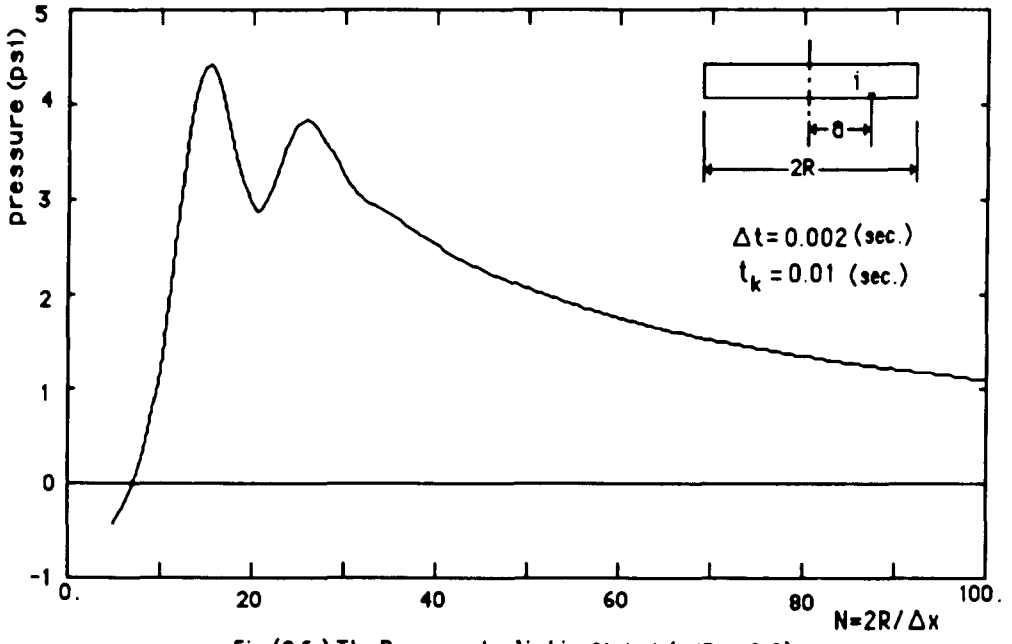

Fig.(8.6) The Pressure Applied in Strip i (a/R=-0.2)

Versus Width of Strip Δx at Time (t=0.01sec.)

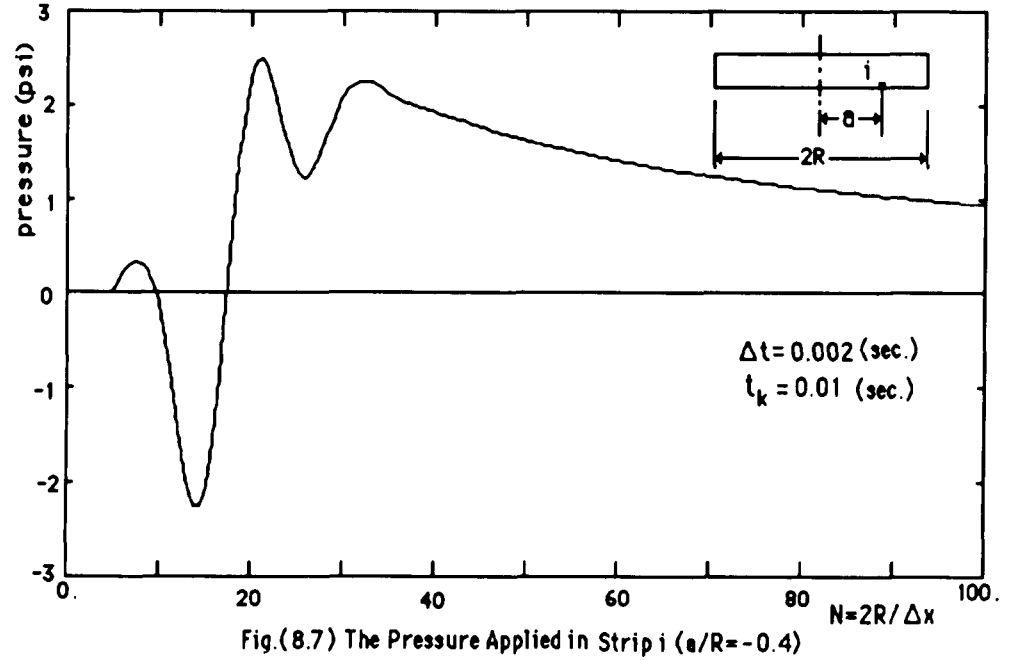

Fig.(8.7) The Pressure Applied in Strip i (a/R=-0.4)

Versus Width of Strip Δx at Time (t=0.01sec.)

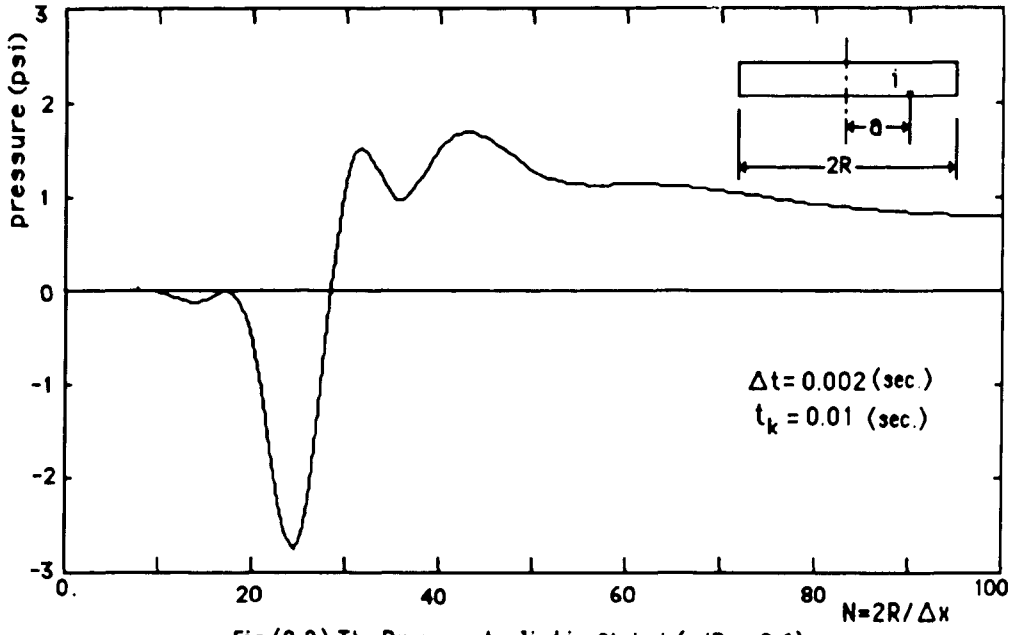

Fig.(8.8) The Pressure Applied in Strip i (a/R=-0.6)

Versus Width of Strip Δx at Time (t=0.01sec.)

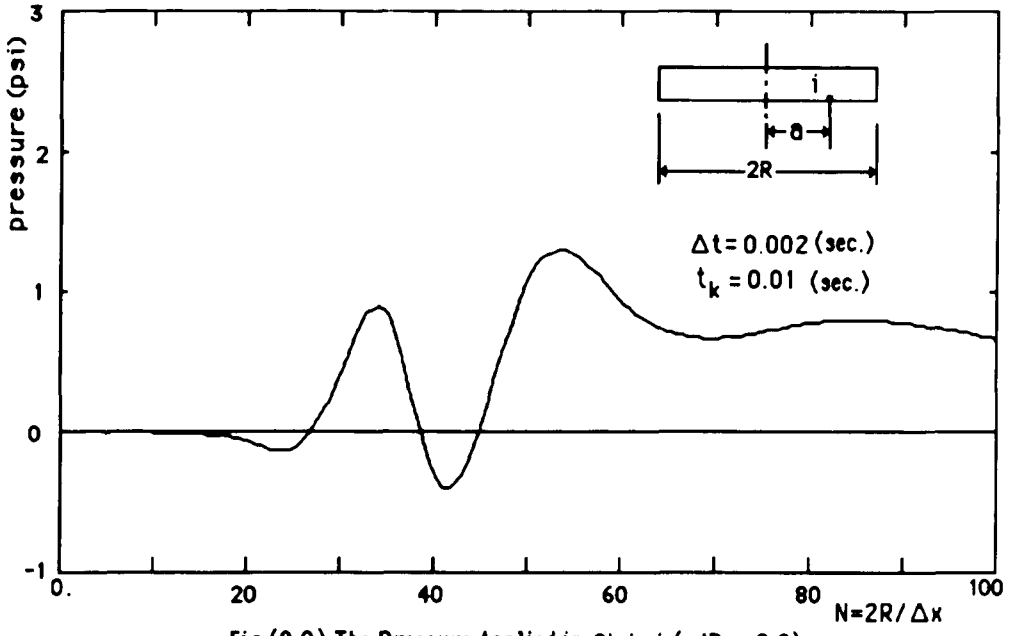

Fig.(8.9) The Pressure Applied in Strip i (a/R=-0.8)

Versus Width of Strip Δx at Time (t=0.01sec.)

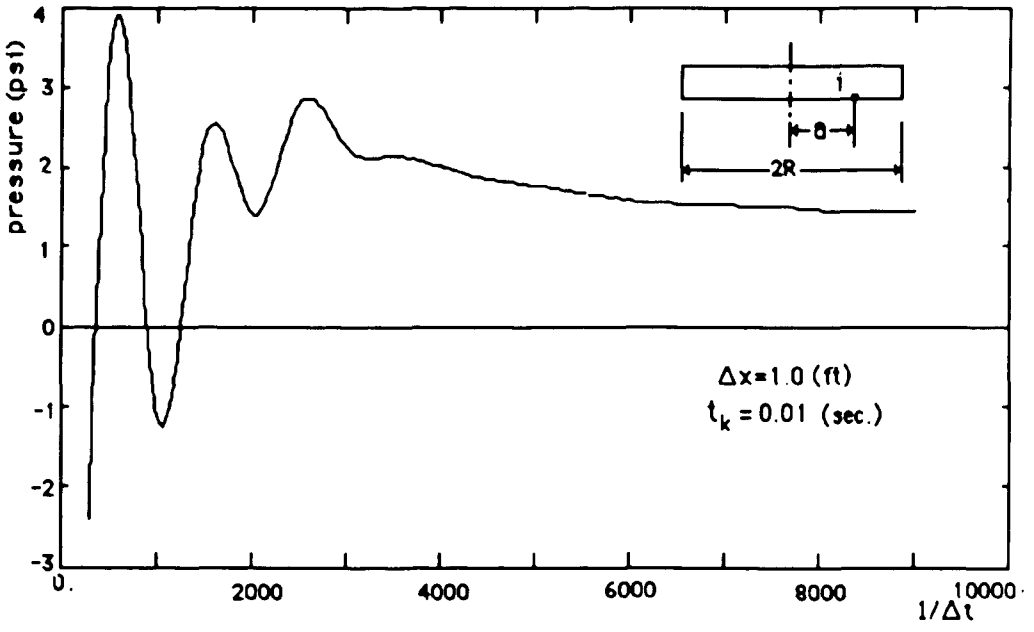

Fig(8.10) Pressure Applied in Strip i (a/R=1.0)

Versus Time Step Δt

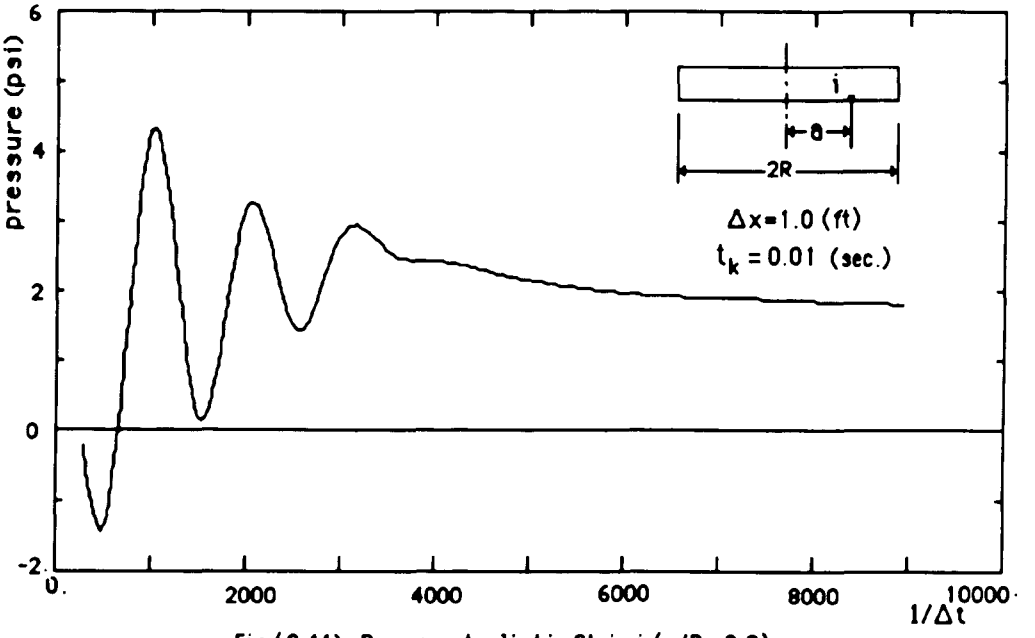

Fig (8.11) Pressure Applied in Strip i (a/R= 0.2)

Versus Time Step Δt

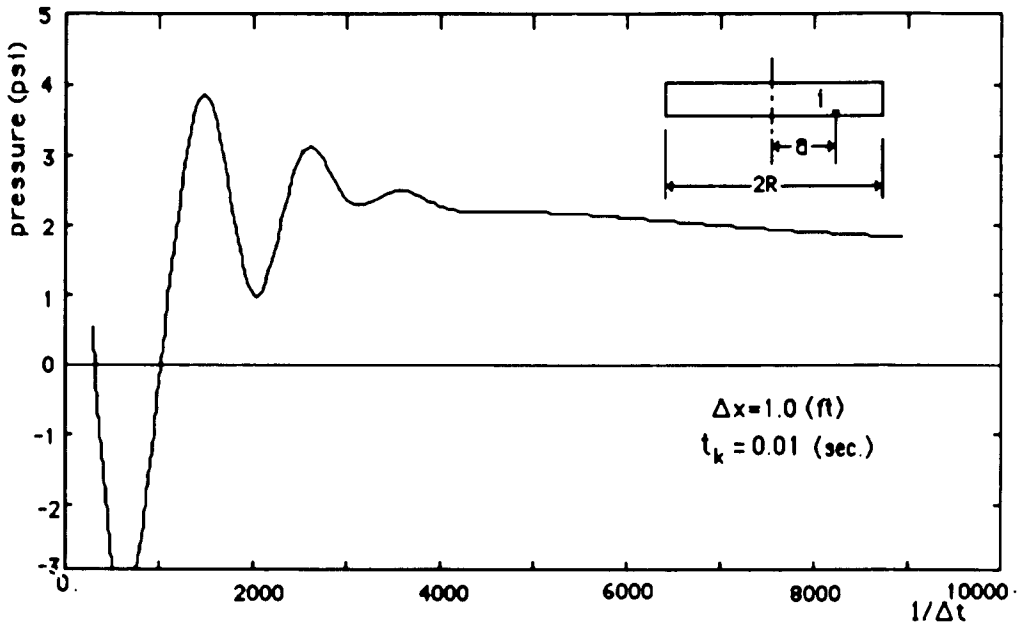

Fig (8.12) Pressure Applied in Strip i (a/R= 0.4)

Versus Time Step Δt

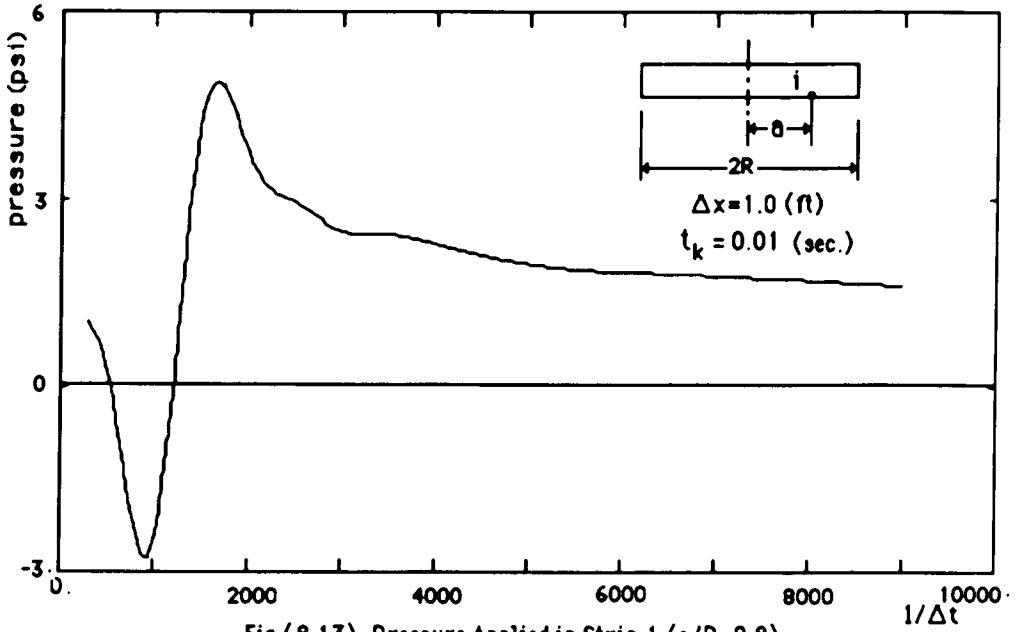

Fig (8.13) Pressure Applied in Strip 1 (a/R=0.8)

Versus Time Step Δt

Chapter 9
Numerical Results

Numerical results are generated using the model developed in Chapter 7. The first set of solutions generate frequency dependent interaction coefficients as was done with the discrete model in Chapter 4. The objective of these results, discussed in section 9.1, is to demonstrate that this analysis give reliable results for the no liftoff case. The second set of solutions is based on comparison with the large scale SSI test [30]. The objective of these solutions,presented in section 9.2, are to compare the results obtained with this model with results obtained with the discrete model and with experimental data. The final set of solutions presented in section 9.3, has the objective of assessing the effect of liftoff.

9.1 Study of Dynamic Stiffness Coefficient

Similar to the work presented in Chapter 4, the dynamic stiffness coefficients obtained by the methods of Chapter 7 are studied in this section. Liftoff effects are neglected for this solution since the analytical model is based on a welded assumption. As shown in Fig (9.1), a rigid disc is resting on the surface of an elastic half space. The forcing function P(t) can be generated by this method in time domain if a vertical displacement $U_0=\cos(\omega t)$ is imposed on the mass M_0.

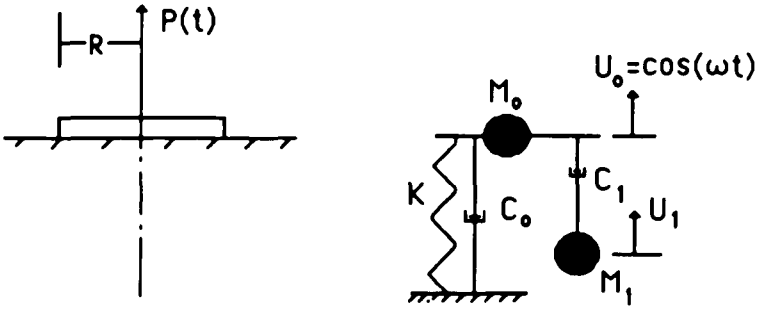

FIG (9.1) DISC IN VERTICAL MOTION

Similar to the Chapter 4, the frequency dependent dynamic stiffness coefficient $K_v(\omega)$ and $C_v(\omega)$ can be obtained as follows

$$K_v(\omega t) = \frac{\omega}{\pi}\int_{-\frac{\pi}{\omega}}^{\frac{\pi}{\omega}} P(t)\cos(\omega t)dt \qquad (9.1)$$

$$C_v(\omega t) = \frac{\omega}{\pi}\int_{-\frac{\pi}{\omega}}^{\frac{\pi}{\omega}} P(t)\sin(\omega t)dt \qquad (9.2)$$

The rocking coefficients $K_r(\omega)$ and $C_r(\omega)$ can be obtained in a similar manner.

For the purpose of generating numerical results using the code described in the previous Chapter, the following properties of the structure and soil are used:

radius of disc	R=10 ft
mass of disc	M_o=47 k.sec^2/ft
mass moment of inertia	J_o=4712 k.ft sec^2
shear modular of soil	G_s=980 ksf
Poisson's ratio	μ=0.25
density of soil	γ=0.11 kcf
shear wave velocity	C_s=535.61 ft/sec

The dynamic stiffness coefficients $K_r(\omega)$,$C_r(\omega)$,$K_v(\omega)$ and $C_v(\omega)$ varying with dimensionless frequency ($\omega_o=\omega R/C_s$) are illustrated in Fig (9.2) and (9.3). As shown in the figures, the coefficients predicted by the continuum mechanic method neglecting lift off are in good agreement with that from Wolf's model.

9.2 Comparison with Experimental Data.

The acceleration data measured in the large scale SSI test [30] are used to test

the validity of the model. The dimension of the structure and the properties of the soil have been described in Chapter 4. The structure is at the surface of an elastic half space rather than embedded in the soil.

The acceleration spectra predicted by the discrete model developed in Chapter 3 are used to compare with the results calculated by this second liftoff model.

1) No liftoff

When liftoff is neglected, the acceleration spectra computed from both the discrete liftoff model and the continuum mechanic method are illustrated in Fig (9.4) to (9.6). It may be seen that the results are in good agreement with that from these two models.

2) Liftoff occurs

Fig (9.7) to (9.9) shows the comparison of the results predicted by the discrete model and the continuum mechanic model when lift off occurs. When frequencies are less then 5 cps the results from both models are in good agreement with each other. The results from the discrete model are 10 to 20 percent higher than that from the second model in the higher frequency region. It might be that the discrete model can only represent the responses in the lower frequency region.

9.3 Effects of LiftOff

In order to study the influence of lift off on the soil structure interaction process, the pressures on the interface between soil and foundation are calculated . The input acceleration data are based on 1.0 and 2.0 times that measured in the Taiwan Seismic Experiment [30]. Since the soil cannot carry tensile force the pressure in the lift off portion must be less than the stress due to the gravity of structure. As shown in Fig (9.10) and (9.11), liftoff will occur at a peak acceleration of 0.15 G's. Fig (9.12) and (9.13) illustrate the variation of the pressure on the foundation base along the diameter for 1.0 and 2.0 times the input data respectively.

During the liftoff the stresses in the contact area of foundation and soil are increased

Fig (9.14) and (9.15) illustrate the variation of the acceleration of structure during the lift off. By using of amplification of input data as 2.0, the accelerations are computed in time region (from 3.0 to 6.0 sec.) that lift off happened. It can be seen that the absolute values of peak acceleration are increased when liftoff effects are considered. However, the maximum negative vertical accelerations keep a constant value (G) that is the acceleration of gravity.

Solutions are obtained for peak accelerations of 1.0 (0.15G's) and 2.0 (0.3G's) times the lift off acceleration. Two percent equipment damping spectra are obtained for the horizontal, vertical, and rocking motion. The results obtained including lift off are divided by the spectra obtained by neglecting the lift off. The results are shown in Fig (9.16) through Fig (9.18).

Similar to the results presented in Chapter 5, liftoff has no effect on the horizontal motion. However, liftoff has a great effect on the vertical and rocking motion. It should noticed that liftoff has a large effect in the frequency range (0.7 to 4.0 cps) of the rocking spectra. This frequency range is important for earthquake design. For the vertical motion, lift off has a important effect for frequencies greater than 5 cps.

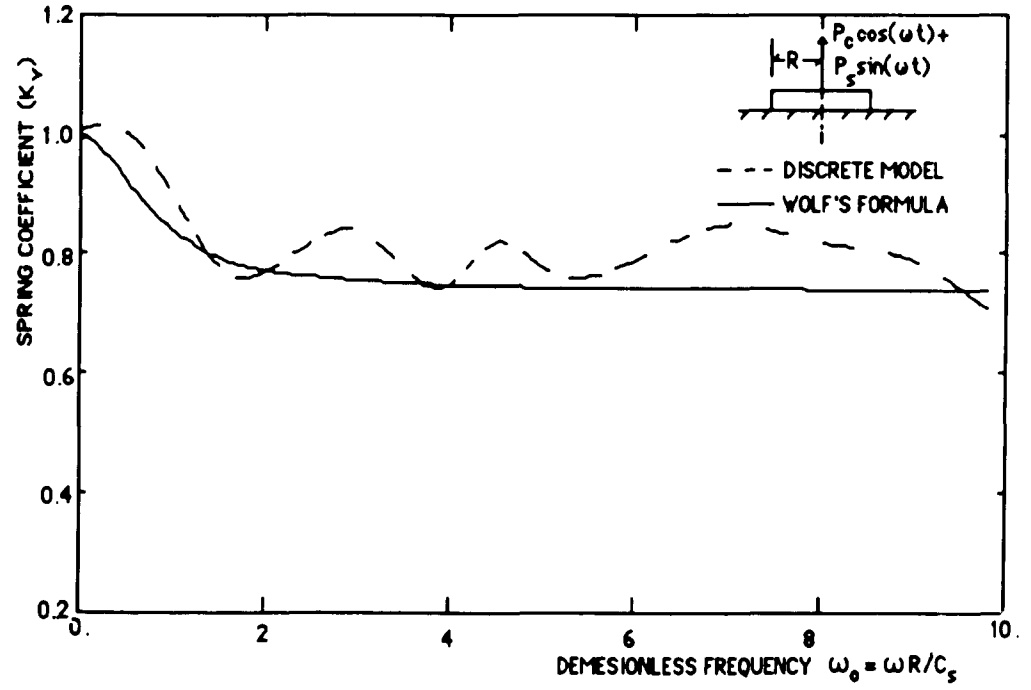

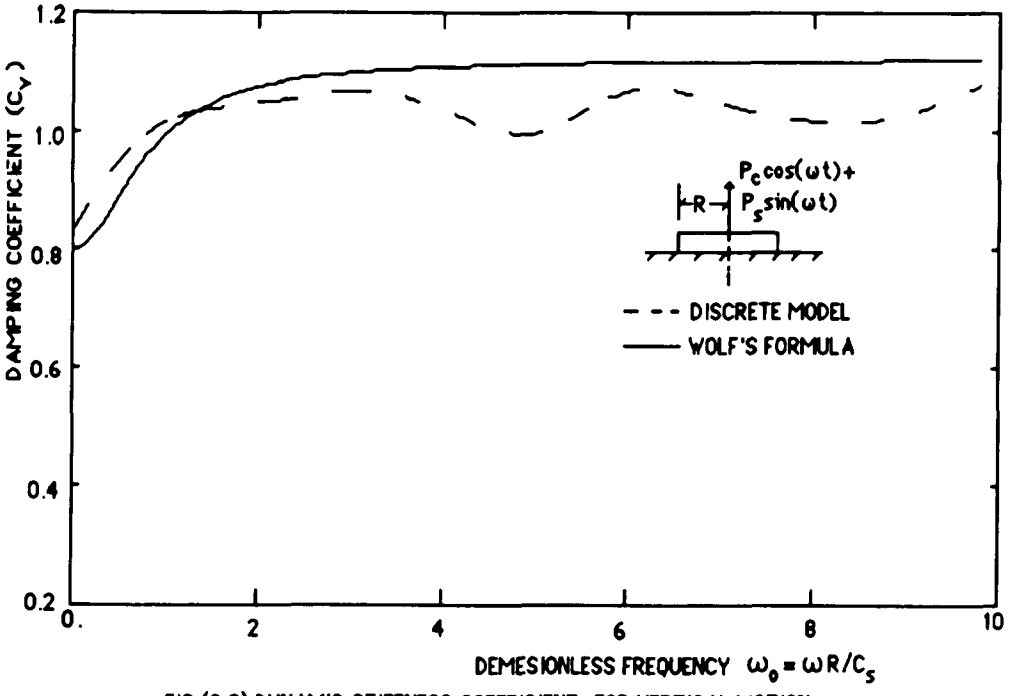

FIG (9.2) DYNAMIC STIFFNESS COEFFICIENT FOR VERTICAL MOTION

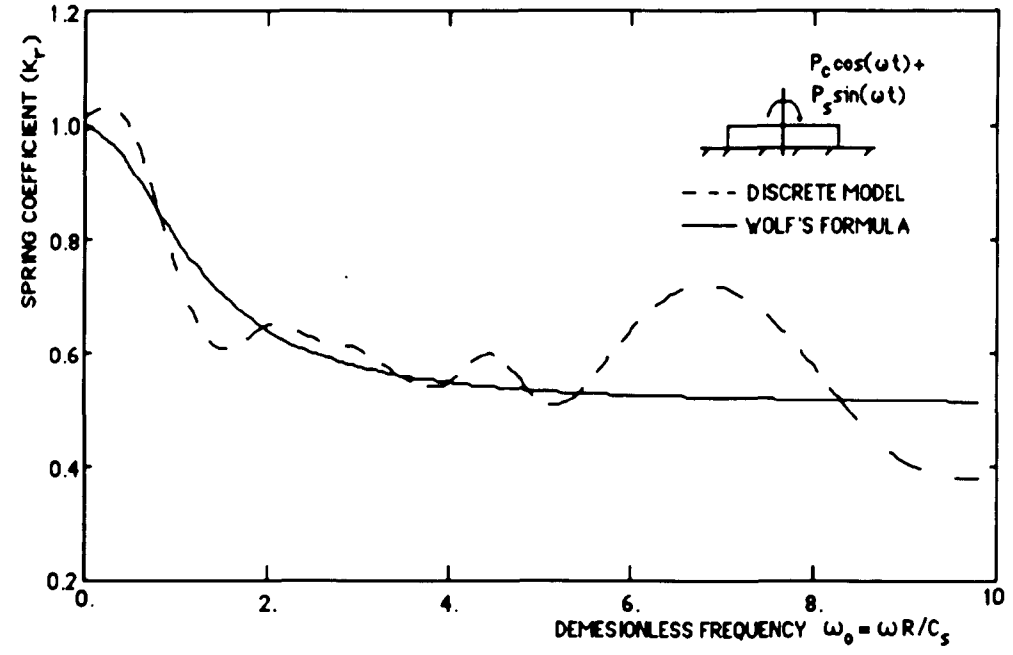

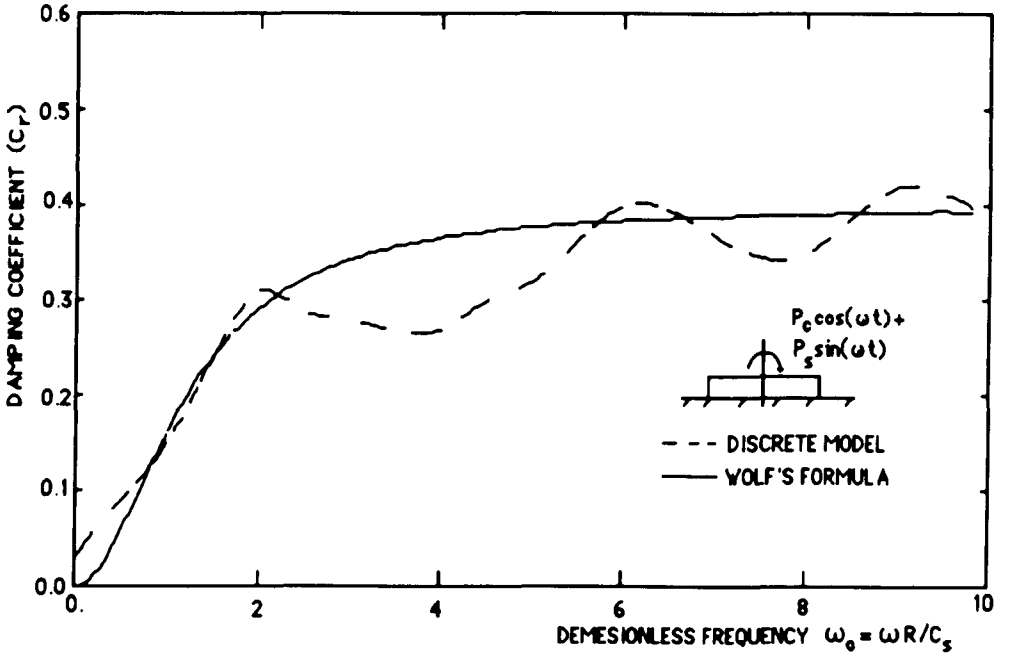

FIG(9.3) DYNAMIC STIFFNESS COEFFICIENT FOR ROCKING MOTION

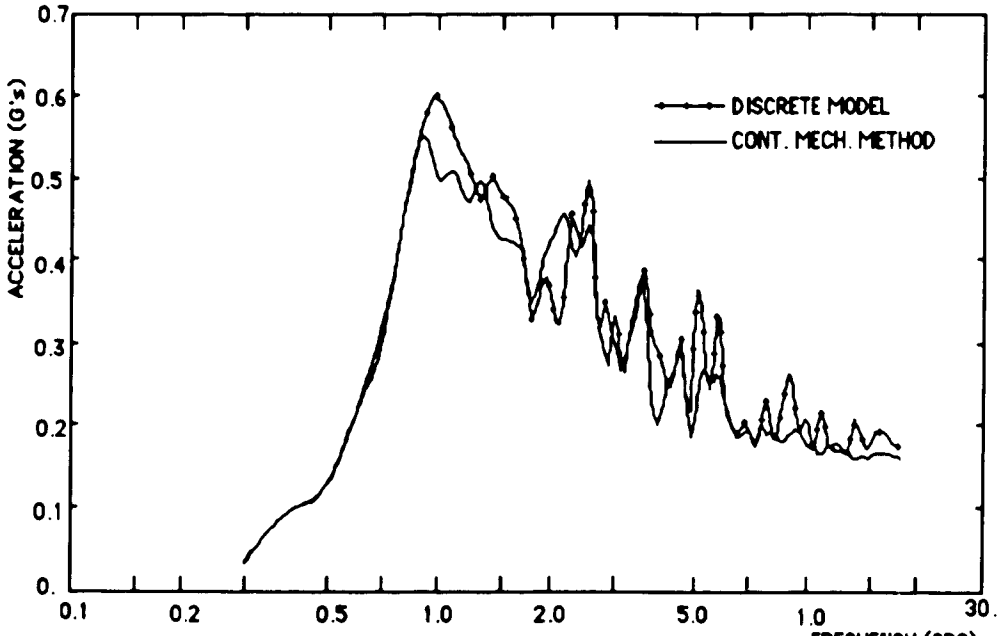

FIG (9.4) COMPARISON OF HORIZONTAL (EW) ACCELERATION SPECTRA NEGLECTING LIFT OFF

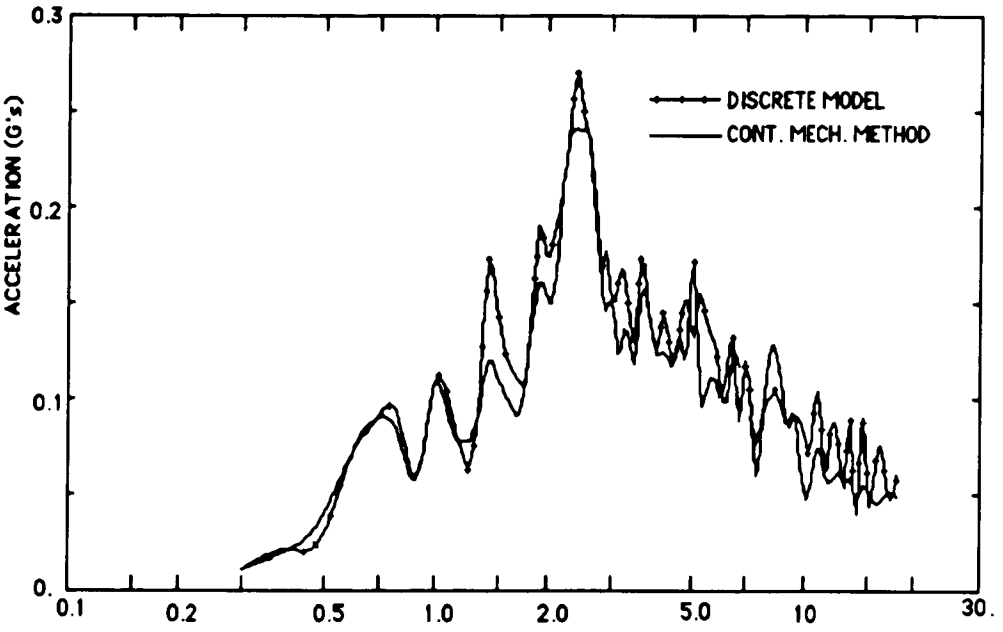

FIG (9.5) COMPARISON OF VERTICAL ACCELERATION SPECTRA NEGLECTING LIFT OFF

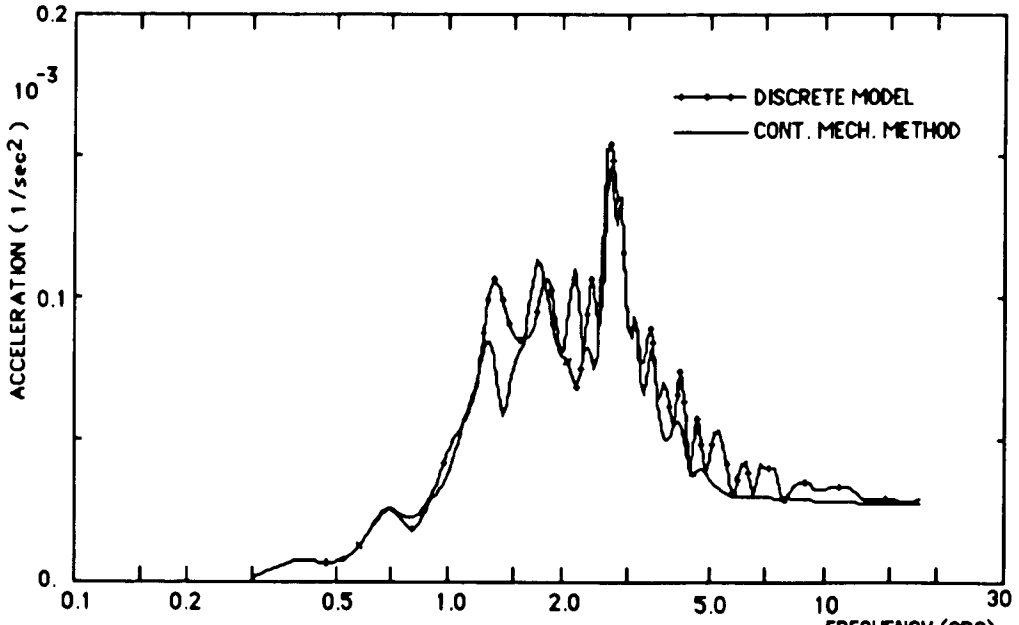

FIG (9.6) COMPARISON OF ROCKING (EW) ACCELERATION SPECTRA NEGLECTING LIFT OFF

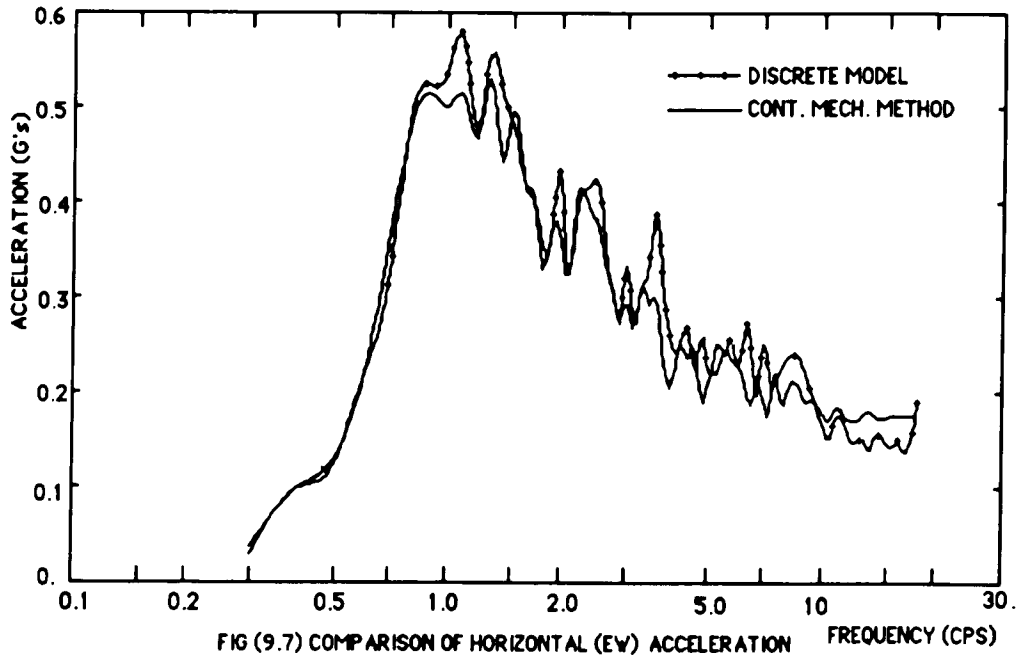

FIG (9.7) COMPARISON OF HORIZONTAL (EW) ACCELERATION SPECTRA WITH LIFT OFF

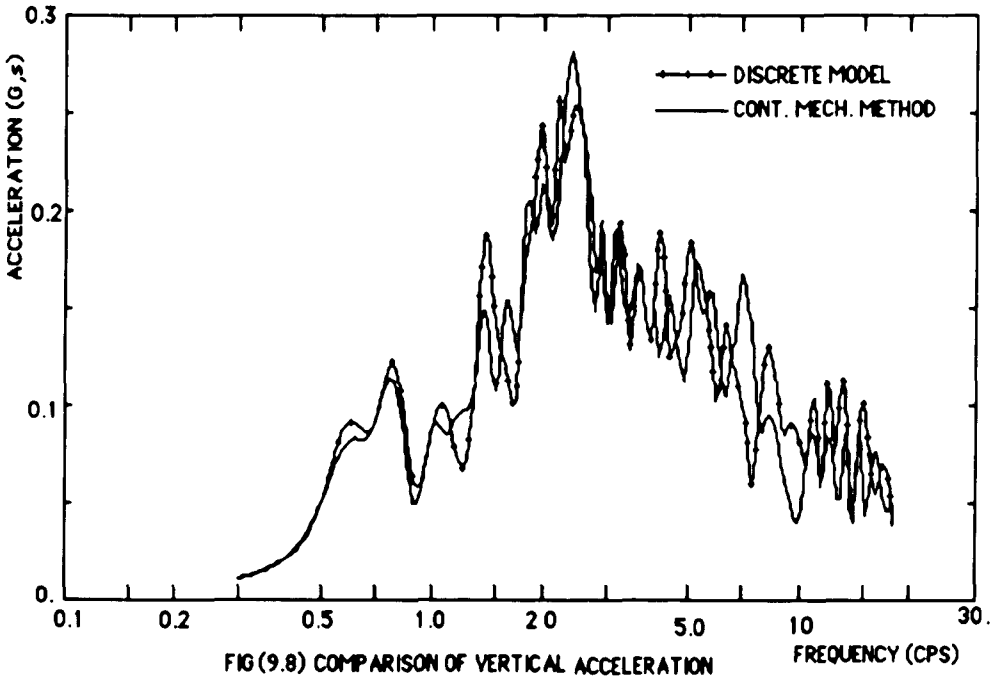

FIG (9.8) COMPARISON OF VERTICAL ACCELERATION SPECTRA WITH LIFT OFF

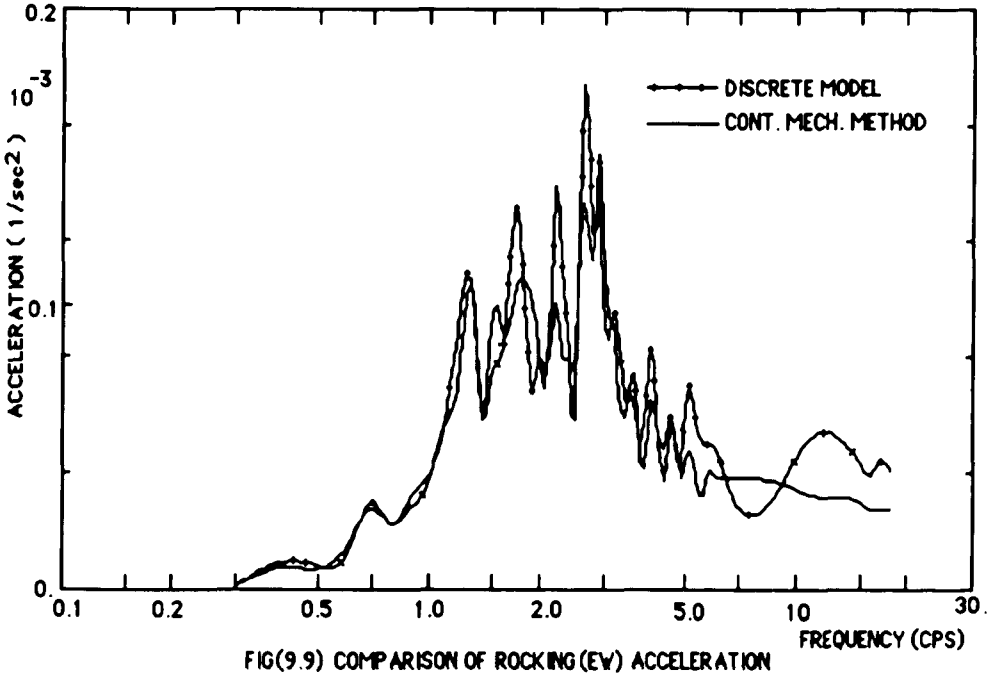

FIG(9.9) COMPARISON OF ROCKING (EW) ACCELERATION SPECTRA WITH LIFT OFF

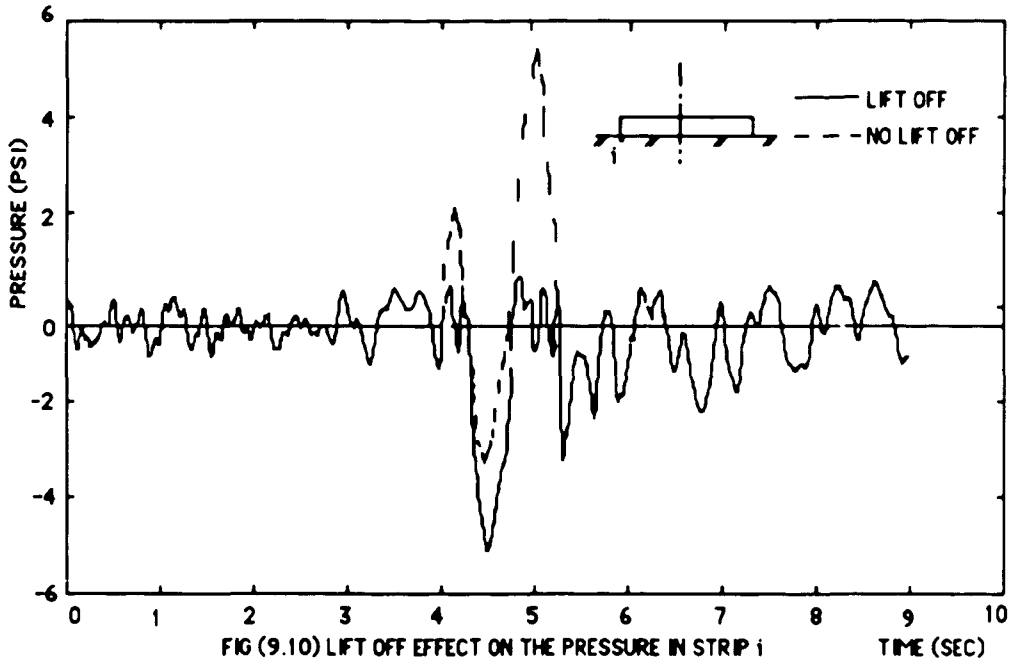

FIG (9.10) LIFT OFF EFFECT ON THE PRESSURE IN STRIP i
AMPLIFICATION FACTOR $\Psi = 1$

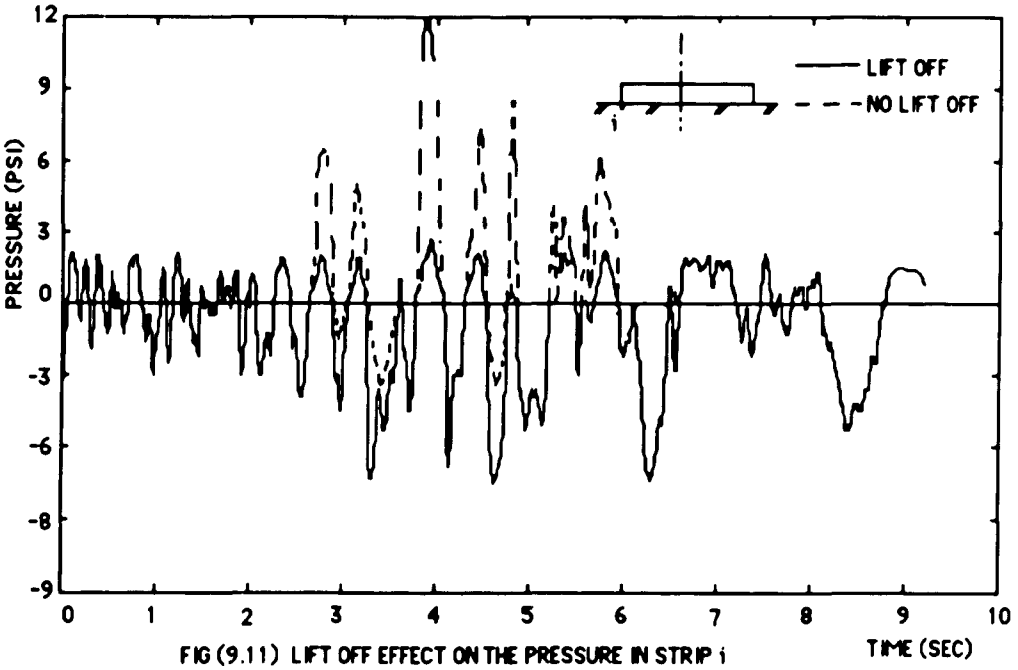

FIG (9.11) LIFT OFF EFFECT ON THE PRESSURE IN STRIP i
AMPLIFICATION FACTOR $\Psi = 2$.

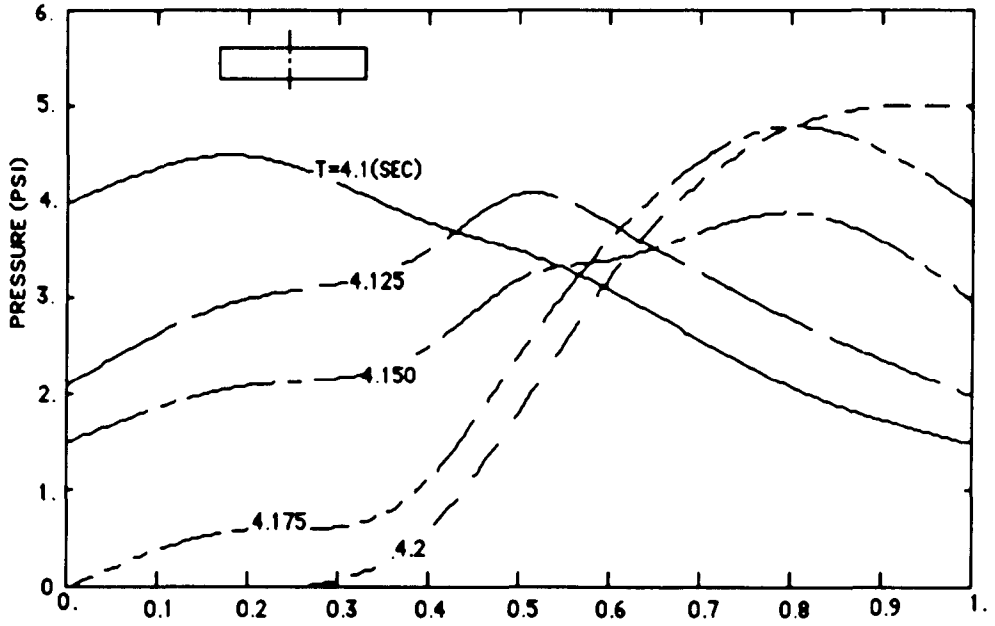

FIG (9.12) THE VARIATION OF PRESSURE IN THE FOUNDATION AMPLIFICATION FACTOR ACTOER (ν=1) (T=4.1-4.2 SEC)

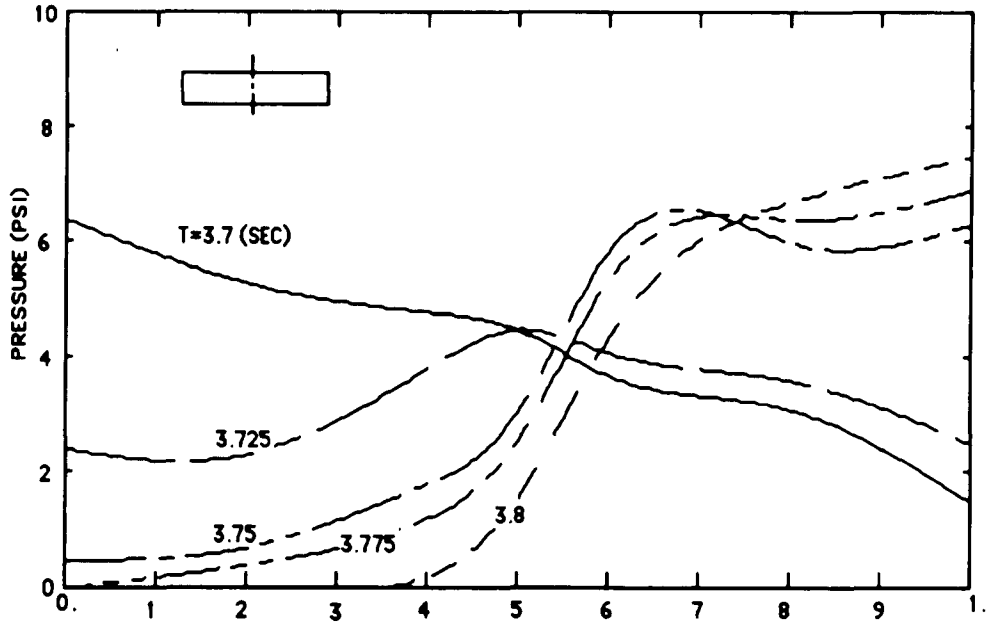

FIG (9.13) THE VARIATION OF PRESSURE IN THE FOUNDATION AMPLIFICATION FACTOR (ν=2) (T=3.7-3.8 SEC)

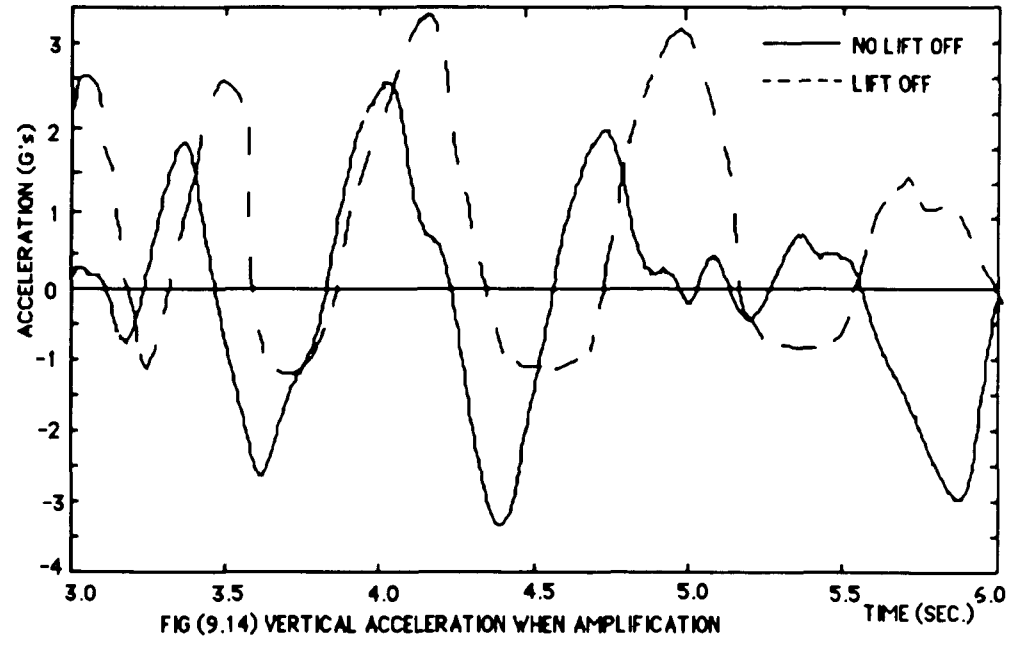

FIG (9.14) VERTICAL ACCELERATION WHEN AMPLIFICATION FACTOR IS 2.0

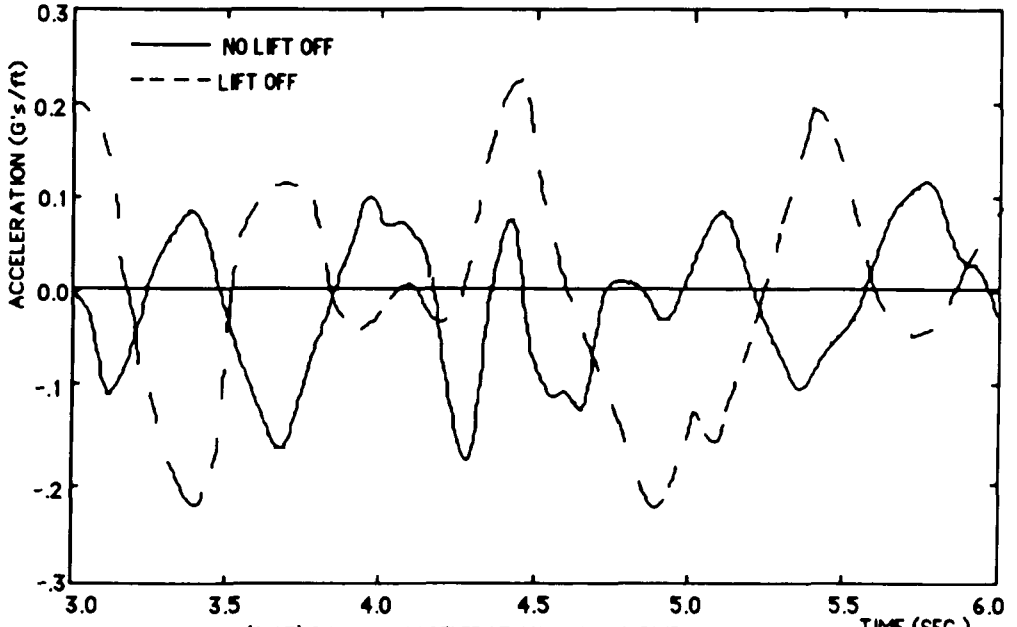

FIG (9.15) ROCKING ACCELERATION WHEN AMPLIFICATION FACTOR IS 2.0

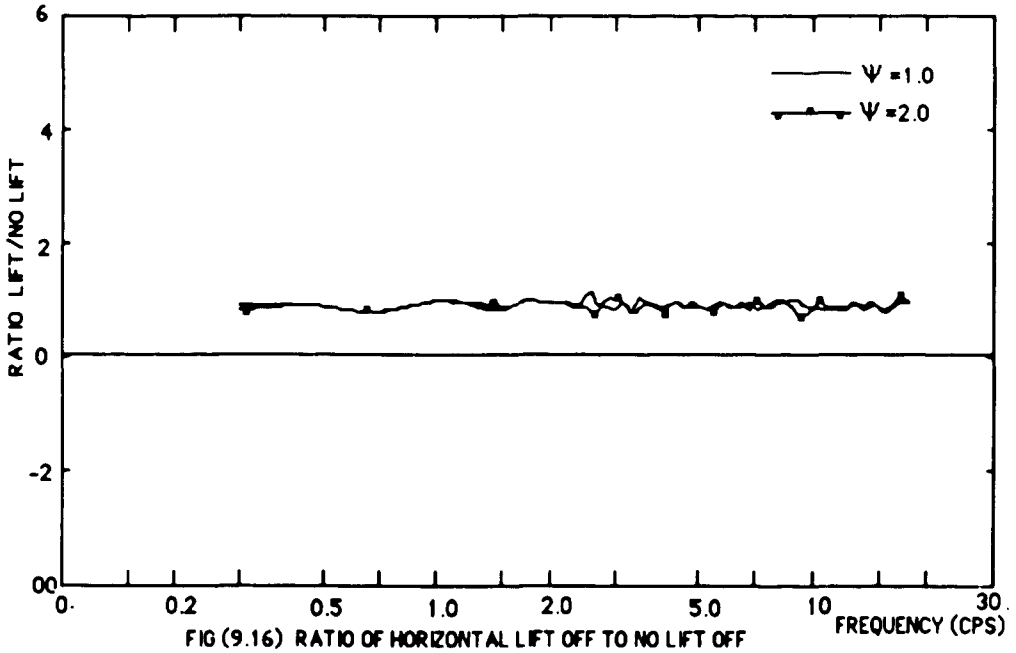

FIG (9.16) RATIO OF HORIZONTAL LIFT OFF TO NO LIFT OFF FOR ACCELERATION SPECTRA

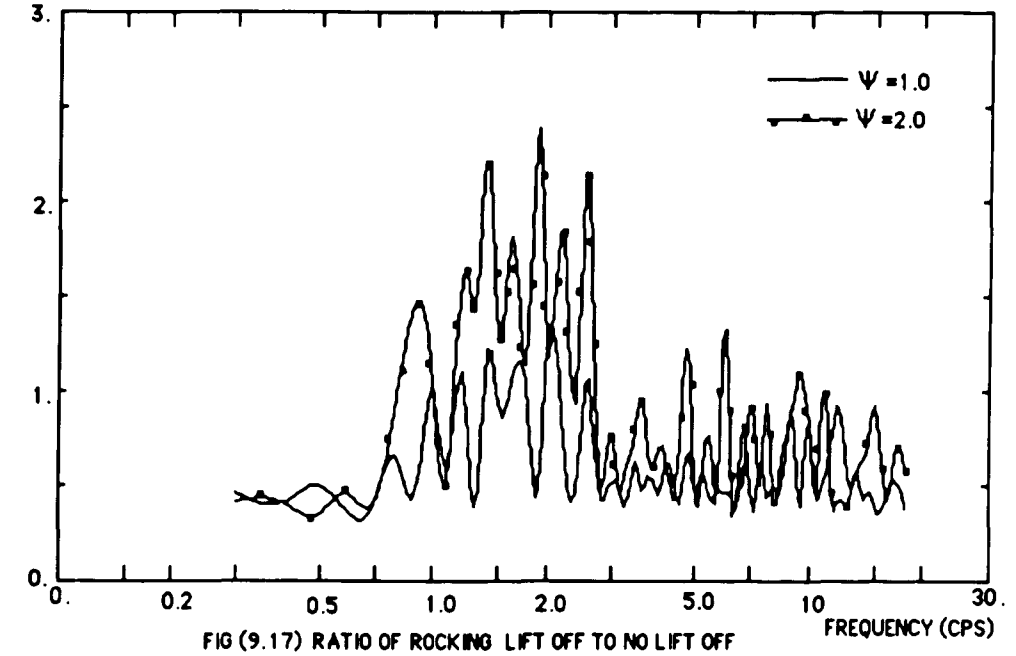

FIG (9.17) RATIO OF ROCKING LIFT OFF TO NO LIFT OFF FOR ACCELERATION SPECTRA

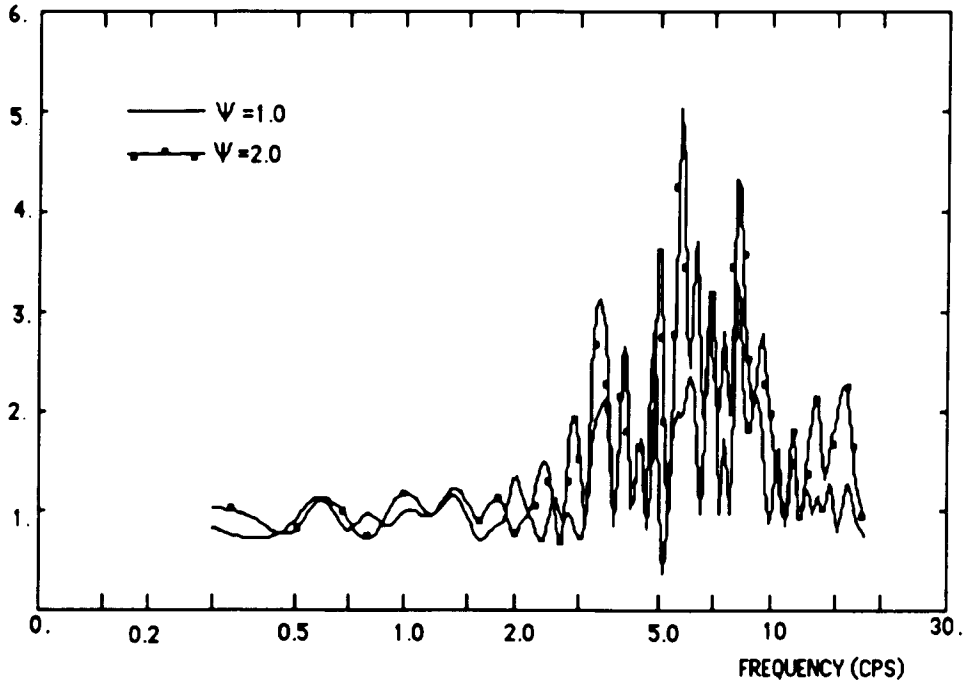

FIG (9.18) RATIO OF VERTICAL LIFT OFF TO NO LIFT OFF FOR ACCELERATION SPECTRA

Chapter 10
Conclusions and Suggestions

The effects of lift off on the soi-structure interaction process are represented in this dissertation. Two different lift off model,discrete model and continuum mechanic method, have been established here for analyzing the influence of lift off on SSI. The discrete model is modified from the Wolf's model. The vertical and moment interaction springs,dampers and masses from wolf's model are used to determine an equivalent foundation modulus acting over the entire foundation area. Two different distribution models,uniform and parabolic distribution, are developed to obtain that equivalent foundation modulus. During the response the pressure acting in distributed parameters are restricted to compression and set equal to the weight of the structure bearing the pressure when the foundation separates from the soil. The foundation area is divided into several segments so that the force is evaluated in each segment. The magnitude approach of the interaction parameters is proportion to the contact area of the foundation. Since this discrete model include the additional masses and damping that represent some behaviors of the soil, certain energy dissipation could be considered. Another lift off model is based on the continuum mechanic method. The foundation base is also divided into strips so that the influence functions due to a unit uniform pulse can be established for each strip. The Pekeris and Chao's solutions are used obtained these influence functions. The compatibility equations and equilibrium equations of motion are derived to solve the pressure of each strip and response of the structure. During an earthquake, tensile pressure must be set zero ,lift off occurring,since soil can not carry tensile stress.

The validity of the models is evaluated in two ways. The first one is to calculate the dynamic stiffness coefficient by use of the models developed in this dissertation, then to compare it with wolf's theoretical result. The second is to compare the predictions from both models with the measured data from Simquake II and Taiwan earthquake test. The results predicted by the both lift off model are good agreement

with the measured data. In discrete model, the parabolic parameter distribution manner gives more reasonable results than uniform one does.

According to the computation, Both of these two lift off models could be used in analysis SSI problem directly. The continuum mechanic method might give more accuracy results since this model can present the response in higher frequency region. However, the computing time of discrete model are much less than another model. Therefore in general earthquake engineering design for the building analysis, it is more convenient to use discrete model than continuum mechanic method. From the analysis, the lift off will occur when the ground peak acceleration are in range 0.1 to 0.5 cps. it is important to consider the effect of lift off on SSI specially for the structure like nuclear power plant. The peak acceleration required to lift off will increase with the depth of embedment and material damping coefficient, and decrease with the height of the center of gravity of structure. During an earthquake, if lift off occurs, the vertical and rocking motion will be coupled each other. The vertical and rocking motion have a great effect on the lift off. During lift off, the stress in part of foundation become zero since those parts of area are separated from soil. The pressure in rest of contact area will be redistributed, and increased. It should be noticed that the base might be failed if the compression stress in the contact area are greater than the soil's strength.

Since one of the assumptions in continuum mechanic method is the rigid cylinder sitting on the surface of the soil ground, the embedment effect can not be considered in this model. It is hope that for the further research the structure should be modified as a embedded cylinder. From the analysis in Chapter 6, the base of the foundation seems better to be divided in two directions for more accuracy results.

APPENDIX A

The Wilson θ Method

In order to solve equations A1

$$[M]\{\ddot{U}\} + [C]\{\dot{U}\} + [K]\{U\} = \{R\} \qquad A1$$

at time $t+\Delta t$, the equations are considered at time $t + \theta\Delta t$.

Since the acceleration in this method are assumed to very linearly during step Δt, the equation A1 employed is

$$[M]\{\ddot{U}\}_\theta + [C]\{\dot{U}\}_\theta + [K]\{U\}_\theta = \{R\}_\theta \qquad A2$$

where,

$$\{R\}_\theta = \{R\}_t + \theta(\{R\}_{t+\Delta t} - \{R\}_t) \qquad A3$$

1. Set initial condition $\{U\}_0$, $\{\dot{U}\}_0$, $\{\ddot{U}\}_0$

If time step is Δt, $\theta = 1.4$ the parameters for integration are

$$a_0 = \frac{6}{(\theta\Delta t)^2} \quad , \quad a_1 = \frac{3}{\theta\Delta t} \quad , \quad a_2 = 2a_1 \quad , \quad a_3 = \frac{\theta\Delta t}{2} \quad , \quad a_4 = \frac{a_0}{\theta}$$

$$a_5 = \frac{-a_2}{\theta} \quad , \quad a_6 = 1 - \frac{3}{\theta} \quad , \quad a_7 = \frac{\Delta t}{2} \quad , \quad a_8 = \frac{\Delta t^2}{2}$$

2. For each time step, solve equations A4 for $\{U\}_\theta$

$$[\hat{K}]\{U\}_\theta = \{\hat{R}\}_\theta \qquad A4$$

in which,

$$[\hat{K}] = [K] + a_0[M] + a_1[C] \qquad A5$$

$$(\hat{R})_0 = (R)_t + \theta\left((R)_{t+\Delta t} - (R)_t \right) + [M]\left(a_0 (U)_t + a_2 (\dot{U})_t + 2(\ddot{U})_t \right)$$

$$+ [C]\left(a_1 (U)_t + 2(\dot{U})_t + a_3 (\ddot{U})_t \right) \qquad \text{A6}$$

3. Calculate displacements, velocities, and accelerations at time $t+\Delta t$

$$(\ddot{U})_{t+\Delta t} = a_4 \left((U)_0 - (U)_t \right) + a_5 (\dot{U})_t + a_6 (\ddot{U})_t \qquad \text{A7}$$

$$(\dot{U})_{t+\Delta t} = (\dot{U})_t + a_7 \left((\ddot{U})_{t+\Delta t} + (\ddot{U})_t \right) \qquad \text{A8}$$

$$(U)_{t+\Delta t} = (U)_t + \Delta t (\dot{U})_t + a_8 \left((\ddot{U})_{t+\Delta t} + 2(\ddot{U})_t \right) \qquad \text{A9}$$

APPENDIX B

1) Pekeris Solution

1. Vertical Displacement Due to a Vertical Step Load

$$\text{If} \quad \tau=\frac{c(t_k - t_m)}{|r - r_1|} \quad , \quad \gamma=\frac{1}{2}\sqrt{3+\sqrt{3}}$$

$$V_p(\tau) = V_p(|r-r_1|, t_k - t_m)$$

$$=0 \qquad (\tau < \frac{1}{\sqrt{3}})$$

$$=-\frac{1}{32\pi\mu|r-r_1|}\left[6-\frac{\sqrt{3}}{\sqrt{\tau^2-1/4}}-\frac{\sqrt{3\sqrt{3}+5}}{\sqrt{\frac{3}{4}+\frac{\sqrt{3}}{4}-\tau^2}}+\frac{\sqrt{3\sqrt{3}-5}}{\sqrt{\tau^2+\frac{\sqrt{3}}{4}-\frac{3}{4}}}\right] \quad (\frac{1}{\sqrt{3}} < \tau < 1)$$

$$=-\frac{1}{16\pi\mu|r-r_1|}\left[6-\frac{\sqrt{3\sqrt{3}+5}}{\sqrt{\frac{3}{4}+\frac{\sqrt{3}}{4}-\tau^2}}\right] \qquad (1 < \tau < \gamma)$$

$$=-\frac{3}{8\pi\mu|r-r_1|} \qquad (\tau > \gamma)$$

2. Horizontal Displacement Due to a Vertical Step Load

$$U_p(\tau) = U_p(|r-r_1|, t_k - t_m)$$

$$=0 \qquad (\tau < \frac{1}{\sqrt{3}})$$

$$=\frac{\sqrt{1.5}\,\tau}{16\pi^2\mu|r-r_1|}\{6I(k)-II(8k^2,k)+(6-4\sqrt{3})III[-(12\sqrt{3}-20)k^2,k]$$
$$+(6+4\sqrt{3})III[(12\sqrt{3}+20)k^2,k)]\} \qquad (\frac{1}{\sqrt{3}} < \tau < 1)$$

$$=\frac{\sqrt{1.5}\,\tau k}{16\pi^2\mu|r-r_1|}\{6I(k)-II(8k\ ,k)+(6-4\sqrt{3})III[-(12\sqrt{3}-20)k\ ,k]$$
$$+(6+4\sqrt{3})III[(12\sqrt{3}+20)k\ ,k)]\} \qquad (1 < \tau < \gamma)$$

$$=\frac{\sqrt{1.5}\,\tau}{16\pi^2\mu|r-r_1|}\{6I(k)-II(8k^2,k)+(6-4\sqrt{3})II[-(12\sqrt{3}-20)k^2,k]$$

$$+(6+4\sqrt{3})II[(12\sqrt{3}+20)k^2,k)]\}+\frac{\gamma}{8\pi\mu|r-r_1|\sqrt{\tau-\gamma^2}} \qquad (\tau>\gamma)$$

where,

$c=\sqrt{\frac{G}{\rho}}$ shear wave velocity

$r=\sqrt{x^2+y^2}$, $r_1=\sqrt{x_1^2+y_1^2}$

2) Chao's Solution

1. Horizontal displacement due to a Horizontal Step Load

If $\tau=\frac{c(t_k-t_m)}{|r-r_1|}$, $\beta^2=(3-\sqrt{3})/4$, $\gamma^2=(3+\sqrt{3})/4$

$U_c(\tau)=U_c(|r-r_1|,t_k-t_m)$

$=0$ $\qquad (\tau<\frac{1}{\sqrt{3}})$

$$=-\frac{\tau^2}{\pi\mu|r-r_1|}\left[\frac{3\sqrt{3}}{8\sqrt{\tau^2-1/4}}-\frac{\sqrt{3\sqrt{3}+5\sqrt{2}}}{8\sqrt{\frac{3}{4}+\frac{\sqrt{3}}{4}-\tau^2}}+\frac{\sqrt{3\sqrt{3}-5\sqrt{2}}}{8\sqrt{\tau^2+\frac{\sqrt{3}}{4}-\frac{3}{4}}}\right] \quad (\frac{1}{\sqrt{3}}<\tau<1)$$

$$=-\frac{\tau^2}{\pi\mu|r-r_1|}\left[\frac{1}{2}-\frac{\sqrt{3\sqrt{3}+5\sqrt{2}}}{8\sqrt{\frac{3}{4}+\frac{\sqrt{3}}{4}-\tau^2}}\right] \qquad (1<\tau<\gamma)$$

$$=-\frac{1}{2\pi\mu|r-r_1|} \qquad (\tau>\gamma)$$

2. Vertical Displacement Due to a Horizontal Step Load

$V_c(\tau)=U_p(\tau)$

BIBLIOGRAPHY

1) John P. Wolf and Dario R. Somain, Approximate Dynamic Model of Embedded Foundation in Time Domain. Earthquake Engineering and Structural Dynamics, Vol. 14, 1986.

2) C. A. Miller,and C. J. Costantino, SSI Methods-SIM Code. Brookhaven National Laboratory, NUREG/CR-1717, vol. 3, sept. 1979 .

3) J. Lysmer, Vertical Motion of Rigid Footing. Report No, 3-115, Dept. of CE Univ. of Michgon, 1965.

4) C. A. Miller, Soil-Structure Interaction Vol.2 Influence of Lift off, NUREG,/CR-4588, BNL-NUREG-51983,vol.2,April,1986

5) J. Elorduy , J.A. NIEBO AND E.M. SZEKELY, Dynamic Response of Bases of Arbitrary Shape Subjected to Periodic Vertical Loading. Proc. Int. Symp. on Wave Propagation And Dynamic Properties of Earth Mechanics,1967.

6) C.L. Pekeris, The Seismic Surface Pulse. National Academy of Science Proceedings-Geophyics,Vol,41,1955.

7) C. C. Chao, Dynamic Response of An Elastic Half Space To tangentical surface loadings. J. Appl. Mech. Trans. ASME, Vol. 27, PP 559-567, 1960.

8) T. Kobori, Dynamical Response of Rectangular Found on An Elastic Space. Proc. Japan Natl. Symp. Earthq. Eng.,Tokyo, Japan,81-86,1962.

9) I. A. Robertson, Forced Vertical Vibration of Rigid Circular Disc on A Semi-Infinite Elastic Solid. Proc. Camb. Phil. soc. 41-62, 1966

10) H. Tajimi, Dynamic Analysis of Struture Embeded in An Elastic Stratum. Proc. Fouth Wold conf. Earthq., Santiago, chile 3. A-6, 53-64, 1969.

11) R. A. Parmelee, Building-Foundation Interaction Effects. Proc. ASCE, 93(EM2), 131-152, 1967.

12) E. L. Wilson, A Method of Analysis For The Evaluation of Foundation-Structure Interaction.Proc. Fourth Wold Conf. Earthq. Eng. Santiago,Chile, 3 A-6,87-89,1969.

13) J. W. Meek, Effect of Foundation Tipping on Dynamic Response. Journal of

The Structure Division. ASCE, July 1975.

14) A. K. Chopra, and S. C. S. Yim, Simplified Earthquake Response Analusis of Structure with Up Lift. Journal of Structure Division, ASCE, Aug, 1985.

15) A. A. Huckelbrrge,abd R. W. Chough, Seismic Response of Uplifting Building Freme. Journal of Structure Division. ASCE, Aug,1897

16) I. N. Pychris, Dynamic Behavior of Rocking structure Allowed to up lift. Report No. EERL 81-02, California Institute of Technology, Aug 1981

17) J.E. Luco, Dynamic Interaction of Shear Wall With The Soil. J. Eng. Mech Div., ASCE, 95, 333-346, 1969.

18) M. D. Trifunac, Interaction of A Shear Wall With The Soil for Incident Plane SH Waves. Bull. Seism.,Soc.,Am., 62, 63-83, 1972

19) H.L.Wong, Dynamic Soil-Structure Interaction. Report EERL-76-01,EArthq. Research Lab.,m California Inst. of Tech., Pasadena, California, 1975.

20) M.A. Oien, Steady Motion of A Rigid Strip Bonded to An Elastic Half Space. J. Appli., Mech. ASME, 38, 328-344, 1971.

21) T.R Kobori and Y. Shinozaki, Vibration of Rigid Circular Disk on An Elastic Half Space Subjected to Plane Waves. Theo. and Appli. Mech., 21, 109-119, Univ. of Tokyo press. 1976.

22) J.E. Luco, Tosinal Response of Structures for Obliquely Incident Seismic Waves, Earthq. Foundation Earthq. Eng. and Stru. Dynamics, 4 119-127, 1976.

23) S. Tani, J. Sakurai and M. Iguchi, The Effect of Plane Shape and Size of Buildings On The Input Earthqake. Motion. Proc. 5th Wold Conf. on Earthq. Eng. Rome, 1973.

24) R.H. Scanlan, Seismic Wave Effects on Soil-Structure Interaction. Earthqake. Eng. and Stru. Dynamic, 4, 379-388, 1976.

25) S.M. Dag, Finite Element Analysis of Seismic Scatter Problems. Phd. Dissertation, Univ. of Calif. Sendiego, La Jolla, California 1977.

26) J. Dominguez, Respopnse of Embeded Found to Travelling Waves. Publication R 78-24 Dept. of CE, MIT ,1978.

27) M.j. Kaldjian, Torsional Stiffness of Embadded Footing. Soil Mech. Found. Div. ASCE, 95, No SM1, 969-980, 1969

28) Y. O. Berdugo and M. Novak, Coupled Horizontal and Rocking Vibration of Embeded Footing. Canadian Geotech. Journal, p747, 9,1972.

29) SIMQUAKE 2 , An Explosive Test to Simulate Earthquake Ground Motion Effects on Model Nuclear Power Plant Structure. University of New Mexico for EPRI, vol.1 to 8, Feb. 1979 .

30) Large-Scale Soil-Structure Interaction Test, EPRI, NP-5513-SR, Special Report, 11,1987.